

PROPERTIES OF HADRONIZATION IN e^+e^- -ANNIHILATION

Jari Häkkinen



Department of Theoretical Physics, Lund University, Sweden
1996

PROPERTIES OF HADRONIZATION IN e^+e^- -ANNIHILATION

Jari Häkkinen

Department of Theoretical Physics
Lund University, Sweden

Thesis for the degree of Doctor of Philosophy

To be presented, with the permission of the Faculty of Mathematics and Natural Sciences of Lund University, for public criticism in Lecture hall A of the Department of Physics on Wednesday June 5, 1996, at 13.15.

This thesis is based on the following publications/papers:

- I Λ -polarization in e^+e^- -annihilation at the Z^0 -pole
Gösta Gustafson and Jari Häkkinen, *Phys. Lett.* **B303** 350 (1993)
- II Deuteron production in e^+e^- -annihilation
Gösta Gustafson and Jari Häkkinen, *Z. Phys.* **C61** 683 (1994)
- III Colour Interference and Confinement Effects in W-pair Production
Gösta Gustafson and Jari Häkkinen, *Z. Phys.* **C64** 659 (1994)
- IV Colour connections in e^+e^- -annihilation
Christer Friberg, Gösta Gustafson, and Jari Häkkinen, LU-TP 96-10
Submitted to *Nucl. Phys.* **B**
- V $b\bar{b}$ fragmentation and $B\pi$ correlations
Jari Häkkinen, LU-TP 96-11
Submitted to *Z. Phys.* *C*
- VI Colour: A Computer Program for QCD Colour Factor Calculations
Jari Häkkinen and Hamid Kharraziha, LU TP 96-08
Submitted to *Comp. Phys. Comm.*

why spend time learning,
when ignorance is instantaneous?

Hobbes

Foreword

When people, non scientists, ask me what I do for a living, I usually hesitate before giving an answer. I try to judge the person I am speaking with and decide whether I should answer 'I am a Ph.D. student in theoretical particle physics', 'I do physics', or just try to ignore the question. When I make use of the first option I have found out that people love to hear me say the sentence 'Ph.D. student in theoretical particle physics' in Swedish (doktorand i teoretisk elementarpartikelfysik), rather than actually hear me try to explain what I do. This could of course reflect upon my way of explaining things. The second option is more rewarding, many people go around thinking about everyday phenomena. Since I claim that I do physics, people expect me to be able to answer *any* question about Nature. The questions do not have to do explicitly with physics, my opinion is asked for anyway. The last option is usually the easiest way out, but works only with people you meet once, or at least rarely. Sooner or later I end up trying to explain what I do, but I cannot say that I have been successful when I have tried. This thesis will probably not shed any light upon my doings during the last 4+ years for most people, and is not intended to. If someone feels neglected I will gladly try to make up for this in some other ways.

The Papers

To be able to perform experiments and theoretical predictions in high energy physics, computers have become a very important tool. Theoretical physicists tend to have different views on computers and Monte Carlo programs. Some of us would never use, and become dependent on, computers, while others do not hesitate to use them. The power of Monte Carlo simulations was realized early in Lund, and has resulted in a few event generators during the past two decades.

The papers which this thesis rests upon could not have been written without MC's and computers. In papers I, II, and V available MC's have been used as calculation tools. In the work presented in papers III and IV there was a need to modify available MC's, not to solve imperfections in them, but rather to introduce possible new (interference) effects in the gluon cascade/hadronization phase. Paper VI describes a non MC program for QCD colour factor calculations.

Paper I

Strange quarks (or generally down type quarks) produced in the reaction $e^+e^- \rightarrow Z^0 \rightarrow s\bar{s}$ are strongly longitudinally polarized in the standard model. It is interesting to investigate

to which extent the spin of the initial quark can be transferred to hadrons formed in the hadronization process. In the constituent quark model the spin of Λ particles is determined by the spin of the s quark, and energetic Λ particles are expected to contain the initial strongly polarized s quark. Λ particles are also well suited to study experimentally since they are produced in a fairly large number, and they decay into a $p\pi$ pair with a large asymmetry,

$$\frac{1}{N} \frac{dN}{d[\cos \theta^*]} = 1 + \alpha P \cos \theta^*$$

where θ^* is the decay angle between the proton and the Λ momenta boosted to the rest frame of the Λ , α is the decay asymmetry, and P is the longitudinal polarization of the Λ .

In this paper we estimate how much of the initial s quark polarization can be observed in Λ decay after hadronization. There are two different production modes of Λ hyperons. The Λ can be directly produced in the hadronization with either an initial s quark or an s quark produced within the hadronization process. A Λ containing an initial s quark inherits the longitudinal polarization of the quark, while a Λ containing an s quark produced in the hadronization is longitudinally unpolarized. Λ particles are also produced as decay products of heavier resonances. If the resonance contains an initial s quark the polarization is assumed to be transferred into the Λ to some degree. These fractions are obtained by studying the SU(6) and Clebsch-Gordan coefficients in the decay of the resonances.

Summing up the different contributions we find that, from the non relativistic quark model, a considerable amount of the initial s quark polarization should be expected in the decay of energetic Λ particles. The ALEPH Collaboration has recently made a Λ polarization measurement with an analysis similar to the one we present in paper I, and they find a very good agreement between experiment and the theoretical expectation if the initial quark spin is inherited by the final state hadrons [1].

Paper II

In nucleus collisions it is suggested that the formation of deuterons can be described as a coalescence process of neutrons and protons, and that the production rate is given by the overlap of the neutron-proton pair wave function with the deuteron wave function. The overlap depends on the deuteron binding energy and the production volume which is a free parameter in the model. Assuming non correlated neutron and proton distributions the suggested model gives the observed deuteron production rate in nucleus collisions. Applying the same model to Υ decays (with the interaction volume fixed from nucleus collision data) gives too energetic and too few deuterons as compared with experimental data.

In the study of deuteron production in Υ decay, we advocate the use of the same model (and the overlap) as proposed in nucleus collisions, but note that some care must be taken. i) In order to apply the model correctly, the nucleon distributions must be assumed to be given by a model which does not take the attractive pn-potential into account, i.e.. the attractive potential between the nucleons should be possible to treat as a perturbation. ii) At low energies, there is an (anti-)correlation of the neutron and proton distributions, which must be included in the calculations. Protons and neutrons avoid being in the same event since

a production of two baryons also implies a production of two anti-baryons. A production of four (anti-)baryons would require a large fraction of the available total energy.

The calculations include non relativistic quantum mechanics for the deuteron wave function, and the use of a Monte Carlo description of the Υ decay (and $q\bar{q}$ continuum) in order to take the neutron and proton correlations into account. We find that deuteron production data in Υ decays are well reproduced with a production volume of about 3fm. Using the production volume obtained from the Υ decay studies, we also make a prediction for deuteron production at LEP1 energies.

In 1995, The OPAL Collaboration made a search for charged particles with unusual mass and/or charge [2], where an upper limit on the deuteron production was given. This value is consistent with the prediction of the total production of deuterons that we make in paper II.

Paper III

In $e^+e^- \rightarrow W^+W^- \rightarrow q_1\bar{q}_2Q_1\bar{Q}_2$ events the two hadronic systems could in principle interact with each other, either through perturbative gluon exchange or in the hadronization phase. If no interferences occur then the final state is given by a superposition of two independently fragmenting hadronic systems. The presence of interference will naturally give a different final state, with implications on the W mass determination at LEP2. The (non) existence of interference can also provide information about the structure of the QCD vacuum and the non perturbative phase of strong interactions.

In paper III we want to study if effects from colour interference in the hadronization phase of $e^+e^- \rightarrow W^+W^- \rightarrow q_1\bar{q}_2Q_1\bar{Q}_2$ events are possible to detect experimentally at LEP2. We also discuss which recoupling probabilities (probability of interference) can be expected. It is, however, not possible to theoretically estimate an absolute recoupling probability due to the non perturbative character of the effects, but we suggest that it may be conceivable to expect that states with shorter “strings” are favoured if recoupling occurs in Nature. A model of colour interference is proposed, and implemented into an MC, where the recoupling probability is a free variable.

If interference occurs, and is favoured when the interference decreases the total string length of the system, we find a possible experimental signal on an event-by-event basis. The signal is small and depends on the recoupling probability. Using the expected sample of $e^+e^- \rightarrow W^+W^- \rightarrow$ hadrons at LEP2, we expect the signal to be visible down to a 10% recoupling probability level.

In the MC we have made two approximations which have an impact on the experimental detection possibility: i) we have assumed isotropic W^+W^- decays, ii) all gluons with energy below Γ_W are neglected (deleted), and in consequence energy is not conserved. The effects from interference are still present when the W^+W^- correlations and energy conservation are included into the MC. The experimental signal derived in paper III is decreased by a factor 2, and in consequence interference effects at a 10% level cannot be found at LEP2 due to the expected small sample of $e^+e^- \rightarrow W^+W^- \rightarrow$ hadrons. Larger recoupling probabilities

can still be detected at LEP2, and the signal should not be ruled out. The major part of the decrease in the signal arises from the introduction of W^+W^- correlations whereas energy conservation only gives a small effect [4].

Several other models for colour interference effects in the decay of the two W 's have been presented [3]. Some of the model presentations are not yet public, but have been used to calculate effects on the W mass determination from colour interference. We have not studied effects on the determination of the W mass in paper III, but results obtained from the proposed model is available in [3], where also the results from other models are presented.

Paper IV

In paper III we discuss colour interference in $e^+e^- \rightarrow W^+W^- \rightarrow$ hadrons at LEP2. In this paper we address the possibility to have similar effects at Z^0 decay events. The two reactions are complementary and a comparison of interference effects in the two reactions would be valuable. No interference can take place in the large N_c limit, but for $N_c = 3$, partons in the QCD cascade can obtain the same colour. In the decay $Z^0 \rightarrow q\bar{q}$ there could in principle be colour interference as soon as two gluons have been emitted.

If identical colours are emitted, how does Nature decide which configuration to choose. Are the possible interferences important? Do they occur in the perturbative phase or in the soft phase, or maybe in both? In paper IV we discuss these problems, and what we can learn about the QCD vacuum from the interface between the hard and the soft phases. We study two models of interference, one where the interference play a rôle in the soft phase only, and another where the effects come into play in the hard *and* the soft phases. We are in particular interested in finding an observable where effects from interference can be detected.

The two models are compared to normal Ariadne runs, and a difference between the models is found. This signal is found in heavy quark events, and is dependent on a double tag of the initial quark directions. Therefore the signal is rather weak, but should be possible to detect (if interferences occur in Nature in the way we propose).

If it is found that interferences occur in $e^+e^- \rightarrow q\bar{q}$ this does not prove that similar effects occur at $e^+e^- \rightarrow W^+W^+ \rightarrow$ hadrons, but it is an indication that interferences can be important at LEP2. A search of interference effects is important at LEP1 where a large data sample is available, since statistics at LEP2 is a problem.

Paper V

This paper is divided into two parts. First we discuss the b quark fragmentation within the Lund string model. In the second part of the paper we study $B^0\pi$ correlations, and the possibility of using the pion charge as a tag of the B meson flavour in CP violation studies.

The “left-right” symmetric splitting function within the Lund string model gives too hard heavy meson distributions, and in consequence too low multiplicity in $b\bar{b}$ events. Experimental groups have instead used the Peterson *et al.* function for the heavy quark frag-

mentation, combined with the symmetric Lund splitting function for the remainder of the string.

In this paper we make a comparison between different fragmentation models implemented in the Jetset MC. An optimization of the different models is done in order to retain experimental data. We find that the best results are obtained when we use the Bowler-Morris imposed modification to the splitting function in the Lund model. The modification gives a softer B meson energy spectrum, the observed multiplicity difference between uds and b events at LEP1, and a smooth rapidity distribution for particles irrespective to flavour and rank in the string. Such a smooth distribution is also expected from PQCD assuming LPHD or cluster fragmentation.

It is suggested that the pion charge can be used to tag the B^0 flavour in CP violation studies. The efficiency of this method is always diluted due to the tagging method. In the second part of paper V we discuss how the $B^0\pi$ correlations (and through this the efficiency of the flavour tag) are affected by B resonance production, and by flavour correlations between neighbouring $q\bar{q}$ pairs produced in the Lund string fragmentation. The dilution (efficiency) of the tagging method is also calculated as a function of the $B\pi$ invariant mass.

The OPAL Collaboration has made a $B^+\pi$ correlation study, and calculate the efficiency of the proposed tagging method. From iso-spin invariance the $B^+\pi$ correlations are related to $B^0\pi$ correlations, and we can compare the OPAL measurement with our results. We find that MC simulations with tensor meson production agree well with the OPAL measurement.

Paper VI

Paper VI is the only work in this thesis not dependent on Monte Carlo simulations. In this work we have written a computer program which can be used to calculate the group theoretical (colour) factor of QCD Feynman diagrams. The program, and the description on how to use the program, have no new scientific results, but give the user a possibility to calculate, and ask about, non trivial colour factors of QCD diagrams, e.g. calculate how the interaction probability between two gluons depends on their common colour state. An introduction on how to obtain these non trivial results is given.

A similar computer program was published in 1988, but is dependent of a commercially available program package [5]. Another difference is that we also present ideas on how to use the programs for other than trivial calculations. The authors of [5] have also implemented their algorithm into the freely available program CompHEP [6], but this program can only handle tree level diagrams and is optimized for other purposes than calculating colour factors.

Acknowledgments

I want to express my warm gratitude to my supervisor Gösta Gustafson for guidance. I also want to thank the people at the Department of Theoretical Physics for interacting with me. Finally, I will make up for all laundry, dishing and dinners at home, thanks Ivet.

References

- [1] The ALEPH Collaboration, *CERN-PPE/96-04*, Submitted to *Phys. Lett. B*
- [2] The OPAL Collaboration, *Z. Phys. C67* 203 (1995)
- [3] Physics at LEP2, Editors G. Altarelli, T. Sjöstrand, and F. Zwirner, CERN/96-01
- [4] Work in progress
- [5] A.P. Kryukov, and A.Ya. Rodionov, *Comp. Phys. Comm.* **48** 327 (1988)
- [6] E.E.Boos *et al.* , CompHEP, Specialized package for automatic calculations of elementary particle decays and collisions, preprint HEP-PH/9503280, SNUTP 94-116, INP MSU-94-36/358

Paper I

Λ -polarization in e^+e^- -annihilation at the Z^0 -pole

Gösta Gustafson¹, Jari Häkkinen²
Department of Theoretical Physics,
University of Lund
Sölvegatan 14A,
S-22362 Lund, Sweden

Published in
Phys. Lett. **B303** 350 (1993)

Abstract:

Strange quarks produced in e^+e^- -annihilation at the Z^0 -pole are very strongly polarized. To study to which extent this polarization is transferred to the observable hadrons would give interesting information on the hadronization mechanism. Λ -particles produced with relatively large x -values are expected to frequently contain an originally produced s -quark. We estimate that Λ -particles with $x > 0.3$ should have a longitudinal polarization of about 30%.

¹E-mail: gosta@thep.lu.se

²E-mail: jari@thep.lu.se

Strange quarks produced in e^+e^- -annihilation at the Z^0 -pole are very strongly polarized. This is a result of interference between the vector and axial vector couplings in the standard model for electro weak interaction. To study to which extent this polarization is transferred to the observable hadrons would give interesting information on the hadronization mechanism.

In hadronic reactions strange particles often show polarization effects transversely to the scattering plane [1]. The polarization is most easily observed experimentally in Λ -particles, which are easy to identify and have a particularly large decay asymmetry. In the non-relativistic quark model a Λ -particle consists of a strange quark together with a ud quark pair with spin and iso-spin zero. Thus in this model the spin of the Λ equals the spin of the s -quark. Various models attempting to explain the polarization of Λ -particles are also generally based on the assumption that the spin of the Λ is determined by the spin of the s -quark [2].

Fast Λ -particles in e^+e^- -annihilation are expected to often contain an initial s -quark, produced at the electro weak vertex, together with an ud spin 0 diquark system produced in the hadronization process. Consequently these Λ 's are expected to reveal the longitudinal polarization of the initial s -quark. In this note we attempt to estimate how much this polarization effect is diluted because many Λ contain s -quarks which are produced in the hadronization process or are the decay products of heavier resonances.

Before discussing the hadronization process we first want to study the polarization of the initial s -quark. At the Z^0 -pole we can neglect the contribution from an intermediate photon. In the standard electro weak theory the longitudinal polarization of the strange quarks (or charge $-\frac{1}{3}$ quarks in general) is given by the following expression, valid for unpolarized electron and positron beams (see e.g. ref [3])

$$P = \frac{a(1 + \cos^2 \theta) + b \cos \theta}{c(1 + \cos^2 \theta) + d \cos \theta}. \quad (1)$$

$$\begin{aligned} a &= -2(v_e^2 + a_e^2)v_d a_d & v_e &= -1 + 4 \sin^2 \theta_W \\ b &= -4v_e a_e (v_d^2 + a_d^2) & a_e &= -1 \\ c &= (v_e^2 + a_e^2)(v_d^2 + a_d^2) & v_d &= -1 + \frac{4}{3} \sin^2 \theta_W \\ d &= 8v_e a_e v_d a_d & a_d &= -1 \end{aligned}$$

Here θ is the CMS angle between the electron and the s -quark and v_e, a_e, v_d, a_d are the vector and axial vector couplings of the electron and a down-type quark.

Because $\sin^2 \theta_W$ is close to $\frac{1}{4}$ the polarization is only slowly varying with the angle θ . For $\sin^2 \theta_W = \frac{1}{4}$ we would have obtained $b = d = 0$ and

$$P = \frac{a}{c} = -2 \frac{a_d v_d}{a_d^2 + v_d^2} = -\frac{12}{13} \approx -0.92 \quad (\sin^2 \theta_W = \frac{1}{4}) \quad (2)$$

For the real value $\sin^2 \theta_W = 0.22-0.23$ the polarization is slowly varying as shown in Fig 1. The angular variation of the unpolarized cross section is determined by the expression

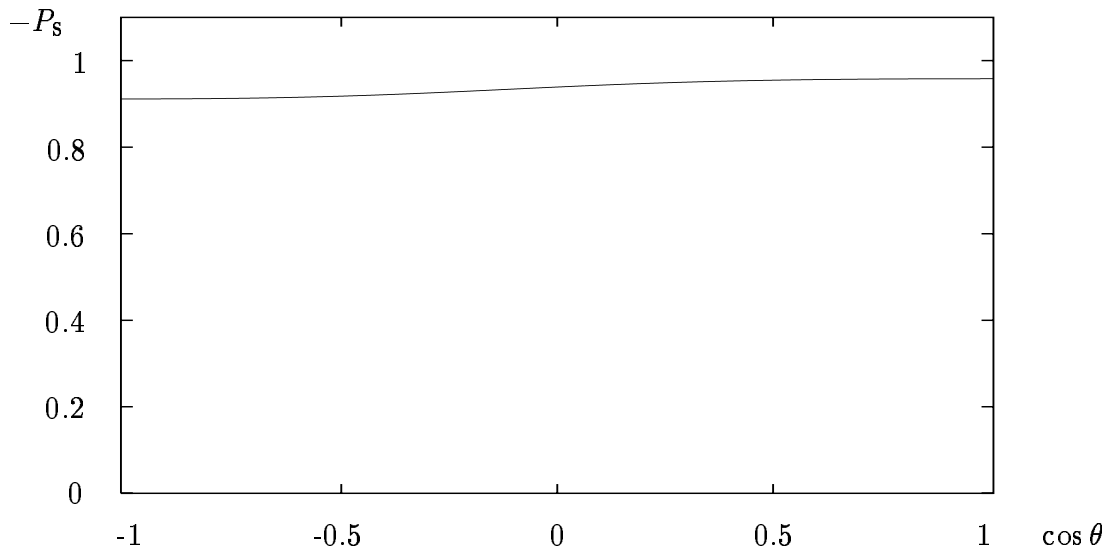


Figure 1: Polarization of the s-quark as a function of $\cos \theta$

$\sigma^0 = c(1 + \cos^2 \theta) + d \cos \theta$ in the denominator of Eq (1). Thus the polarization weighted by the cross section, $\langle P \rangle$, is also given by the same ratio $\frac{a}{c}$:

$$\langle P \rangle = \frac{\int P \sigma^0 d(\cos \theta)}{\int \sigma^0 d(\cos \theta)} = \frac{a}{c} \approx -0.94 \quad (\sin^2 \theta_W \approx 0.225) \quad (3)$$

Our conclusions are that the polarization of the s-quarks is varying very little with the angle θ , and the average polarization is approximately 94%. Of course the \bar{s} -quarks have the same degree of polarization, however with *opposite* helicity.

We now want to study how the polarization of the s-quarks is reflected in the polarization of Λ -particles. We will use the Lund string fragmentation model [4], implemented in the JETSET MC program [5], to estimate the contributions to Λ -production from different sources. The model parameters are adjusted to fit the experimental data on strange baryon production from OPAL [6].

We distinguish between directly produced Λ 's and Λ 's which are decay products of heavier resonances, and we also distinguish between Λ 's which contain an initial strange quark and those which contain an s-quark produced in the hadronization process. To estimate the polarization in these different categories we use the following assumptions:

- i) As mentioned above strange baryons produced in high energy reactions show strong polarization effects transversely to the scattering plane. There are however very little polarization in the longitudinal direction. For this reason we assume that quarks produced in the hadronization process are only very weakly polarized longitudinally.
- ii) If the Λ contains an initially produced u- or d-quark, this quark is part of a spin 0 ud quark pair. Therefore we assume that the initial polarization of this u- or d-quark is lost in the formation of the Λ .

- iii) Because the ud pair in a Λ has spin 0, the Λ spin is determined by the s-quark spin. Thus a directly produced Λ , which contains an initial s-quark, ought to be polarized in the same way as the strange quark.
- iv) Some Λ 's contain an initial s-quark but are decay products of heavier resonances. These Λ -particles are assumed to inherit part of their parent's polarization. We assume again that the polarization of the parent is determined by the initial s-quark, while those quarks of the parent, which are produced in the hadronization process, are not longitudinally polarized.

From these assumptions follows that the polarization of the Λ should be negligible if it does not contain an initially produced s-quark. If it, however, does contain an initial s-quark the polarization depends on the type of parent in the following way:

Directly produced Λ : For these Λ 's we have

$$P_\Lambda = P_s \quad (4)$$

where P_Λ and P_s are the polarization of the Λ -particles and the s-quarks respectively.

$\Sigma^0 \rightarrow \Lambda\gamma$: The ud quark pair in Σ^0 has iso spin and spin 1. Thus in the non-relativistic quark model we have $P_{\Sigma^0} = -\frac{1}{3}P_s$. In the electro-magnetic decay $\Sigma^0 \rightarrow \Lambda\gamma$, the spin-iso-spin 1 ud-diquark is changed to a spin-iso-spin 0 ud-diquark. In the simple quark model the s-quark is not affected by this process, which implies that

$$P_\Lambda \approx -\frac{1}{3}P_{\Sigma^0} = +\frac{1}{9}P_s. \quad (5)$$

$\Sigma(1385) \rightarrow \Lambda\pi$: $\Sigma(1385)$ has spin $\frac{3}{2}$, and if the non strange diquark is randomly polarized we will get $P_{\Sigma(1385)} = \frac{5}{9}P_s$. In the P-wave decay to $\Lambda\pi$ the Λ will get the same polarization as the parent $\Sigma(1385)$. Thus we find

$$P_\Lambda = P_{\Sigma(1385)} = \frac{5}{9}P_s. \quad (6)$$

$\Xi \rightarrow \Lambda\pi$: The quark model wave function of the Ξ implies that $P_\Xi = \frac{2}{3}P_s$. The parity non-conserving decay into a $\Lambda\pi$ system is dominantly an S-wave decay. Averaged over decay angles the Λ polarization is given by $P_\Lambda = (\frac{1}{3} + \frac{2}{3}\gamma)P_\Xi$, where $\gamma \approx 0.87$ [7]. Consequently

$$P_\Lambda \approx 0.9P_\Xi = 0.6P_s. \quad (7)$$

$\Xi(1530) \rightarrow \Xi\pi \rightarrow \Lambda\pi\pi$: In the same way as for $\Sigma(1385)$ we find $P_\Xi = P_{\Xi(1530)} = \frac{5}{9}P_s$. From $P_\Lambda \approx 0.9P_\Xi$ then follows

$$P_\Lambda \approx 0.9\frac{5}{9}P_s = 0.5P_s. \quad (8)$$

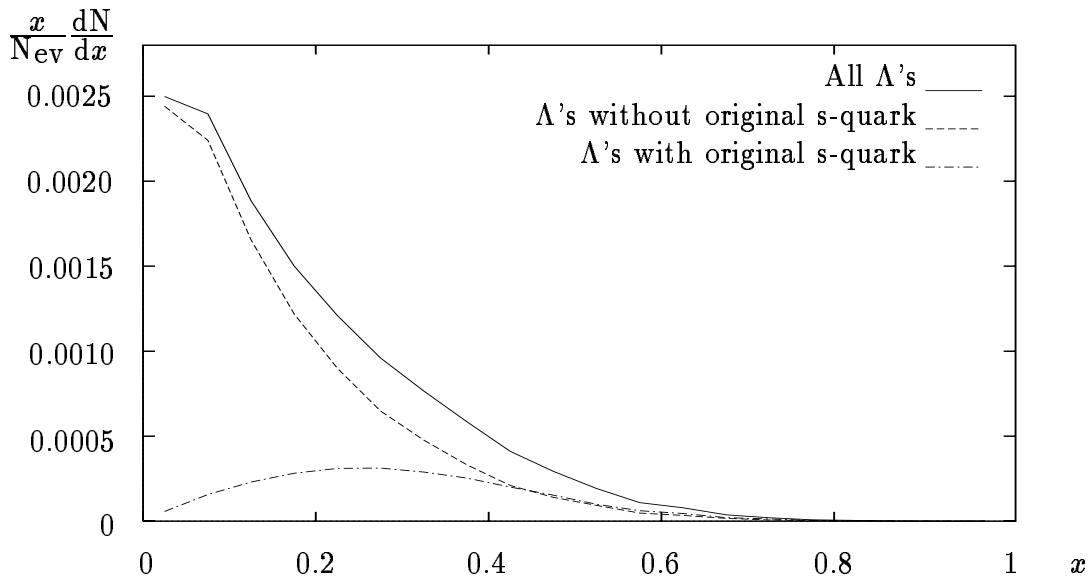


Figure 2: The contributions to the production of Λ 's

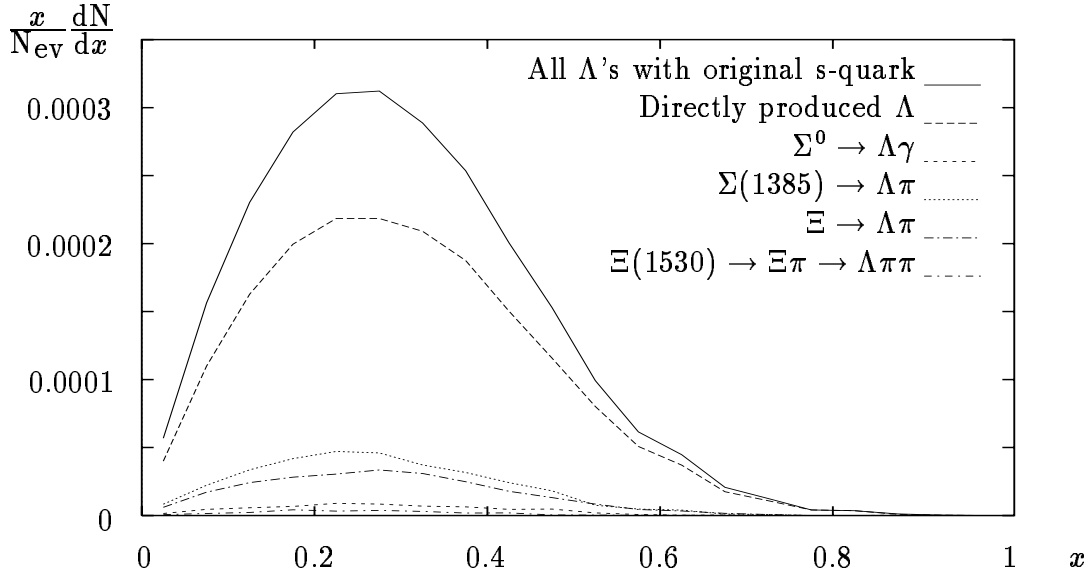


Figure 3: The contributions to the production of Λ 's containing an initial s-quark

The contributions from other possible decays, $\Sigma(1385) \rightarrow \Sigma^0 \pi \rightarrow \Lambda \gamma \pi$, $\Omega^- \rightarrow \Lambda K^-$, and $\Omega^- \rightarrow \Xi^- \pi \rightarrow \Lambda \pi \pi$ give very small contributions which can be neglected.

The contributions to the Λ -production from the different sources are shown in Fig 2 and Fig 3. In Fig 2 we show the contributions to the production from Λ 's with and without the original s-quark, together with the total yield of Λ 's. Fig 3 shows how the Λ 's, which do contain an initial s-quark, can be separated into contributions from directly produced Λ 's and decay products from different baryon resonances. We see that the probability that the Λ contains an initial s-quark is relatively large for $x > 0.3$, but, as expected, rapidly decreasing for smaller x -values. (We note that the largest resonance contribution comes from $\Sigma(1385)$). For this reason we have used the hadronization parameter set, determined by the OPAL

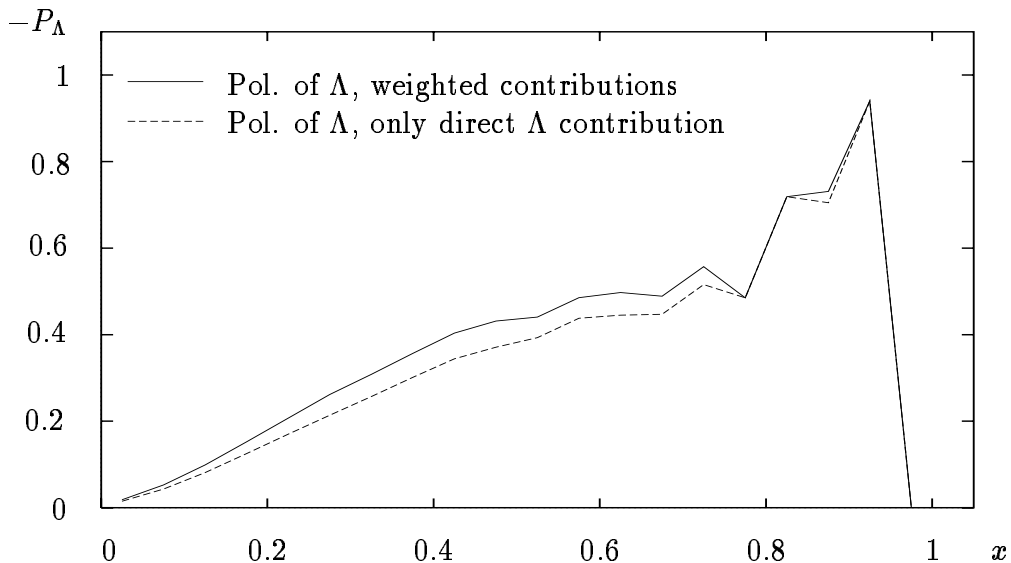


Figure 4: Expected longitudinal polarization of Λ as a function of x

Collab., which fits the $\Sigma(1385)$ production [6].)

The polarization expected is shown in Fig 4. The dashed curve is the fraction of the Λ 's, which is directly produced with an initial s-quark, multiplied with the factor 0.94, corresponding to the s-quark polarization. The solid line is the result after adding the contribution from resonance decays in accordance with Eqs (5-8). We see that this only gives a small correction. A minor dilution of the polarization of the direct Λ 's may be expected from the hadronization process. We also note that with default values for the hadronization parameters, the polarization would be decreased by about 0.07 units. This is due to a smaller fraction of directly produced Λ 's and a larger production of strange baryon resonances.

Our conclusion is that the estimated longitudinal Λ -polarization is about 25-30% for $x > 0.3$. (Note that for larger x -values, where the polarization is larger, the rate is also rapidly decreasing.) In $\frac{1}{4}$ million events we expect (with 100% detection efficiency) about 3000 Λ or $\bar{\Lambda}$ in this x -range, which should be sufficient for a determination of the polarization with a statistical uncertainty of about 0.05. This estimate is based on the non-relativistic quark model, and to see whether it agrees or disagrees with experimental results will give interesting information on the hadronization process. We also note that, given enough statistics, it would be interesting to study how the polarization varies off the Z^0 -pole due to Z^0 - γ interference.

Acknowledgement

We want to thank prof B Andersson and dr P Mättig (who draw our attention to this problem) for valuable discussions.

References

- [1] See e.g. K. Heller, Proceedings of the 9th International Symposium on High Energy Spin Physics, Bonn, Germany, 6-15 Sept. 1990. p97-105
- [2] B. Andersson, G. Gustafson, and G. Ingelman, *Phys. Lett.* **85B** (1979) 417
T. DeGrand and H. Miettinen, *Phys. Rev.* **D24** (1981) 2419
J. Swed, *Phys. Lett.* **105B** (1981) 403
- [3] J.E. Augustin and F.M. Renard, Proceedings of the LEP summer study, CERN 79-01, Vol 1 (1979) p185-199
- [4] B. Andersson, G. Gustafson, G. Ingelman, and T. Sjöstrand, *Phys. Rep.* **97** (1983) 31
- [5] T. Sjöstrand, *Comp. Phys. Comm.* **39** (1986) 347
T. Sjöstrand and M. Bengtsson; *ibidem* **43** (1987) 367
- [6] OPAL Collab., P.D. Acton *et al.*, *Phys. Lett.* **291B** (1992) 503
- [7] Particle Data Group, "Review of particle properties", *Phys. Rev.* **D45** (1992)

Paper II

Deuteron production in e^+e^- -annihilation

Gösta Gustafson¹, Jari Häkkinen²
Department of Theoretical Physics,
University of Lund
Sölvegatan 14A,
S-22362 Lund, Sweden

Published in
Z. Phys. **C61** 683 (1994)

Abstract:

We argue that in e^+e^- -annihilation (including Υ -decay) deuteron production should be given by the overlap of the deuteron wave function with the wave function of a pn-pair. The production rate depends sensitively upon the size of the production region. Taking into account the strong correlation between protons and neutrons, experimental results for Υ -decay are consistent with the size expected in the Lund string fragmentation model. A prediction is given for the deuteron production in Z -decay.

¹E-mail: gosta@thep.lu.se

²E-mail: jari@thep.lu.se

1 Introduction

The Argus Collab. at Doris has observed a relatively sizable production of (anti-)deuterons in the decay of Υ [1]. The production rate has been compared to the production of deuterons in nucleus collisions. For this latter situation different models have been proposed. It has been suggested that deuterons are formed in the collisions between protons and neutrons [2]. It has also been proposed that the production can be described as a coalescence process, and the production rate can be determined from the overlap between the wave functions for a proton and a neutron with the wave function of a deuteron [3, 4]. This overlap depends not only on the deuteron wave function, thereby on its binding energy, but also on the interaction volume.

If the overlap is dominated by situations where $\vec{p}_p \approx \vec{p}_n \approx \vec{p}_d/2$ we get the following relation with some constant C

$$\frac{E}{\sigma_{\text{tot}}} \frac{d^3\sigma(d)}{d^3p} = C \frac{E_p E_n}{\sigma_{\text{tot}}} \frac{d^6\sigma(p,n)}{d^3p_p d^3p_n} = C \frac{m_p}{8} \frac{E}{\sigma_{\text{tot}}} \frac{d^6\sigma}{d^3p d^3k} \Big|_{\vec{k}=\vec{0}} \quad (1)$$

Here $\vec{p} \equiv \vec{p}_d/2 \approx \vec{p}_p \approx \vec{p}_n$, $E \equiv E_d/2 \approx E_p \approx E_n$ and

$$\vec{k} = \frac{\vec{p}_p - \vec{p}_n}{2} \Big|_{\text{pn-cms}} \quad (2)$$

is the pn relative momentum in the pn cms. In a simulation process the number of deuterons corresponds to the number of pn-pairs with $|\vec{k}| < k_{\text{cut}}$, where

$$C \frac{m_p}{8} = \frac{4\pi}{3} k_{\text{cut}}^3 \quad (3)$$

If the proton and neutron distributions are equal and *uncorrelated*, this can be written as

$$\frac{E}{\sigma_{\text{tot}}} \frac{d^3\sigma(d)}{d^3p} = C \left(\frac{E}{\sigma_{\text{tot}}} \frac{d^3\sigma(p)}{d^3p} \right)^2 \quad (4)$$

The constant C depends on the deuteron wave function and the size of the interaction volume. With the notation $C = \frac{4\pi}{3} p_0^3 / m_p$ ($p_0 = 2k_{\text{cut}}$) the observed deuteron production rate in nucleus collisions is obtained for $p_0 \approx 130\text{MeV}$ [5].

Applied to Υ decay, with the same value of C (corresponding to $p_0 = 130\text{MeV}$), Eq (4) predicts roughly the observed number of deuterons. Ref [1] finds that the prediction is about a factor 2/3 times the experimental value, but the predicted energy distribution is somewhat too hard, with too many deuterons with high energy and too few with low energy.

In this article we want to

- i) argue that in e^+e^- -annihilation reactions (including Υ decay) the deuteron production should indeed be given by the overlap of the deuteron wave function, provided the nucleon distributions are determined by a model, which does not take the attractive pn potential into account.

- ii) demonstrate that a careful analysis, including the correlation between protons and neutrons, reproduces the observed energy distribution. The observed rate is consistent with estimates of the interaction volume based on the Lund string fragmentation model.
- iii) make predictions for deuteron production in e^+e^- -annihilation into $q\bar{q}$ -pairs, e.g. at LEP.

2 Wave function overlap

In an e^+e^- -annihilation event a $q\bar{q}$ or $3g$ system is transformed into hadrons. This transformation is determined by the Hamiltonian

$$H = H_0 + H_I \quad (5)$$

where H_I describes an attractive force between a proton and a neutron with a deuteron bound state, and H_0 describes the remaining strong interaction. We assume that the final state interaction H_I can be treated as a perturbation.

Thus H_0 describes the transition to hadronic states (denoted Ψ_k) containing free protons and neutrons. A model for this transition is given by the Lund fragmentation model [6]. The full Hamiltonian H gives transitions to states Ψ'_i , which contain deuterons as well as pn states in the continuum, orthogonal to the deuteron wave function. To the lowest order in a perturbation expansion the probability to obtain a definite state Ψ'_i is in this case simply given by the overlap with the unperturbed states Ψ_k .

We note that this case is different from the (more complicated) situation in nucleus collisions, where the initial state is an eigenstate to the full Hamiltonian H , i.e. a state of type Ψ'_i . If this state contains an unbound pn-pair, the wave function for this pair is orthogonal to that of a deuteron. Thus such a pair can be transformed into a deuteron only by the interaction with some other particle.

The overlap with the deuteron wave function is estimated in ref [4]. Here we will use a different formalism, but our results are very similar. The binding energy of the deuteron is small and therefore the wave function is quite extended. To get an intuitive feeling for the result we first study the situation when the range of the attractive potential is very small compared to the extension of the wave function. Results from a more accurate calculation will be presented afterwards.

Separating the cms motion and the relative motion we introduce the variables $\vec{r} = \vec{r}_p - \vec{r}_n$ and $\vec{k} = (\vec{p}_p - \vec{p}_n)/2$ (from Eq (2)) as measured in the pn cms. The approximate deuteron wave function has the following form

$$\Psi_d(r) \approx N \frac{e^{-\kappa r}}{r} \quad (6)$$

$$\kappa = \sqrt{m_p \mathcal{E}}; \quad N = \sqrt{\frac{\kappa}{2\pi}}$$

Here \mathcal{E} is the deuteron binding energy and the reduced mass equals $m_p/2$. For the free pn-pair we could imagine a plane wave ansatz

$$\Psi_{\text{pn}} = \frac{1}{\sqrt{V}} e^{i\vec{k}\vec{r}} \quad (7)$$

where V is the quantization volume. The square of the overlap is then

$$A(k) = |\langle \Psi_{\text{d}} | \Psi_{\text{pn}} \rangle|^2 = \frac{8\pi\kappa}{V} \frac{1}{(\kappa^2 + k^2)^2} \quad (8)$$

This expression falls off rapidly with increasing momentum k , and the probability for a pn-pair to join into a deuteron is large only for $k \lesssim \kappa$. If the production cross section is approximately constant within this region the result in Eq (1) is justified, and we obtain

$$C \frac{m_p}{8} = \frac{3}{4} \int A(k) d^3k = \frac{3(2\pi)^3}{4V} \quad (9)$$

The factor $3/4$ is a spin factor representing the probability to form a total spin 1 state.

This result depends on the quantization volume, which indicates that it is sensitive to the production volume for the pn-pair. Therefore we replace the plane wave equation in Eq (7) by a wave package

$$\tilde{\Psi}_{\text{pn}} = \tilde{N} e^{-r^2/2\sigma^2 + i\vec{k}\vec{r}} \quad \tilde{N}^{-2} = \sigma^3 \sqrt{\pi^3} \quad (10)$$

We then get

$$C \frac{m_p}{8} = \frac{3}{4} \int |\langle \tilde{\Psi}_{\text{pn}} | \Psi_{\text{d}} \rangle|^2 d^3k = 6\sqrt{\pi} \kappa \sigma^{-2} e^{\kappa^2 \sigma^2} \text{erfc}(\kappa/\sigma) \approx \frac{6\sqrt{\pi} \kappa \sigma^{-2}}{\kappa \sigma \ll 1} \quad (11)$$

Here erfc is an error function and the last approximation is obtained when κ is small compared to σ^{-1} . Expressed in the variable k_{cut} or p_0 , defined above, this approximation implies

$$(2k_{\text{cut}})^3 = p_0^3 = \frac{36}{\sqrt{\pi}} \kappa \sigma^{-2} \quad (12)$$

To improve this approximate result we replace the wave function in Eq (6) by a wave function corresponding to a square well potential with radius $R = 1.7$ fm and depth $V_0 = 36.4$ MeV. This function has the form

$$\Psi_{\text{d}} = \begin{cases} N_1 \frac{\sin k' r}{r} & r < R & k' = \sqrt{m_p(V_0 - \mathcal{E})} \\ N_2 \frac{e^{-\kappa r}}{r} & r > R & \kappa = \sqrt{m_p \mathcal{E}} \end{cases} \quad (13)$$

The overlap with the wave package in Eq (10) is calculated numerically, and the result is shown in Fig 1. We have also studied a different wave package, with separate production points for the nucleons

$$\tilde{\Psi}'_{\text{pn}} = N' e^{-(\vec{r}-\vec{\mu})^2/2\sigma^2 + i\vec{k}\vec{r}} \quad (14)$$

It turns out that the result is very similar to that in Fig 1 if only σ^2 is replaced by $\sigma^2 + \mu^2$.

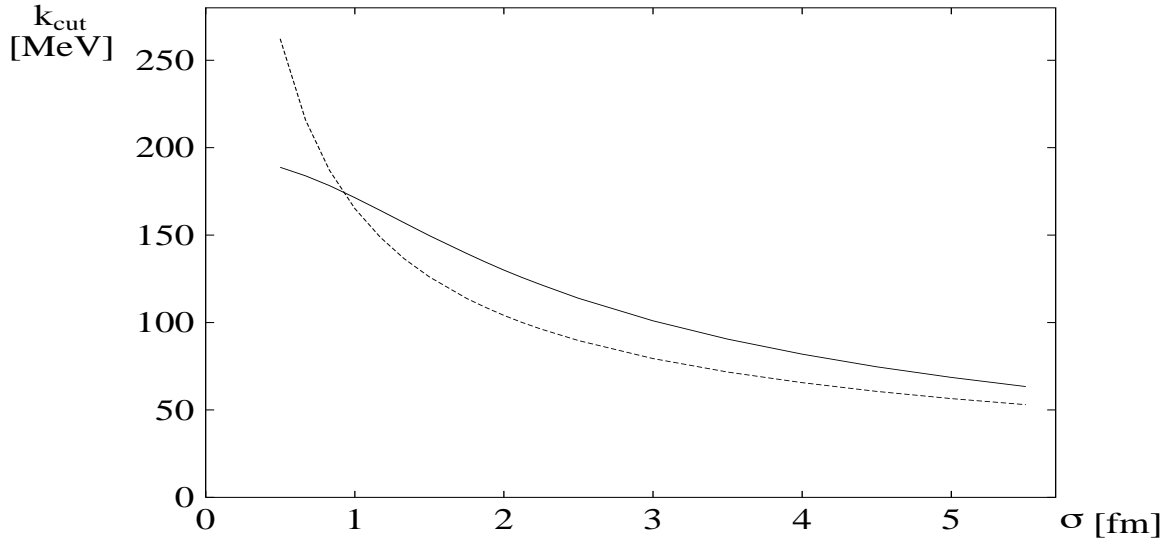


Figure 1: Wave function overlap expressed in the parameter k_{cut} as a function of the size σ of the production region. The solid line corresponds to the wave function in Eq (13), and the dashed line to the approximation in Eq (12). Note that the production probability is proportional to k_{cut}^3 .

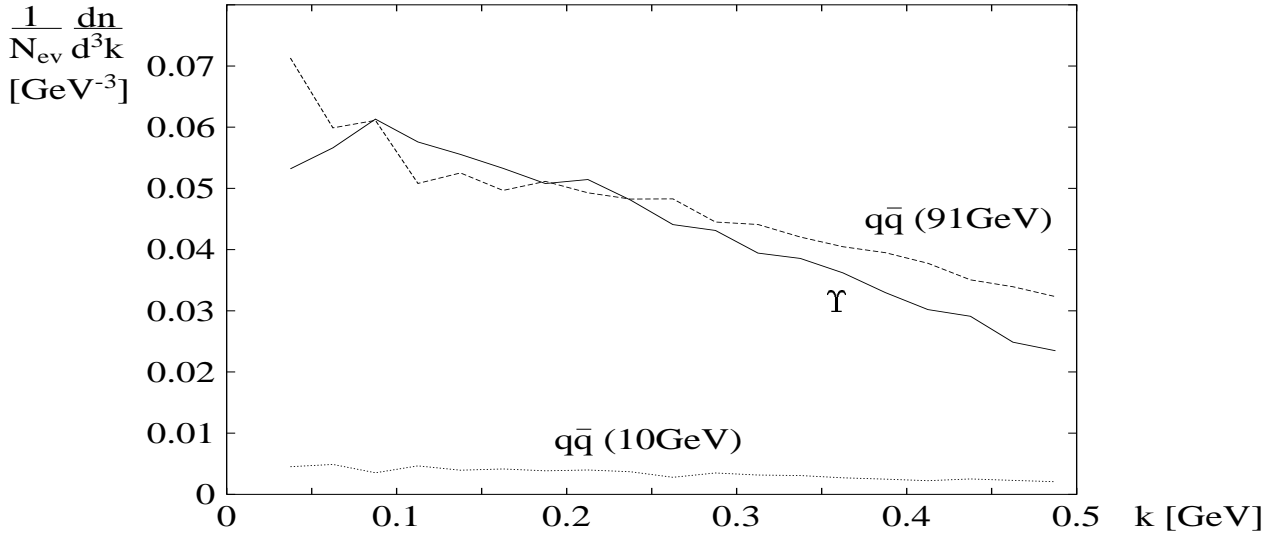


Figure 2: Distribution of pn pairs as a function of the relative momentum k . (Included nucleons are either directly produced or Δ -decay products). Results are shown for Υ -decay (solid line), $q\bar{q}$ continuum at 10 GeV (dotted line), and Z -decay (dashed line).

3 Correlations and resonances

To take into account the pn -correlations and the effect of resonances we simulate events with the Lund fragmentation model as implemented in the JETSET MC [7]. We have first checked that the distribution in \vec{k} is almost constant for $k \lesssim 200\text{MeV}$. This is demonstrated in Fig 2. The result implies that only the integral over the overlap, $\int A(k)d^3k$, is important

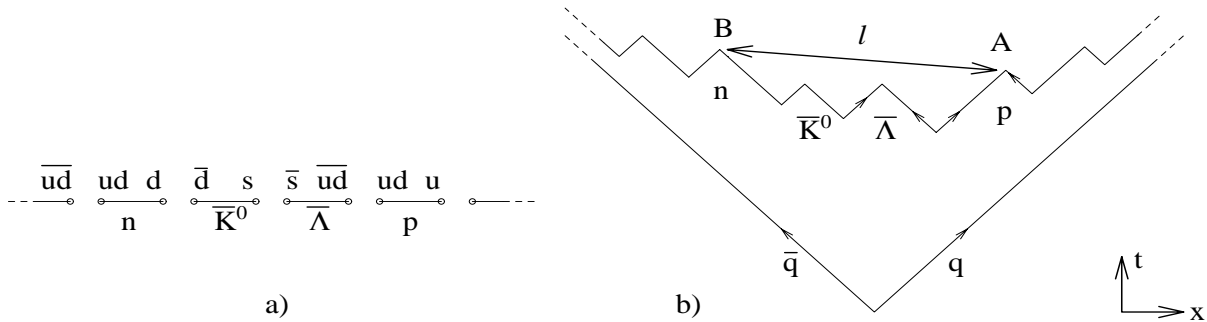


Figure 3: a) Possible string breakup process with a pn pair. b) Space-time structure of the breakup.

and that the cross section is given by Eqs (1) and (9).

When estimating the number of pn pairs, which can combine to form a deuteron, it is important to note that not all nucleons are directly produced in the hadronization process. Thus nucleons from the decay of strange baryons with very long lifetimes, are not expected to be able to form deuterons. For Δ -resonances the lifetime is so short that a decay product should have a possibility to join another nucleon into a deuteron, although with a larger production region.

In our simulations we have found that for 24% of the pn pairs both nucleons are directly produced. For 38% at least one nucleon is a Δ -decay product, and the other nucleon is either directly produced or also a Δ -decay product. (In most of these pairs the other nucleon is directly produced, and in only 1/4 of them both nucleons originate from Δ -particles.) For the remaining 38% at least one nucleon is a decay product of a strange baryon. In most of these pairs, 30% of the total number, at least one nucleon comes from a Λ . These fractions are practically independent of the total energy of the pair. We note that only in a relatively small fraction of the pn pairs both nucleons are directly produced.

To evaluate the number of deuterons we must first estimate the production volume for the pn pairs. In string fragmentation particles, which are close in momentum space, are also produced close in coordinate space. Thus it is possible to understand that the pion pair production region, obtained in HBT-analyses, is of the order of 1 fm, also at high energies when the string length may be tenths of fm or more. For pn pairs the production volume must be somewhat larger than for pions, because nucleons are more massive, and when the string breaks there must be at least one anti-baryon between the proton and the neutron. A typical example is shown in Fig 3. A space-time diagram for the string motion and breakup is shown in Fig 3b.

It is not obvious how to define the production points for the different hadrons. The simplest alternative is the point where the constituents meet for the first time. This corresponds to the points A and B in Fig 3b, for the proton and the neutron respectively. We have used the MC to calculate the distribution in the invariant distance, l , between these points for a straight string. Fig 4 shows the result for pairs with a small relative momentum

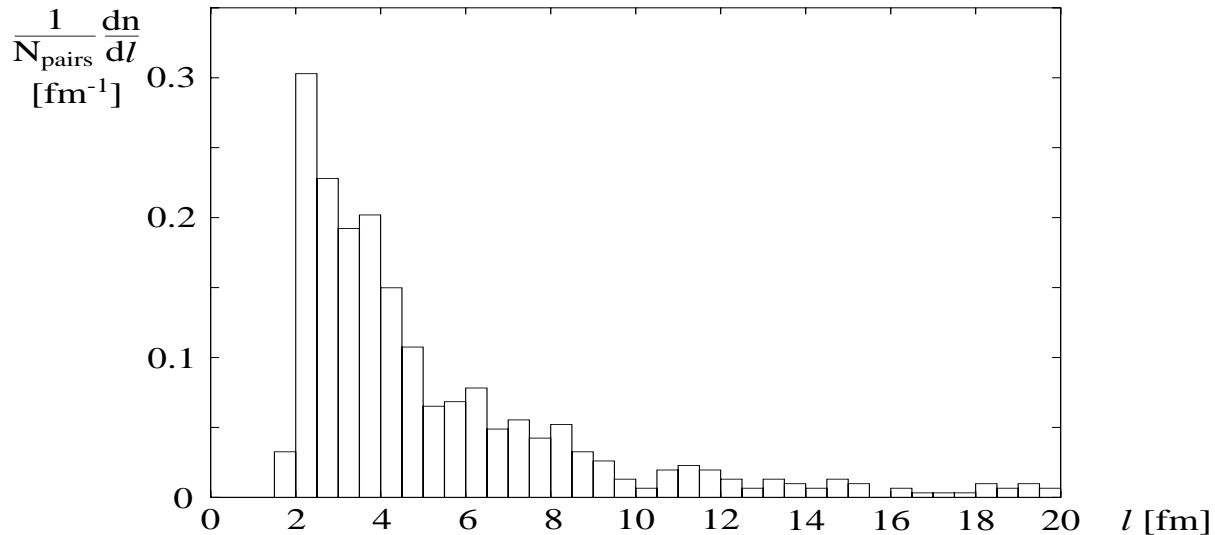


Figure 4: *Distribution in invariant distance between the production points for pn pairs with low relative momentum. (For 5% of the pairs the distance is larger than 20fm.)*

($k < 150\text{MeV}$). (In this figure only directly produced nucleons are included). We note that there is a large peak around 3fm, with a rather limited tail stretching to large volumes, and very few pairs below 2fm. The result presented corresponds to 91GeV, which implies that the maximum distance is 91fm (we assume a string tension $\kappa = 1\text{GeV}/\text{fm}$). As there are very few pairs with low relative momentum which have distances larger than 15fm, we see that these results essentially also correspond to an infinitely long string.

The situation in Υ -decay does not correspond to an infinitely long string. In the Lund string model it is represented by a closed string, which is stretched out by the three gluons to a triangular shape. In view of the difficulties to define the production points in an unambiguous way, we have not found it meaningful to perform a complicated simulation calculating the location of the production points for such a triangular string. For a closed string with total energy 10GeV the maximum distance is 5fm. Thus the large distance tail in Fig 4 is not relevant for the Υ -decay, and we think that a reasonable estimate for the average distance between the production points is around 3fm.

The Δ -resonance has a lifetime of 1.7fm. If this is added in quadrature to an original distance of $\sim 3\text{fm}$ it will increase the distance by about 0.5fm.

4 Results

4.1 Υ -decay

The experimental results for deuteron production in ref [1] are well reproduced with σ about 3fm. In Fig 5 we have presented results from MC simulations obtained using $\sigma = 3.5\text{fm}$ for directly produced pn pairs and $\sigma = 4\text{fm}$ when one nucleon comes from a Δ -decay and the other is either directly produced or another Δ -decay product. According to Fig 1 these

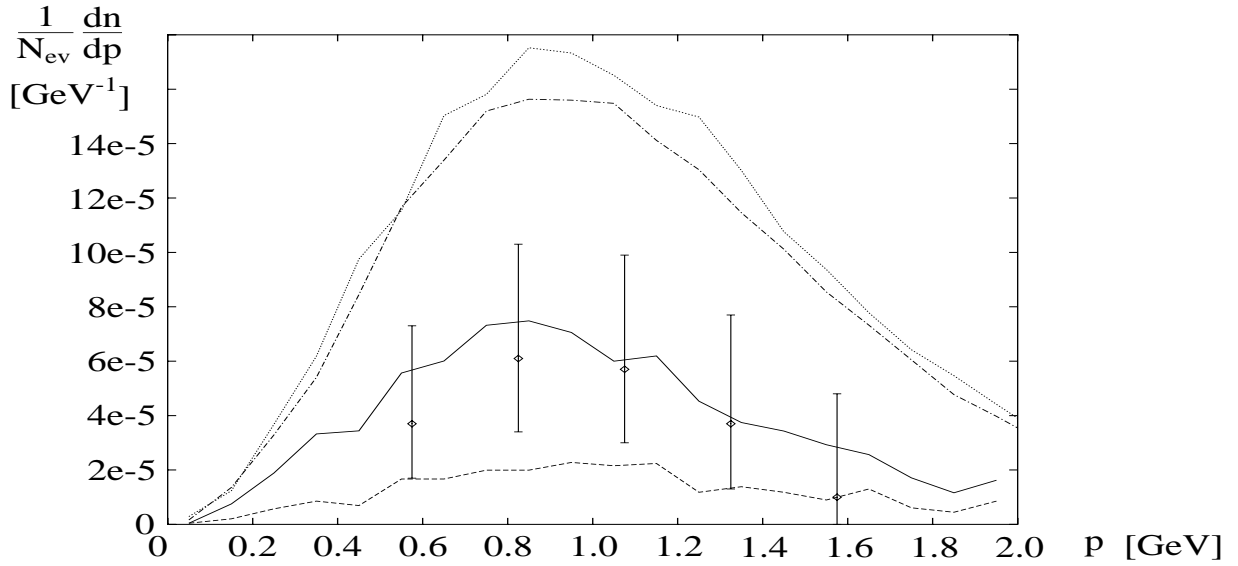


Figure 5: *The momentum distribution for deuterons in Υ -decay. The solid line is the result including directly produced nucleons and Δ -decay products as described in the text. The dashed line corresponds to only directly produced nucleons. The other curves are the results from Eq (4) assuming uncorrelated nucleons, including only direct nucleons and Δ -decays (dashed-dotted line) and including also strange baryons other than Λ (dotted line).*

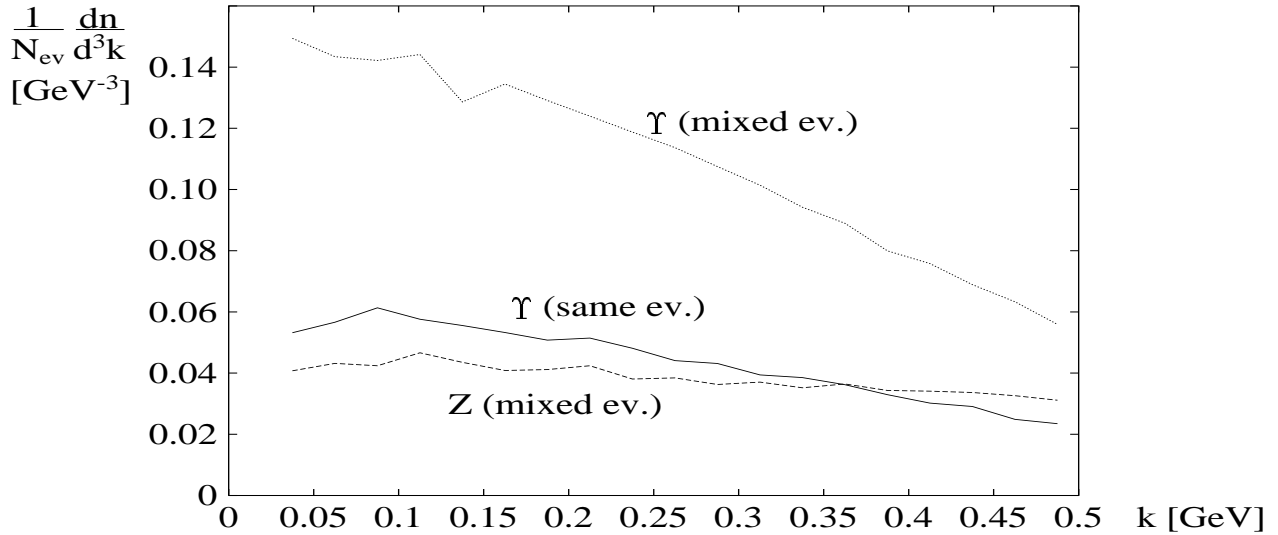


Figure 6: *Distribution in relative momentum k of pn pairs, where the nucleons in the pair are taken from different events. The dotted line is for Υ -decay, and the dashed line is for Z -decay. For comparison the solid line shows the distribution for correlated pairs in Υ -decay from Fig 2.*

values correspond to $k_{\text{cut}} = 90\text{MeV}$ and $k_{\text{cut}} = 82\text{MeV}$ respectively. We note that also σ -values as low as 2.8 and 3.3, instead of 3.5 and 4, would give results within the experimental errors.

In Fig 5 is also shown results obtained if the nucleons in a pair were uncorrelated, which

corresponds to Eq (4). If we do not include nucleons from strange baryon decays and use an average value of k_{cut} (86MeV), the result is about a factor 2.5 larger. This shows that the nucleons are strongly correlated. The correlation is not so much because a proton and a neutron in the same event avoid having the same momentum. They rather avoid being in the same event. This is seen in Fig 6, which shows the distribution in relative momentum, k , for pn-pairs from different events. This curve is similar in shape to the distribution in Fig 2, but the normalization is much higher. We interpret this as a consequence of the limited energy available. A proton and a neutron must be accompanied by two anti-baryons, and together these four particles would take a large part of the total Υ -energy. (If also nucleons from strange baryons other than Λ 's were included the result would be even larger, as indicated by the dotted line in Fig 5. Including also Λ -decays would increase the result by another factor of 1.5).

If the nucleons were uncorrelated we would thus need a much smaller k_{cut} -value, and hence a larger production region. In ref [1] it is pointed out that in this case a fair agreement with data is obtained for $k_{\text{cut}} = p_0/2 = 65\text{MeV}$. Not including strange baryon decays this would also be the result from our simulations. From Fig 1 we see that this corresponds to a σ -value around 5.3fm, which seems to be an unrealistically large production region.

We note that in our simulation the shape of the spectrum is rather similar if we use the approximation in Eq (4) with uncorrelated nucleons. The main difference lies in the normalization. This was not the case for the analysis in ref [1], using experimental data for proton production. The main discrepancy is however for the first bin, where the experimental uncertainty in the proton spectrum is very large.

4.2 $q\bar{q}$ continuum

In the process $e^+e^- \rightarrow q\bar{q}$ the particle density is lower than for $e^+e^- \rightarrow \Upsilon \rightarrow 3g$. Thus the production rate for deuterons is also lower. From Fig 2 we see that the number of low mass pn pairs in the $q\bar{q}$ continuum at 10GeV is only about 4% of the number at Υ . This is consistent with the upper limit in ref [1], which corresponds to $1.7 \cdot 10^{-5}$ d/event or about 25% of the production rate in Υ -decay.

At LEP energies the total particle multiplicity is larger, and therefore also the number of pn pairs. To, in an approximate way, take into account the tail in the distribution of production point distances in Fig 4, we have used the larger σ -values 4 and 4.5fm for directly produced pairs and pairs including Δ -decay. Fig 7 shows the predicted momentum distribution at 91GeV. The total production rate is $5 \cdot 10^{-5}$ deuterons per event.

In Fig 6 we also show results for pairs from mixed Z-decay events. Here we do not get a very large result using mixed events. This is a natural consequence of the pronounced jet structures in the events from Z-decays. Thus if we would like to use Eq (4) to estimate the deuteron production, the larger σ -value in Z-decay compared to Υ -decay would imply a smaller value for C or p_0 , but this is counteracted by the smaller anti-correlation (cf. Fig 6 and 2) which gives a larger value for C .

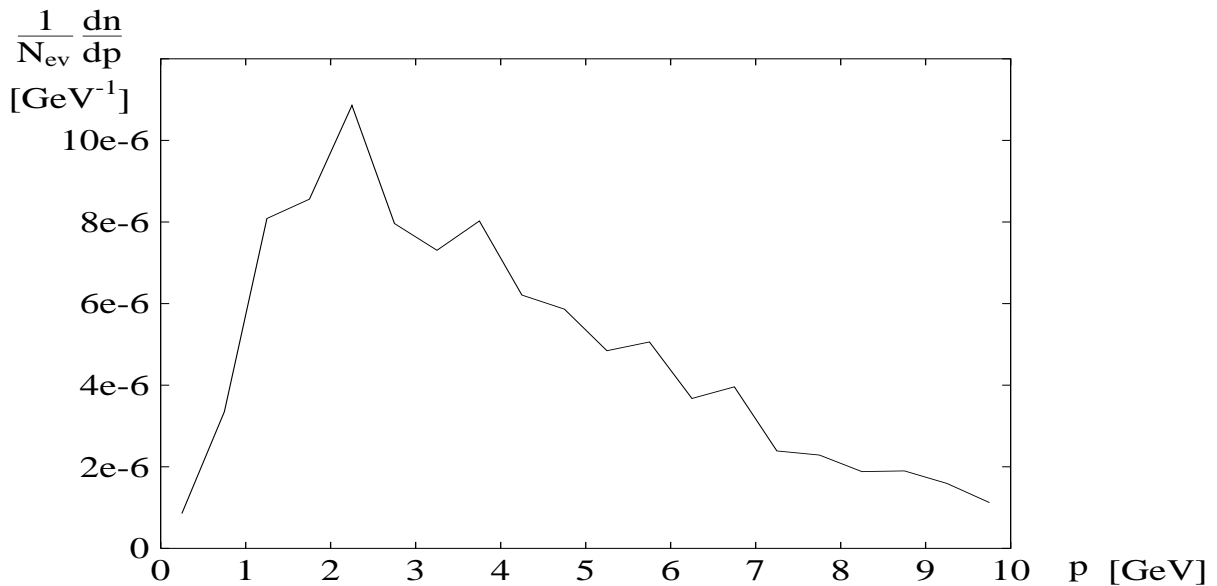


Figure 7: *The predicted momentum distribution for deuterons at 91 GeV.*

5 Conclusions

We have argued that in e^+e^- -annihilation (including Υ -decay) deuteron production should be given by the overlap of the deuteron wave function with the wave function of a pn-pair, provided the nucleon distributions are determined by a model which does not take the attractive pn potential into account. This situation is simpler than the situation in nucleus collision, for which a coalescence process has been proposed in refs [3] and [4].

When calculating the deuteron production rate it is very essential to take the pn correlations into account. Protons and neutrons are strongly anti-correlated so that the number of pn-pairs (with low invariant mass) in an Υ event is about a factor 2.5 smaller than the number obtained by mixing events.

The production rate depends on the size of the production region. The experimental results for Υ -decay from ref [1] are consistent with the size expected in the Lund string fragmentation model. (Also the momentum distribution is well reproduced by the model calculations). If the anti-correlation was not taken into account an unrealistically large production region would have been needed. We have here taken into account that nucleons from Δ -decay correspond to a larger production region, and that the lifetime of strange baryons is so long that their contributions can be neglected.

We have made a prediction for deuteron production in Z-decay. The integrated production rate corresponds to $5 \cdot 10^{-5}$ deuterons per event.

References

- [1] ARGUS Collab., H. Albrecht *et al.*, *Phys. Lett.* **236B** 102 (1990)
- [2] R. Hagedorn, *Phys. Rev. Lett.* **5** 276 (1960)
W.D. Myers, *Nucl. Phys.* **296A** 177 (1978)
J. Gosset, J.J. Kapusta, G.D. Westfall, *Phys. Rev.* **18C** 844 (1978)
- [3] S.T. Butler, C.A. Pearson, *Phys. Rev. Lett.* **7** 69 (1961)
S.T. Butler, C.A. Pearson, *Phys. Lett.* **1** 77 (1962)
A. Schwarzschild, Č. Zupančič, *Phys. Rev.* **129** 854 (1963)
- [4] H. Sato and K. Yazaki, *Phys. Lett.* **98B** 153 (1981)
- [5] H.H. Gutbrod *et al.*, *Phys. Rev. Lett.* **37** 667 (1976)
J. Gosset *et al.*, *Phys. Rev.* **16C** 629 (1977)
M.C. Lemaire *et al.*, *Phys. Lett.* **85B** 38 (1979)
V.B. Gavrilov *et al.*, *Z. Phys.* **324A** 75 (1986)
- [6] B. Andersson, G. Gustafson, G. Ingelman, and T. Sjöstrand, *Phys. Rep.* **97** 31 (1983)
- [7] T. Sjöstrand, M. Bengtsson *Comp. Phys. Comm.* **43** 367 (1987)
T. Sjöstrand, JETSET 7.3, program and manual

Paper III

Colour Interference and Confinement Effects in W-pair Production

Gösta Gustafson¹, Jari Häkkinen²
Department of Theoretical Physics,
Sölvegatan 14A,
SE-223 62 Lund, Sweden

Published in
Z. Phys. **C64** 659 (1994)

Abstract:

In the reaction $e^+e^- \rightarrow W^+W^- \rightarrow (q_1\bar{q}_2)(Q_1\bar{Q}_2)$ we expect that normally the colour singlet systems $(q_1\bar{q}_2)$ and $(Q_1\bar{Q}_2)$ hadronize independently into two hadron chains or strings. However also the pairs $(q_1\bar{Q}_2)$ and $(Q_1\bar{q}_2)$ form colour singlets with probability $1/N_c^2 = 1/9$. This probability could be further enhanced by gluon exchange. We therefore expect that the hadronization can give “recoupled” colour strings between these quark–anti-quark pairs with some small probability, and a study of this effect will give interesting information about the vacuum structure. In this paper we discuss a possible experimental signal for recoupled events and show that such events can be identified also when the effect of gluon emission before the recoupling is taken into account.

¹E-mail: gosta@thep.lu.se

²E-mail: jari@thep.lu.se

1 Introduction

At LEP2 it will be possible to study the reaction $e^+e^- \rightarrow W^+W^-$ where each of the two W 's decay into a $q\bar{q}$ system. Normally it is assumed that these two $q\bar{q}$ systems hadronize independently, thus producing two independent strings or chains of hadrons. As the lifetimes of the W 's are very short the $q\bar{q}$ systems are essentially produced on top of each other, and it is therefore conceivable that the hadronization processes interfere, and a study of this interference (or the absence of an interference) would give valuable information about the confinement mechanism and the vacuum structure. In this paper we discuss possible experimental signals of this effect.

Let us assume that the two W 's decay into quark-anti-quark pairs called $q_1\bar{q}_2$ and $Q_1\bar{Q}_2$ respectively. The W lifetime is approximately 0.1fm, which implies that the distance in space and time between the decay points, at LEP2 energies, is of the order $\Delta x \sim 0.05\text{fm}$ and $\Delta t \lesssim 0.1\text{fm}$. These values are small compared to the confinement scale. Therefore, when the quarks and anti-quarks move away from each other, how does the quark q_1 know that its partner is \bar{q}_2 , meaning that a string or a hadron chain should be formed between q_1 and \bar{q}_2 ?

It is true that the pair $q_1\bar{q}_2$ initially forms a colour singlet, but *also* $q_1\bar{Q}_2$ forms a singlet with probability $1/N_c^2 = 1/9$. Thus we might possibly expect that, if the pairs are produced in the same space-time point, the strings are "recoupled" and stretched between the pairs $q_1\bar{Q}_2$ and $Q_1\bar{q}_2$ with a probability of the order $1/N_c^2$. The recoupling probability can be further enhanced as the colour structure can be changed by gluon exchange. A gluon exchanged between e.g. q_1 and Q_1 would imply that the pairs $q_1\bar{q}_2$ and $Q_1\bar{Q}_2$ are colour octets, and strings would naturally form within the pairs $q_1\bar{Q}_2$ and $Q_1\bar{q}_2$. As discussed in refs [1, 2] hard gluons (gluons with $E \geq \Gamma_W$) are emitted independently by the decay products of the W 's. For this reason the exchange hard gluons, or interference effects from hard gluon emission, give only a small effect. The effect of *soft* gluon exchange can however not be easily estimated. It depends on the vacuum structure and cannot be calculated perturbatively.

Possible implications of the vacuum structure on the recoupling probability were pointed out in ref [3]. In a bag-type model the string between a quark and an anti-quark is a colour fluxtube with width of the order 1fm and an essentially homogeneous colorelectric field inside the tube. In this case the vacuum behaves like a type I superconductor. When the two W 's decay, it is then natural to imagine that the quarks and anti-quarks are surrounded by a baglike hole in vacuum, and that recoupling is likely if the distance (in space-time) between the production points for the pairs is less than 1fm.

We may also imagine that the vacuum is more similar to a type II superconductor. Here the string should consist of a thin core surrounded by an extended colorelectric field. The extension of this field ought to be of the order 1fm, but the core may be significantly more narrow. In this case we can imagine that recoupling is more improbable and only likely if the distance between the production points is small compared to the thickness of the core.

We see that a study of the probability for recoupling (and if possible how it depends on the total energy, i.e. on the distance between the W decay points) can give interesting

information about the structure of the vacuum and the confinement mechanism. Two questions are essential, i) what recoupling probability could be expected?, and ii) is it possible to identify recoupled events?

When trying to answer these questions it is important to take into account the effects of emission of (real) gluons. As mentioned above hard gluons are emitted very early [1, 2]. The space-time distance between the W decay points is of the order $1/\Gamma_W$, and therefore gluons with energies larger than Γ_W are produced incoherently by the two pairs $(q_1\bar{q}_2)$ and $(Q_1\bar{Q}_2)$. Thus rather than a possible recoupling between two $q\bar{q}$ systems we have two colour singlets, each containing a $q\bar{q}$ pair and a set of gluons, which can be recoupled, or regrouped into new colour singlet systems, in many different ways.

2 What recoupling probabilities may be expected?

When trying to estimate what recoupling probabilities could be expected it is relevant to compare with a similar situation in the B meson decay $B \rightarrow \psi + X$. If q denotes a light quark this decay can proceed via the reaction $q\bar{b} \rightarrow q\bar{c}W^+ \rightarrow q\bar{c}c\bar{s}$. Here the pairs $q\bar{c}$ and $c\bar{s}$ form colour singlets, and thus the $c\bar{s}$ pair normally forms a colour octet. Consequently the formation of a ψ meson implies the same form of colour recoupling, and some analyses of the branching ratios have indicated a recoupling probability around 15 or 20% [4]. In a B decay the energy is comparatively low and the W^+ is very much off shell and therefore the three quarks c , \bar{c} , and \bar{s} are essentially produced in the same space-time point. Thus we see that at zero distance (between three of the quarks) and lower energies there is apparently a significant recoupling probability.

The situation in W pair production is different from B decay in two respects. First the two W's decay in different space-time points, separated by 0.05–0.1fm. This is expected to reduce the recoupling probability, more in case vacuum is like a type II superconductor and less if it is like a type I superconductor. Secondly the emission of gluons implies that the two initial systems can be recoupled in many different ways, and this fact can in principle increase the total recoupling probability.

Before we discuss these dynamical effects it is interesting to study what the recoupling probability would be, due to only SU(3) Clebsch-Gordan coefficients, if there were *no* effects from gluon emission or the vacuum structure. Assume that two colour singlet systems, $q_1\bar{q}_2$ and $Q_1\bar{Q}_2$, are produced in the same space-time point. The probability that also $q_1\bar{Q}_2$ and $Q_1\bar{q}_2$ form colour singlets is then 1/9, as mentioned earlier. If $q_1\bar{Q}_2$ and $Q_1\bar{q}_2$ form colour singlets we may expect that they also can form separate hadron chains or strings. However, if q_1 forms a colour singlet with both \bar{q}_2 and \bar{Q}_2 , the structure of the observable hadron state can *not* be determined without further dynamical assumptions. As discussed in more detail in the appendix, the algebraic group properties only give a rather weak bound that the recoupling probability, P , must lie in the range $\delta < P < 1 - \delta$, where $\delta = 1/2 - \sqrt{2}/3 \approx 0.03$. Thus the recoupling probability could in principle be anything above a lower limit of 3%.

As mentioned in the introduction hard gluons are emitted early, and therefore gluons with energies larger than Γ_W are produced incoherently by the two pairs $q_1\bar{q}_2$ and $Q_1\bar{Q}_2$ [1, 2].

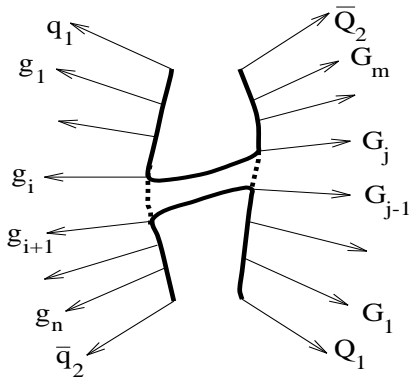


Figure 1: *The gluons $g_1 g_2 \dots g_n$ (with $E > \Gamma_W$) are emitted from the original $q_1 \bar{q}_2$ pair while $G_1 G_2 \dots G_m$ are emitted from the $Q_1 \bar{Q}_2$ pair. The two systems $q_1 g_1 \dots g_i G_j \dots G_m \bar{Q}_2$ and $Q_1 G_1 \dots G_{j-1} g_{i+1} \dots g_n \bar{q}_2$ are then colour singlets with probability $1/9$ for each value of i and j . They may thus form independent hadron chains or strings.*

Thus before the hadronization and before a possible recoupling two sets of colour connected gluons $g_1 g_2 \dots g_n$ and $G_1 G_2 \dots G_m$ (with $E > \Gamma_W$) are emitted independently by the $q_1 \bar{q}_2$ and $Q_1 \bar{Q}_2$ systems respectively³. Every set of particles $q_1 g_1 g_2 \dots g_i$ is now a colour triplet. Thus we can have a recoupling between the two original systems in many different ways. The two sets of particles $q_1 g_1 \dots g_i G_j \dots G_m \bar{Q}_2$ and $Q_1 G_1 \dots G_{j-1} g_{i+1} \dots g_n \bar{q}_2$ are colour singlets with probability $1/N_c^2$ for *every* choice of i and j (see Fig 1). The average number of gluons with $E > \Gamma_W$ (and $k_\perp > k_{\perp cut} = 1\text{GeV}$) is $\langle n \rangle = \langle m \rangle \approx 4.3$, and thus if the probability for recoupling is also of the order $1/N_c^2$ for each of these $(n+1)(m+1)$ possibilities, the *total* recoupling probability could in principle be very large.

We do not believe that all these recoupling possibilities are equally probable. Sjöstrand and Khoze [2, 5] have studied two different scenarios. In scenario II, which corresponds to a type II superconductor, it is assumed that the confining field has a very narrow core, and can be treated as an infinitely thin string. When two strings cross and have a space-time point in common, it is assumed that they can recouple with probability one (if they cross in many points only the one first in time is kept). As a result the recoupling probability is approximately 35% at $\sqrt{s} = 170\text{GeV}$. Scenario I corresponds to a type I superconductor and here the field is treated as a flux tube with radius around 0.5fm. (More precisely the field strength is proportional to $\exp(-r_\perp^2/2r_{had}^2)$, where $r_{had} = 0.5\text{fm}$). In every space-time point, where the flux tubes overlap, there is a constant recoupling probability (with a Gaussian fall off at the tube boundaries). The magnitude of this recoupling probability density is a free parameter, but if it is chosen to be 0.9fm^{-4} the total recoupling probability is 35% just as in scenario II. In both scenarios those recouplings are favoured, in which the initial strings are cut and recoupled in the “middle”, so that the two pieces have approximately the same

³More precisely soft gluons are emitted with a relative probability $1 - \frac{1+x(1-\epsilon)}{1+2x(1+\epsilon)+x^2(1-\epsilon)^2}$ where $\epsilon = v^2 \cos \theta$, v is the speed of the W, θ is the angle between the gluon and W momenta, and $x = \frac{\gamma(v)E_g}{\Gamma_W}$

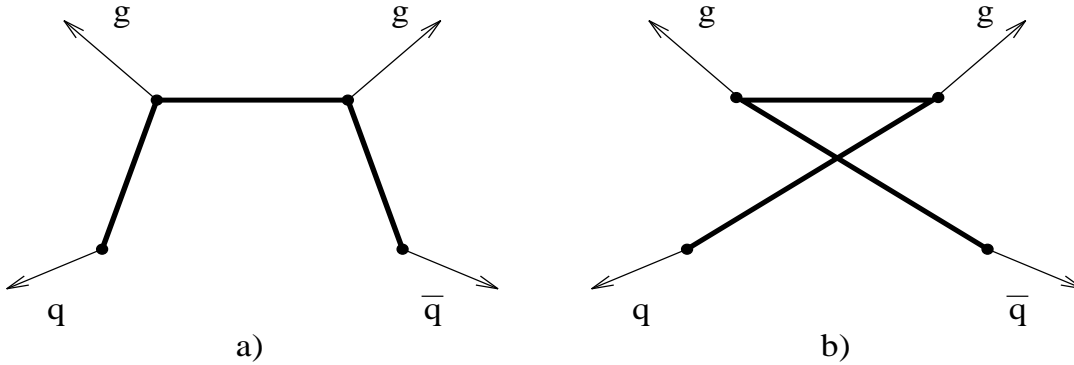


Figure 2: *The production probability for a $q\bar{q}gg$ state is, in perturbative QCD, larger for the colour connection which corresponds to a “shorter string” as in fig a).*

energy. As the normal (not recoupled) systems correspond to “long” strings, stretched across the origin in the cms, it is natural that most recouplings give “shorter” strings (i.e. strings which give fewer hadrons); this is more pronounced for scenario I than for scenario II.

In a type II scenario we think that the recoupling probability of 35% might be regarded as an upper limit. This result was obtained assuming unit probability for recoupling when the strings cross, and the results from B decay may indicate that a recoupling does not always occur when the space-time structure makes it possible. In a type I scenario the flux tubes always overlap to a larger or lesser degree. The recoupling probability cannot be calculated from our present knowledge of QCD, and with all the recoupling possibilities available after the initial gluon emission, the total probability may in principle be very large. The value 0.9 fm^{-4} for the probability density which is studied in refs [2, 5], is just arbitrarily chosen in order to facilitate a comparison between the scenarios, and has no dynamical motivation.

In scenarios I and II studied by Sjöstrand and Khoze it is assumed that the recoupling probability only depends on the geometrical overlap of the field configurations in coordinate space, with no dependence on the kinematical motion of the fields. (Some dynamical effects are included in scenario II', in which only those recouplings are allowed which give “shorter strings” in the sense discussed below.) If we study $q\bar{q}gg$ four jet events, as illustrated in Fig 2, we note that the colour connection in Fig 2b, which corresponds to a “longer” string, is disfavoured. When comparing different possibilities of recoupling, as discussed above, it is conceivable that the tendency in the scenarios studied in refs [2] to favour short “strings” may be further enhanced by dynamical effects. This also means that recoupling might be more probable if it connects gluons which move in approximatively the same direction. In a type I scenario the fluxtubes always overlap in coordinate space, and it is quite conceivable that the properties in momentum space are most important for the recoupling probability.

The “length” of a string is correlated with its invariant mass and thus one possibility would be to select and study that recoupling possibility (i.e. those values of i and j above) for which $s_1 \cdot s_2$ is minimum. (Here $\sqrt{s_1}$ and $\sqrt{s_2}$ are the invariant masses of the two systems after recoupling). A more efficient measure for the “length” of a string state is the quantity λ studied in ref [6]. It corresponds to an “effective rapidity length”, and is

closely correlated to the hadronic multiplicity. For hard gluons it is approximately given by $\lambda \approx \sum \ln(p_i + p_{i+1})^2/m_0^2$, where p_i are the (colour-ordered) parton momenta and the hadronic mass scale m_0 is around 1GeV. Thus it is conceivable that those recouplings for which $\lambda_1 + \lambda_2$ is significantly reduced may be dynamically favoured (where λ_1 and λ_2 are the λ -measures for the two recoupled strings). An extreme case corresponds to the assumption that only the recoupling for which $\lambda_1 + \lambda_2$ is minimum is likely, perhaps with a probability around 10%. It is also possible that all states, for which $\lambda_1 + \lambda_2$ is significantly reduced, have a fair recoupling probability, which could give a larger total recoupling probability.

We note that for the recoupled states with minimum $\lambda_1 + \lambda_2$, the average change $\langle \Delta\lambda \rangle$ is around 2 units. (For a sample with a cut on thrust, as studied in the next section, the value of $\langle \Delta\lambda \rangle$ is even larger). This can be compared with the recoupled states studied in ref [2], which are selected only from purely geometrical considerations, for which $\langle \Delta\lambda \rangle$ is of order 0.7 for scenario I (and somewhat smaller for scenario II). In the same way as this geometrically selected sample, also the states with minimum $\lambda_1 + \lambda_2$ normally corresponds to recoupling where the initial states are cut in two approximately equal pieces. The average value of the quantity $d_{\text{rec}} = |E_1 - E_2|/(E_1 + E_2)$ (where E_1 and E_2 are the energies of the two pieces of a split W decay system) is given by $\langle d_{\text{rec}} \rangle \approx 0.2$ which is comparable to the result in ref [2].

3 Can recoupled events be identified?

The question whether the recoupled events can be identified was addressed in ref [3]. In this older analysis the emission of gluons before recoupling was neglected, and with this simplifying treatment a very clear difference was seen between recoupled and “normal” events. If the angle between the outgoing q_1 and \bar{Q}_2 is fairly small, e.g. around 30° , the two recoupled strings move apart in the cms with large velocities, thus producing few particles in the central region. Looking at the number of central particles, e.g. particles with $|y| < 2$, the recoupled events could easily be identified on an event by event basis.

However the gluons emitted independently by the two systems in the early phase, as discussed above, will give extra particles in the central region, which will reduce the difference between the recoupled and non-recoupled events. Sjöstrand and Khoze [2, 5] studied effects of recoupling on the determination of the W mass and on *average* distributions, and in their analysis they found small effects. Our aim here is different. We want to study if there are *some* possible recoupled systems which are sufficiently different from the “normal” systems so that they can be identified experimentally.

As mentioned above recoupled systems with two “short strings” may be particularly favoured. They are also the ones which differ most from the non recoupled systems, because the two short strings move away in opposite directions in a way which is most similar to the situation without primary gluon emission, studied in ref [3]. They will thus be more easily identified and we will in the following concentrate on those recoupling possibilities which give the shortest strings, i.e. those for which $\lambda_1 + \lambda_2$ is minimum.

In order to have a large difference between the recoupled and non recoupled systems,

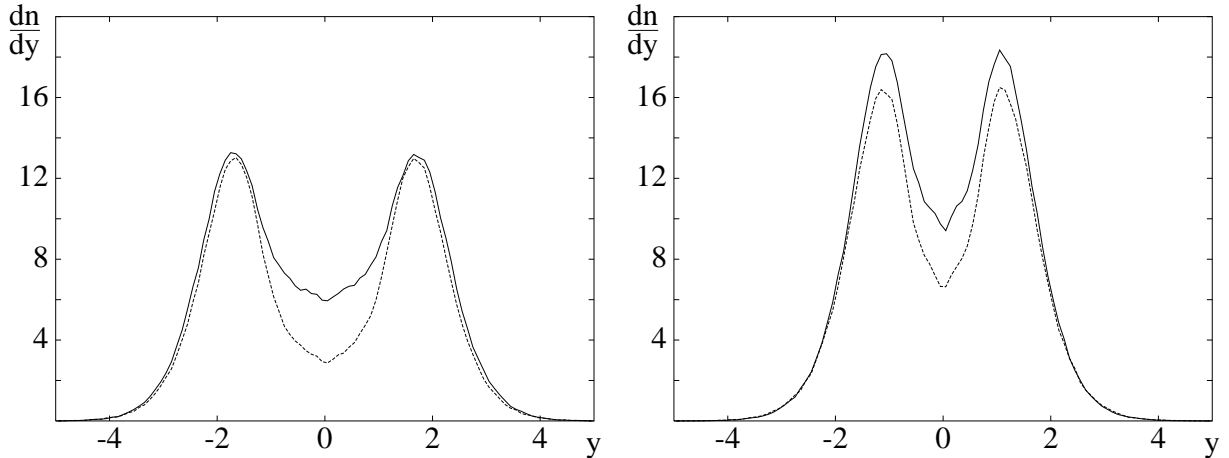


Figure 3: Rapidity distributions for “normal” events (solid line) and recoupled events (dashed line) with thrust cuts $T > 0.92$ (fig a) and $T > 0.76$ (fig b).

the angle between e.g. q_1 and \bar{Q}_2 should not be too large. In ref [3] (and also in ref [2]) events where this angle was 30° were selected. In our analysis we found that the recoils from gluon emission imply that a cut on this angle is less suitable, and instead we study here events with a cut on the thrust variable T .

As mentioned above it would be interesting to study how the recoupling probability varies with the total energy, which implies a variation in the distance between the W decay points. However, as discussed in ref [2], also at the threshold energy, $\sqrt{s} = 2m_W$, the width of the W’s implies that they are not produced at rest. Therefore the distance varies very little in the LEP2 range from threshold to 180GeV. For this reason we here present results only for 170GeV where the effect of the spread in the W mass is small and can be neglected. These results are representative also for energies close to threshold, where the average W momenta are of the same order of magnitude [2].

In our simulations gluons with $E \gtrsim \Gamma_W$ are emitted using the Ariadne MC [7], and the recoupled events are chosen to give minimum values for the sum $\lambda_1 + \lambda_2$, as discussed above. For the hadronization process we have used the Lund string model [8] implemented in the Jetset MC [9]. In string fragmentation soft gluons with $E < \Gamma_W$ give very little effect, and they have therefore been neglected. In Fig 3 we show the inclusive rapidity distribution for “normal” and “recoupled” events. We see that the central region is suppressed in the recoupled events, but due to the initial gluon emission it is not totally empty. Therefore this average distribution can not be used as an experimental signal for the recoupled events. It would not be possible to ascertain an admixture of recoupled event of the order 10%. (We note that the results in Fig 3 are similar to the corresponding results obtained by Sjöstrand and Khoze [2]).

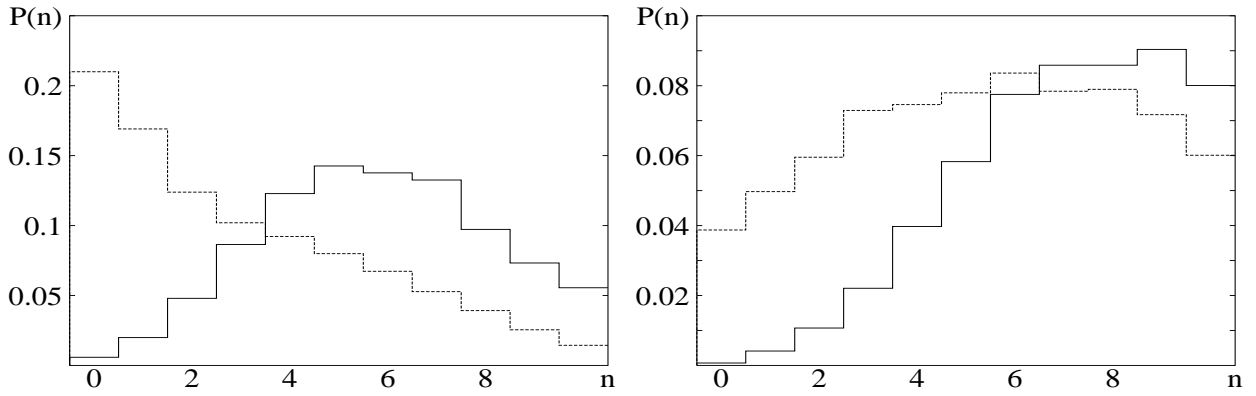


Figure 4: *Multiplicity distributions for $|y| < 0.5$ for “normal” events (solid line) and recoupled events (dashed line) with thrust cuts $T > 0.92$ (fig a) and $T > 0.76$ (fig b).*

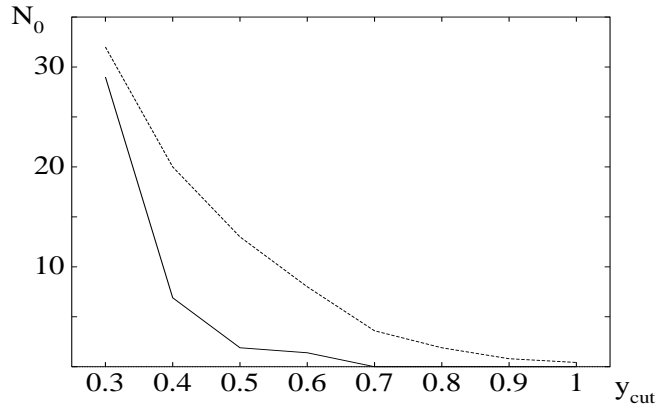


Figure 5: *Expected number of events with zero central particles, N_0 , as a function of the rapidity bin size $|y| < y_{cut}$. The dashed line shows the recoupled events and the solid line shows the normal events. The total sample is assumed to be 5000 hadronic WW decays.*

However, even if the average recoupled event is not sufficiently different from the normal ones, it turns out that events with no central particles are much more common in the recoupled sample. Fig 4 shows the multiplicity distribution (including π^0) in the central region $|y| < 0.5$ for “normal” and recoupled events with the thrust cuts $T > 0.92$ and $T > 0.76$. With the higher thrust cut the difference between normal and recoupled events is larger but statistics become poor as only around 4% of the events pass this cut. For $T > 0.76$ we keep 60% of the events preserving a fairly large difference in the probability to have no particle in the central region. This probability is a factor 55 larger for the recoupled events than for the normal events. With 5000 events with hadronic W-decays, and with 10% probability for recoupling, we expect 13 recoupled events with $n_{central} = 0$ with a background of 1.9 events from normal events. (This signal to background ratio is essentially constant in the entire LEP2 energy range from threshold to 190GeV). The signal to background ratio can be further enhanced if one combines data from different cuts in thrust and rapidity. The dependence on the thrust cut is seen in Figs 3 and 4, and the dependence on the width of the rapidity bin is illustrated in Fig 5. From Fig 4 it is seen that also the probabilities $P(1)$ are very different between normal and recoupled events, and thus information from events

with exactly *one* particle in the central rapidity bin can also be used. The best choice of observables will depend on the resolution and acceptances properties of the detectors, and for those who are interested the MC program for the recoupling is available upon request.

Note that in this example we have assumed that a recoupling occurs only to states with minimal λ . Similar results could of course be obtained if recoupling occurs also to other states with small λ -values, but with a correspondingly larger total recoupling probability.

4 Conclusions and comments

In the reaction $e^+e^- \rightarrow W^+W^- \rightarrow (q_1\bar{q}_2)(Q_1\bar{Q}_2)$ hadron chains or strings are normally expected to be stretched within the colour singlet systems $q_1\bar{q}_2$ and $Q_1\bar{Q}_2$. However also the systems $q_1\bar{Q}_2$ and $Q_1\bar{q}_2$ are singlets with probability $1/N_c^2 = 1/9$, and we could therefore expect “recoupled” chains or strings with a probability of this order of magnitude.

Due to the finite lifetime of the W 's, hard gluons (with $E > \Gamma_W$) are emitted independently by the two initial quark–anti-quark pairs. This reduces the observable difference between the “normal” and the “recoupled” events. On the other hand it may also increase the recoupling probability, because the two initial colour singlet systems can be recoupled in very many ways, each in principle with a probability of order $1/N_c^2$.

The presence or absence of such recoupled events gives valuable information about the vacuum structure. Thus we would e.g. expect a larger recoupling probability if vacuum behaves like a type I superconductor than if vacuum is more like a type II superconductor. In the former case the colour fluxtube would be similar to an elongated bag, while in the latter case the confining colour field would have a more narrow central core.

Sjöstrand and Khoze [2, 5] have studied observable effects if the recoupling probability is determined purely by the geometrical structure of the confining force field, and they have found generally small effects. In this paper we have argued that it is not unlikely that dynamical effects enhance the recoupling probability for states which correspond to “short strings” producing few hadrons. These states are also the ones which differ most from the normal events, and we have seen that they can be experimentally identified if they occur with a rate of about 10%.

Sjöstrand and Khoze have also studied the effects of recoupling on the determination of the W mass [5, 2]. Assuming 35% recoupling probability they find an extra uncertainty of about 40MeV. The recoupling effects the softer hadrons, and the states studied in our analysis will give a similar uncertainty in the mass determination as those studied in refs [5, 2]. Thus as a first approximation the uncertainty in the mass determination will be proportional to the total recoupling probability. This probability cannot be calculated from our present knowledge of QCD, and could in principle be large.

It would also be interesting to study effects of recoupling in other reactions. As mentioned in ref [2] recoupling is also possible in normal Z -decay events. We can e.g. look at the reaction $e^-e^+ \rightarrow q\bar{q}gg$. If both gluons are emitted from the quark or anti-quark legs (cf. Fig 6a) a straightforward calculation shows that the probability for the two gluons to be in a

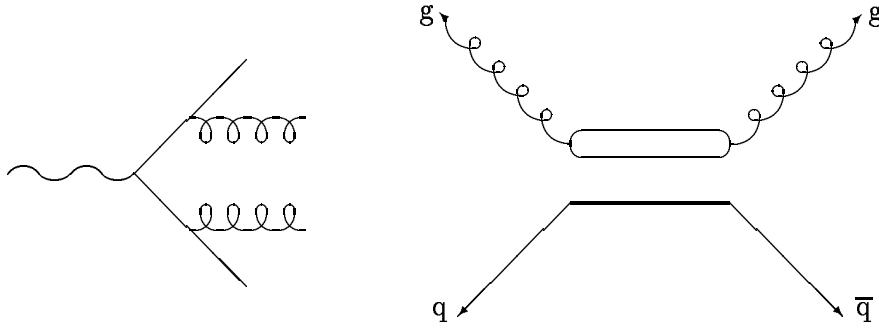


Figure 6: $q\bar{q}$ state and ring of gluons.

colour singlet state is $1/(N_c^2 - 1) = 1/8$. In such a case the hadronization can be expected to correspond to a string between the quark and the anti-quark, together with a closed string loop between the gluons, as shown in Fig 6b. (If the two gluons originate from the process $g \rightarrow gg$ they are of course always in a colour octet state. Thus the momentum distribution for the gluons in Fig 6 is the same as for two emitted photons). In a following paper we want to study observable features of such recoupled systems in this and other reactions.

Acknowledgments

We want to thank dr T. Sjöstrand for valuable discussions.

This research is supported in part by the EEC Programme "Human Capital and Mobility", Network "Physics at High Energy Colliders", contract CHRX-CT93-0357 (DG 12 COMA).

A Appendix

It is interesting to study what the recoupling probability would be, due to only SU(3) Clebsch-Gordan coefficients, if there were *no* dynamical effects from soft gluons and the vacuum structure. For this we study two pairs $q_1\bar{q}_2$ and $Q_1\bar{Q}_2$ produced in the same space-time point, and we define the states $|1\rangle$ and $|2\rangle$ in the following way:

$$\begin{aligned} \text{State } |1\rangle &: q_1\bar{q}_2 \text{ and } Q_1\bar{Q}_2 \text{ form separate colour singlets,} \\ \text{State } |2\rangle &: q_1\bar{Q}_2 \text{ and } Q_1\bar{q}_2 \text{ form separate colour singlets.} \end{aligned} \quad (1)$$

In state $|1\rangle$ there is a probability $1/N_c^2 = 1/9$ that also $q_1\bar{Q}_2$ and $Q_1\bar{q}_2$ form singlets. This does not imply however, that $q_1\bar{Q}_2$ and $Q_1\bar{q}_2$ form independent hadron strings with probability $1/9$. We see that the states $|1\rangle$ and $|2\rangle$ are not orthogonal but satisfy $\langle 1|2\rangle = \sqrt{1/9} = 1/3$.

When the quarks and anti-quarks hadronize we assume that the hadrons are formed in two separate cluster chains or strings, and we then have two possible final states, which we denote $|a\rangle$ and $|b\rangle$.

$$\begin{aligned} \text{State } |a\rangle &: q_1\bar{q}_2 \text{ and } Q_1\bar{Q}_2 \text{ form ends of separate strings,} \\ \text{State } |b\rangle &: q_1\bar{Q}_2 \text{ and } Q_1\bar{q}_2 \text{ form ends of separate strings.} \end{aligned} \quad (2)$$

These states are eigenstates to observables with different eigenvalues and are therefore orthogonal to each other; $\langle a|b\rangle = 0$. States $|1\rangle$ and $|2\rangle$ can be written as linear combinations

of $|a\rangle$ and $|b\rangle$. Due to the symmetry of the situation they can be written as

$$\begin{aligned} |1\rangle &= \alpha |a\rangle + \beta |b\rangle \\ |2\rangle &= \beta |a\rangle + \alpha |b\rangle \end{aligned} \quad (3)$$

The recoupling probability is obviously given by $|\beta|^2$ and the scalar product between $|1\rangle$ and $|2\rangle$ gives the relation

$$\langle 1|2\rangle = 2\text{Re}(\alpha^*\beta) = 1/3. \quad (4)$$

We can choose α real and with the notation $\alpha = \sin\theta$, $\beta = \cos\theta \exp i\varphi$ we obtain

$$\sin(2\theta) \cdot \cos\varphi = 1/3 \Rightarrow |\sin(2\theta)| \geq 1/3 \quad (5)$$

Thus the recoupling probability $|\beta|^2$ is restricted by the relation

$$\delta < |\beta|^2 < 1 - \delta, \quad \delta = 1/2 - \sqrt{2}/3 \approx 0.03 \quad (6)$$

We conclude that we only obtain a rather loose restriction. The recoupling probability could be anything above a lower limit of 3% (and below 97%). (It is easy to see that the same result is obtained if $|a\rangle$ and $|b\rangle$ are not single states but corresponds to two groups of states).

References

- [1] Yu.L. Dokshitzer, V.A. Khoze, L.H. Orr, W.J. Stirling, *Nucl. Phys.* **B403** 65 (1993)
- [2] T. Sjöstrand, V.A. Khoze, *Z. Physik* **C62** 281 (1994)
- [3] G. Gustafson, U. Petterson, P.M. Zerwas, *Phys. Lett.* **B209** 90 (1988)
- [4] M. Neubert *et al.* in Heavy Flavours, Ed. A.J. Buras, M. Lindman, World Scientific 1992
S. Henderson, Proceedings of XXIX Rencontres de Moriond, 1994 and references given in [3]
- [5] T. Sjöstrand, V.A. Khoze, *Phys. Rev. Lett.* **72** 28 (1994)
- [6] B. Andersson, P. Dahlgvist, G. Gustafson, *Phys. Lett.* **B214** 604 (1988), *Z. Physik* **C44** (1989) 455
- [7] U. Petterson, Lund preprint LUTP 88-5 (1988)
L. Lönnblad, DESY preprint DESY 92-046 (1992)
- [8] B. Andersson, G. Gustafson, G. Ingelman, T. Sjöstrand, *Phys. Rep.* **97** 31 (1983)
- [9] T. Sjöstrand, *Comp. Phys. Comm.* **39** 347 (1986)
T. Sjöstrand, M. Bengtsson, *Comp. Phys. Comm.* **43** 367 (1987)

Paper IV

Colour connections in e^+e^- -annihilation

Christer Friberg, Gösta Gustafson, Jari Häkkinen¹

Department of Theoretical Physics, Lund University,
Sölvegatan 14A, S-223 62 Lund, Sweden

Submitted to
Nucl. Phys. B

Abstract:

We have a very limited knowledge about how the confinement mechanism works in processes like $e^+e^- \rightarrow q\bar{q}g \dots g$, when there are identical colour charges. In this case the partons can be connected by a string or a cluster chain in several different ways. We do not know if in such a situation Nature chooses a particular configuration at random, or if some configuration is dynamically favoured. Also in the perturbative parton cascade we have no well founded recipe for describing the interference effects, which correspond to non planar diagrams and are caused by identical colour charges. We have studied two different models, and are in particular interested in the possibility that a colour singlet gluon system hadronizes isolated from the remainder of the state. Using double tagged events with heavy $c\bar{c}$ or $b\bar{b}$ quarks, it appears to be possible to find a significant signal, if such events appear in Nature.

If this type of (re)connected states appear in Z decays it may also be an indication that reconnection might appear between the decay products of two W 's in the reaction $e^+e^- \rightarrow W^+W^- \rightarrow q_1\bar{q}_2Q_1\bar{Q}_2$ at LEP2. This would be important e.g. for a precision measurement of the W mass.

¹christer@thep.lu.se, gosta@thep.lu.se, jari@thep.lu.se

1 Introduction

High energy reactions, e.g. e^+e^- -annihilation, are generally described in terms of two phases: First a short time perturbative phase with large momentum transfers, described in terms of quarks and gluons. This initial phase is described by a parton cascade. Secondly a long time soft interaction phase, in which the energy of the partons is transformed into hadrons. This non-perturbative hadronization phase is successfully described by a string model [1] or a cluster model [2]. These two phases are generally assumed to be well separated from each other. The parton cascade has a cutoff of the order 0.5–1GeV corresponding to a timescale of 0.2–0.4fm, while the hadronization time often is assumed to be 1–2fm. It is believed that the reaction cross section is fully determined by the perturbative phase, while in the soft hadronization phase a definite hadron state is chosen with total probability 1.

In both phases a set of approximations is used, where the number of colours is assumed to be large. Assuming infinitely many colours reduces the possible interference effects. Only planar diagrams contribute in the perturbative cascade, and the way to connect the partons by a string or cluster chain becomes unique. A specific colour charge has to be connected to a parton with the corresponding anti-colour, and with infinitely many colours the probability that two (or more) partons have the same colour is zero.

With only three colours, as in Nature, this is no longer the case. The basic problem is that the direct correspondence between the parton states and the string states (or cluster chains) is lost. The parton state is determined by the momenta, polarization, and colour of all the quarks and gluons. This is not enough to describe the true states in QCD. Also some topological quantum numbers have to be specified, related to the vacuum condensate and the confinement mechanism. 't Hooft has proposed that these extra quantum numbers correspond to gauge singularities similar to the ones appearing in a superconductor [3]. In the string model they correspond to the string topology; the string state is specified by the momenta carried by the string ends (quarks and anti-quarks) and by the corners (gluons), together with a specification of how they are connected.

The most simple example is shown in Fig 1. With two red quarks and two anti-red anti-quarks there are two different possible string states. The string configuration is in principle an observable (reflected in the momenta of the final state hadrons), which corresponds to excitations in the vacuum condensate. When the coloured partons move apart, the confinement mechanism must give a response in the condensate, such that a particular string state is selected. This selection cannot be determined from perturbative QCD, because the distinction between the two string states in Fig 1b does not correspond to any observable related to the parton state in Fig 1a.

The fact that the present models work so well, indicates that these effects are usually small. They are generally of the order $1/N_c^2$, which corresponds to the probability that two gluons have the same colour. They are nevertheless of fundamental importance for our understanding of the confinement mechanism. What determines the response of vacuum to the produced partons, and what is the time scale of the “interface” between the hard and the soft phases? When identical parton charges allow several state topologies, is one topology chosen at random or is some configuration dynamically favoured? Connected to these

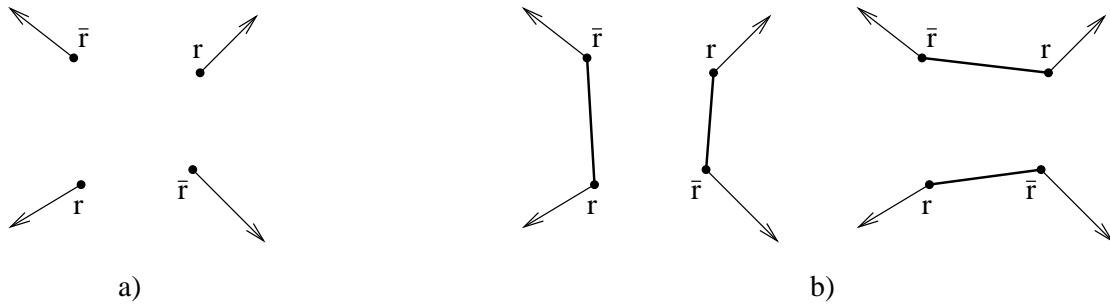


Figure 1: When two red and two anti-red colour charges move apart they can be connected by strings or cluster chains in two ways.

problems are colour suppressed contributions to the perturbative parton cascade, related to non planar diagrams.

As the problems cannot be solved by perturbative QCD we have to rely on experimental measurements. Thus in this paper we want to study possible effects of the finite number of colours, and observables which are sensitive to these effects. The problem has been studied in refs [4, 5, 6, 7] in connection with the reaction $e^+e^- \rightarrow W^+W^- \rightarrow q_1\bar{q}_2q_3\bar{q}_4$ ². At LEP2 the two $q\bar{q}$ pairs originate from points separated by about 0.1fm, which is short compared to the hadronization scale. Here we will study similar effects in the reaction $e^+e^- \rightarrow q\bar{q} +$ a number of gluons at LEP1. With few colours it is possible to obtain a gluonic subsystem, which is in a colour singlet state. This system could hadronize independently, decoupled from the remaining state (in the string model as a closed string), and we want in particular to study if it is possible to experimentally identify such gluonic colour singlets. At LEP1 the whole process starts in a single point, and a comparison of the effects in the two reactions would be very valuable.

There are three different problems we want to address in this paper:

- What can we learn about the interface between the hard and the soft phases?
- How does the confinement mechanism work when there are several ways to connect the partons by a string?
- Is it possible to find a good approximation scheme for the interference effects in the perturbative phase?

These problems will be further discussed in the following sections. The last problem is in principle solvable within perturbative QCD, but this is not the case for the other two problems. We will describe two different models and discuss how these can be experimentally tested. The effects on average event properties are generally small, but it is possible to find an observable signal for special events.

²In the calculations in [4] the polarization of the W 's was neglected. When this is taken into account the reported signal is reduced by approximately a factor 1/2

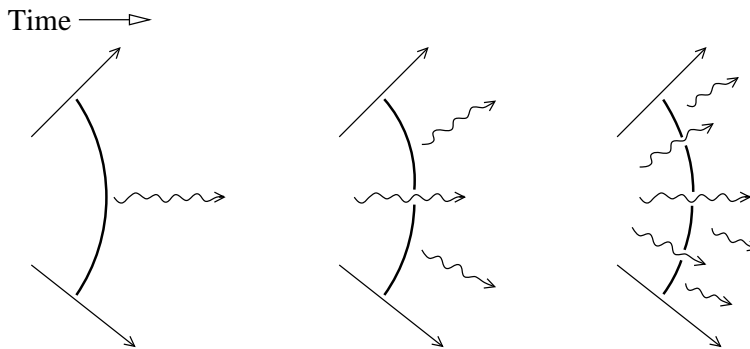


Figure 2: *The dipole picture of a gluon cascade.*

2 Interface between the hard and soft phases

In an e^+e^- -annihilation event full perturbative calculations have been performed only to second order in α_s . This is far from sufficient to reproduce experimental data, and different approximation schemes have been developed to approximate the evolution of a parton cascade. In the dipole cascade model [8], an initial colour dipole between a quark and an anti-quark can emit a gluon and thereby split in two dipoles, which can emit further gluons in a cascade as illustrated in Fig 2. The dipoles form a chain where the colour of one gluon is combined with the anti-colour of a neighbouring gluon. The colour and the corresponding anti-colour radiate coherently producing the 'dipole emission'. This effect is often called soft gluon coherence [9, 2], and can be approximated by an angular ordering of the emitted gluons. In the large N_c limit all the dipoles have different colours, and therefore radiate independently, apart from the recoils experienced due to the emission. With only three different colours we must frequently have a situation with e.g. two red and two anti-red charges, which have to interfere in the further gluon emission. In the original dipole cascade model, implemented in the Ariadne MC [10], this interference is neglected, and also in other versions of the parton cascade, e.g. those implemented in the Herwig [11] or the Jetset [12] MC, the only interference included is the one from a colour charge and the directly associated anti-charge. One approach to include interference effects, which we will discuss further below, is implemented in the latest version of Ariadne (version 4.07).

Thus in the perturbative cascade a quark-gluon state with well specified colours is produced. Via the confinement mechanism the energy of these partons is transformed into colour singlet hadrons. In the string model a string-like force field is stretched from a quark via a set of gluons to an anti-quark. Thus in the example in Fig 3 the string is stretched from red to anti-red, then from blue to anti-blue etc.. With many colours the string configuration corresponds exactly to the chain of dipoles, but if there are more than one red-anti-red pair there may be more than one possible way to stretch the string.

As mentioned in the introduction the string configuration appears as an observable. Even if a certain string state does not correspond uniquely to a definite hadron state, different possible string states produce usually very different hadronic states, and they can therefore be distinguished from each other. We note that in the string model also the direction of a

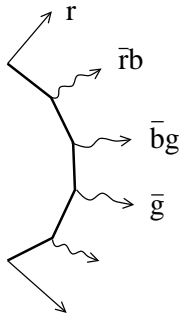


Figure 3: *In the string model a string-like colour field is stretched from red to anti-red, from blue to anti-blue etc.*

closed string, corresponding to a purely gluonic system, is an observable (with the direction defined e.g. from colour to anti-colour). When the string breaks by the production of an $s\bar{s}$ pair the s and \bar{s} are pulled in opposite directions, which implies a rapidity separation between e.g. a final state K and \bar{K} . This means that e.g. the decay $\Upsilon \rightarrow 3g$ can give two differently oriented string loops, which cannot be separated by perturbation theory [13].

Thus the string or cluster chain configuration is an observable, which is not fully determined by the partonic state of coloured quarks and gluons, and the confinement mechanism has to imply that a certain configuration is selected. At which stage in the process is this configuration fixed? Is this fixation purely in the hadronization phase, or does it also affect the initial hard phase. To clarify this problem we will compare with the behaviour of a superconductor, and discuss in more detail the example of Υ decay.

If the vacuum condensate behaves like a type I superconductor, we expect that the bag model is a good representation of the confinement mechanism, and the string should be more regarded as a flux tube with a radius of the order of 1fm. It is then natural to expect that the topology of the string or cluster chain is not determined until the partons are separated by a similar distance, and that this process is totally separated from the perturbative cascade.

If on the other hand vacuum is more like a type II superconductor the string would be more similar to a vortex line, where the energy is concentrated to a thin core, although the field can be smeared out over a larger region. We can then imagine that the topology is fixed at an earlier stage when the parton separation is of the order of the core radius. In this case the mechanism which determines the string configuration could possibly also affect the early hard phase of the reaction.

As an example let us study the reaction $\Upsilon \rightarrow 3g$. The decay amplitude is proportional to the colour factor

$$\frac{1}{2}d^{abc} = \text{Tr} [T^a T^b T^c] + \text{Tr} [T^c T^b T^a] \equiv A + B \quad (1)$$

where a , b , and c are the colours of the three gluons. The two terms correspond to different orientations of the string (see Fig 4). In the large N_c limit the two amplitudes are orthogonal, and the cross section for the two different string states is given by the colour factors (obtained

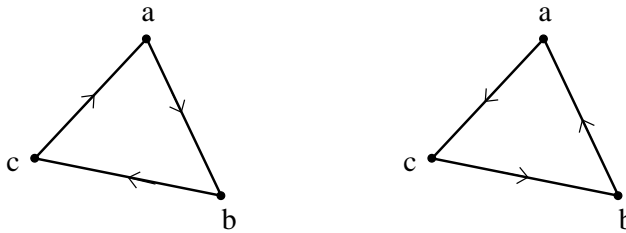


Figure 4: *Two different string configurations are possible in the decay $\Upsilon \rightarrow 3g$. The direction of the string is defined as going from colour to anti-colour.*

by summing over all colours)

$$\sum |A|^2 = \sum |B|^2 = \frac{(N_c^2 - 1)(N_c^2 - 2)}{8N_c} \quad (2)$$

For finite N_c there is however also an interference term

$$\sum AB^\dagger = -\frac{N_c^2 - 1}{4N_c} \quad (3)$$

which corresponds to a part of the cross section, for which the orientation of the final state is not determined. An example is when all three gluons are $r\bar{r}$. Although formally of order $1/N_c^2$ this part is clearly not small; it is negative and for three colours it is a fraction $2/(N_c^2 - 4) = 40\%$ of the total cross section. Since the two states in Fig 4 are eigenstates to an observable with different eigenvalues, the full amplitudes have to be orthogonal. If the topology is fixed at an early stage of the process, it could conceivably interfere with the perturbative phase and thus influence the cross section [13]. If this would imply that the interference term should be neglected in a calculation of the cross section, a determination of α_s to fit experimental data would give a smaller value, not in agreement with α_s measurements at higher energies [14]. Although not a proof, this is at least an indication that the string configuration is determined at a later stage well separated from the initial hard process, which determines the cross section.

Thus, if the string topology is not determined in the hard phase we must face the following problem: Sometimes the initial perturbative process produces a state with several identical colour charges moving apart. What mechanism selects a specific final state topology? Is the topology chosen at random among those which are possible, or is some topology dynamically favoured? In the next section we will discuss some conceivable models.

3 Models

3.1 The hadronization phase

We first want to discuss a model (called the soft reconnection model) in which the perturbative cascade is unchanged, and only the hadronization phase is modified. Let us assume that

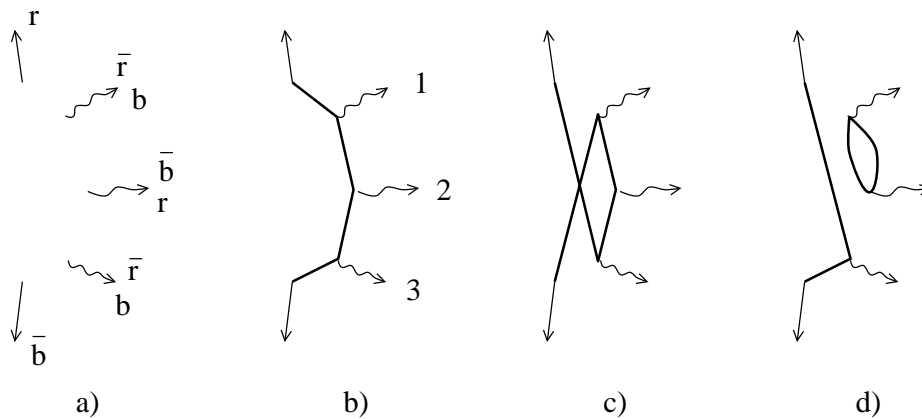


Figure 5: *The partons in a) can be connected in three different ways as in b), c), and d).*

the perturbative phase has resulted in a set of partons with colour charges as shown in Fig 5a. These charges can be connected by a string (or cluster chain) in different ways as illustrated in Fig 5b–d. As discussed above we do not know if Nature chooses one configuration at random, or if some particular configuration is dynamically favoured. The same problem is studied in [4, 5, 6, 7] in connection with the reaction $e^+e^- \rightarrow W^+W^- \rightarrow q_1\bar{q}_2q_3\bar{q}_4$. As in ref [4] we will here study a model where the confinement mechanism preferentially connects a colour with a corresponding anti-colour in the neighbourhood. This implies that “short” string configurations should be favoured, and to decide what is a “short string” we will, as in [4], use the λ measure defined in [15]. This measure corresponds to an “effective rapidity length”, and is closely correlated to the hadronic multiplicity. For hard gluons it is approximately given by $\lambda \approx \sum \ln [(p_i + p_{i+1})^2/m_0^2]$ where p_i are the (ordered) parton momenta and the hadronic mass scale m_0 is around 1GeV.

Assume that the ordering in Fig 5b is the one generated in the hard phase. Then the configuration in Fig 5c is possible provided the gluons numbered 1 and 3 have identical colours. Similarly the configuration in Fig 5d is possible if the colour of gluon 1 corresponds to the anti-colour of gluon 2. As there are 8 different gluon colours, these possibilities appear in general with probability 1/8. The SU(3) colour algebra will be discussed further in Section 4, but the basic property of our model is that a possible colour recoupling of the partons, which results in a smaller value for the λ measure, will be chosen with a probability 1/8. (One constraint is that two or more gluons, which form an isolated colour singlet system as in Fig 5d, must not originate from a single colour octet gluon.)

The possibility to connect the partons as in Fig 5c or 5d is often called colour reconnection or recoupling. This is actually an improper terminology. The partons have not been *reconnected*. They did not start connected as in Fig 5b, and colour connection would be a better term. This is similar to the use of the term recombination time for the time when electrons and protons first combine to neutral atoms after the Big Bang.

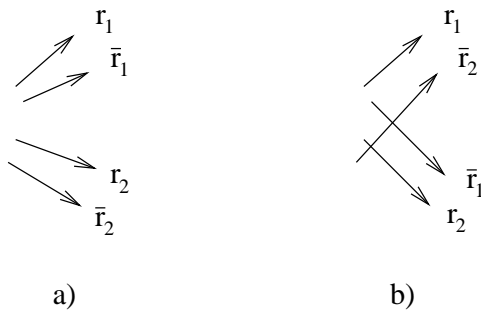


Figure 6: a) Usually a colour charge and its associated anti-colour are close in phase space. b) Occasionally a red charge can be closer to an anti-red charge from a different pair.

3.2 The hard phase

In a second model also the hard perturbative phase is modified. In principle this phase is calculable within perturbative QCD. This is not possible in practise, and as mentioned above, in most parton cascade models all non-planar diagrams are neglected. (An exception is the latest version of Ariadne, which we will comment on further below.) This means that essentially only interference effects from e.g. a red and its adjacent anti-red charge in the same dipole is included. Assume that two $r\bar{r}$ pairs are produced. In principle they would emit further soft gluons as a quadrupole. In most cases the two partners in one dipole are close in phase space, and therefore appears as a neutral object when viewed from the other dipole, as illustrated in Fig 6a. In these cases the neglected interference between the dipoles should be small. Occasionally this is not true, and the situation can look as in Fig 6b. Here a better approximation would be to include interference within the pairs $r_1\bar{r}_2$ and $r_2\bar{r}_1$, but neglect the interference between these pairs. This means that the emission of softer gluons can correspond to a different ordering of the charges in the dipole chain.

Since a proper inclusion of the interference effects is too complicated, we want to study a rather simple model, assuming that this model can give information about possible qualitative features and the expected order of magnitude of the effects. In the parton cascade it can happen that the colour charges can be arranged in a dipole chain in different ways. In the model we assume that in such cases the emission of softer gluons is better approximated if we reorder the gluons, so that the charges in the dipoles are as close in phase space as possible. As a measure, when we compare two different orderings, we also here use the λ measure discussed above.

As in the soft reconnection model the possibility to have identical gluon colours is taken into account by allowing the reconnection with probability $1/8$, if it provides a smaller λ measure.

Thus, at every step in the cascade we check if the gluon chain should be reordered. The colour reconnection of the gluons should be relevant for the emission of softer gluons later in the cascade. The Landau-Pomeranchuk formation time in a gluon emission is related to its transverse momentum, and therefore it is essential that the transverse momentum is used as an ordering parameter in the cascade. For this reason the dipole cascade model,

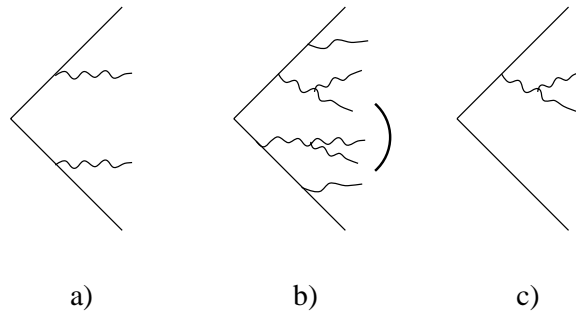


Figure 7: a) A pair of gluons emitted from (anti-)quark legs are in a colour singlet state with probability $1/[N_c^2 - 1] = 1/8$. b) This is also approximately the case for any connected gluon sub-system. c) An exception is two or more gluons originating from a single gluon parent. Such a system is naturally always a colour octet.

implemented in Ariadne, is particularly convenient, and we will use a modification of this program, in spite of the problems discussed below.

A model in which reconnection can occur *both* in the hard phase and in the soft phase will in the following be called the cascade reconnection model.

4 Colour structures and mother-daughter relations

4.1 Colour structures

We are particularly interested in the presence of isolated gluonic systems, as in Fig 5d, because such states can possibly be experimentally identified. Such an isolated system must clearly form a colour singlet state. A gluon pair produced as in Fig 7a is a colour singlet with probability $1/(N_c^2 - 1)$. This is also approximately the case for any connected gluon system, as e.g. the one in Fig 7b. (We note that with 5 gluons, which is the average number in Ariadne at the Z^0 -pole, we have 10 different connected gluon systems. If all of these would have the probability $1/8$ to form an isolated gluonic system, such systems would not be rare.)

An exception is two or more gluons originating from a single initial gluon as in Fig 7c. Such a system is always a colour octet. Thus it is essential to know if a gluon is emitted by a parent quark or a parent gluon. This is no problem in the cascade schemes implemented in the Herwig or the Jetset MC's. However, in the dipole cascade model a gluon is not emitted from a single parent, but is the result of the separation of a colour charge and anti-charge in a colour dipole. Furthermore colour coherence implies that a gluon emitted from a dipole between two parent gluons can be effectively emitted from a parent quark (i.e. colour triplet) charge.

This problem was studied in [16] and some results will be discussed in the next subsection. The colour factor for gluon emission from a quark is $C_F = \frac{1}{2}N_c [1 - 1/N_c^2]$, which is

slightly less than half the corresponding factor for emission from a gluon (which is connected to two dipoles), $C_A = N_c$. The aim of ref [16] was to study how to take into account this colour suppressed contribution to the cascade evolution, but the results can be used also for our purpose analysing the mother-daughter relation.

4.2 Mother-daughter relations in the dipole cascade model

A $q\bar{q}$ pair produced in an e^+e^- -annihilation event emits gluons according to the distribution

$$dn = C_F \frac{\alpha_s}{2\pi} \frac{x_1^2 + x_3^2}{(1-x_1)(1-x_3)} dx_1 dx_3 \quad (4)$$

where x_1 and x_3 are the conventional scaled quark and anti-quark momenta. For soft gluons this approximately equals the ‘‘dipole distribution’’

$$dn \approx C_F \frac{\alpha_s}{\pi} d \left[\ln k_\perp^2 \right] dy \quad (5)$$

where

$$\begin{aligned} k_\perp^2 &= s(1-x_1)(1-x_3) \\ y &= \frac{1}{2} \ln \frac{1-x_3}{1-x_1} \end{aligned} \quad (6)$$

The phase space available is approximately a triangular region, $|y| < \frac{1}{2} [\ln s - \ln k_\perp^2]$, in the $y - \ln k_\perp^2$ -plane, cf Fig 8a.

For the emission of two gluons the hardest one is distributed according to Eq (4) or (5), while the distribution of the softer gluon corresponds to two independent dipoles spanned between the quark and the gluon and between the gluon and the anti-quark respectively. For fixed $k_{\perp 2}$ of the second gluon, the available rapidity range in the two dipoles is $\ln(s_{qg_1}/k_{\perp 2}^2)$ and $\ln(s_{g_1\bar{q}}/k_{\perp 2}^2)$, which results in a total rapidity interval

$$\Delta y = \ln \frac{s_{qg_1}}{k_{\perp 2}^2} + \ln \frac{s_{g_1\bar{q}}}{k_{\perp 2}^2} = \ln \frac{s}{k_{\perp 2}^2} + \ln \frac{k_{\perp 1}^2}{k_{\perp 2}^2}. \quad (7)$$

Thus the available phase space for the second gluon is increased and corresponds to the folded surface in Fig 8b. Here the two dipoles correspond to the surfaces a+b and c+d+e respectively. The emission density in the two dipoles is proportional to $C_A/2$, but there is also a correction term with a relative weight $-1/N_c^2$ corresponding to a dipole between the quark and the anti-quark [17]. The result is a density proportional to $C_A/2$ on surfaces b and c and proportional to $C_F = \frac{1}{2}C_A [1 - 1/N_c^2]$ on surfaces a, d and e. Thus we see that surfaces b and c correspond to emission from the gluon charges (note that this area is determined by the transverse momentum $k_{\perp 1}$ of the first gluon; in the infinite momentum frame this corresponds to the energy times the emission angle) while surfaces a, d and e correspond to emission from a quark (or anti-quark) charge. Here e.g. surfaces a and e can be interpreted as emitted from the quark and the anti-quark. In surface d the quark and the gluon emit coherently as a single triplet charge, due to the soft gluon interference.

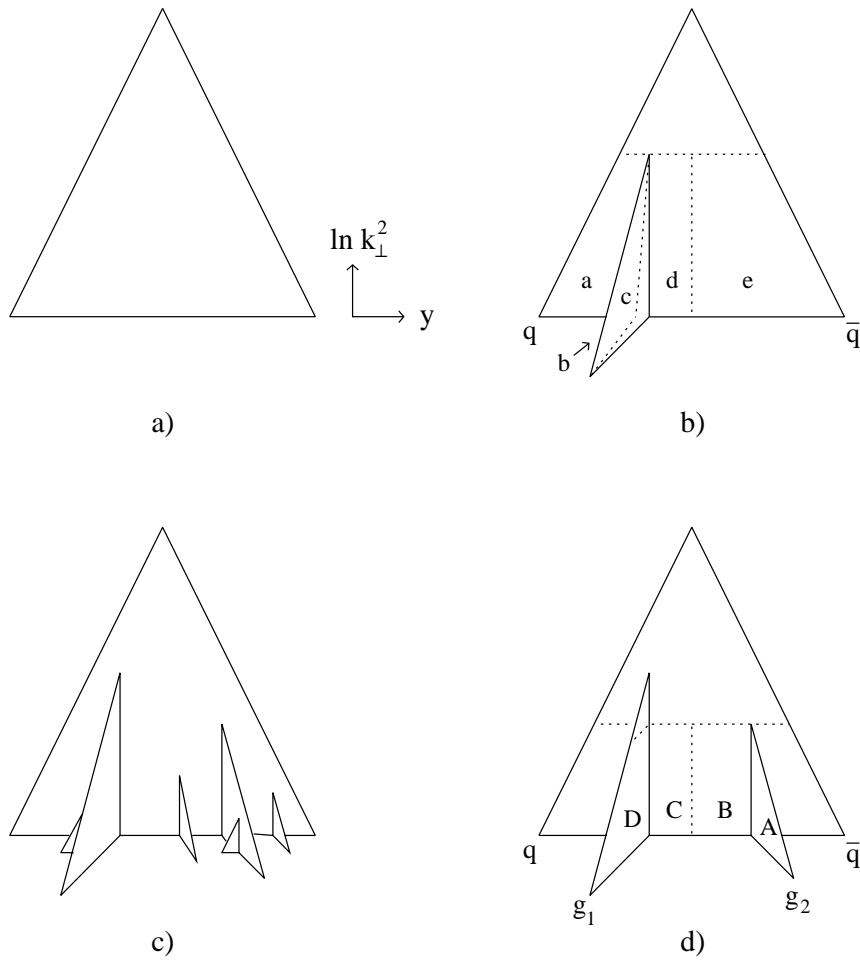


Figure 8: a) *The phase space for gluon emission from a $q\bar{q}$ pair is approximately a triangular region in the $y - \ln k_{\perp}^2$ plane.* b) *If one gluon is emitted the size of the phase space for emission of softer gluons corresponds to this folded surface.* c) *Every gluon emission increase the phase space for softer gluons producing a multi-fractal total phase space.* d) *Gluon emission associated with surfaces B and C corresponds to emission from an effective quark or an anti-quark charge (triplet or anti-triplet).*

In a similar way the emission of a third gluon corresponds to three dipoles etc. Each emission increases the phase space for softer gluons as leading to a multi-fractal structure illustrated in Fig 8c [15]. Consider in particular the emission from a $q\bar{q}g_1g_2$ system as shown in Fig 8d. Here surfaces A, B, C and D correspond to emissions from the dipole between the two gluons. In the same way as above surfaces A and D correspond to emissions from parent gluons, with density $C_A/2$, while in surface C the quark and gluon g_1 emit coherently as a triplet (quark) charge with density C_F . Similarly in surface B the anti-quark and g_2 emit coherently as an anti-triplet charge.

Finally we have to discuss how to associate an emitted gluon (with momentum k) to one of the surfaces in Fig 8d. Assume that the gluon is emitted from the dipole between the

gluons g_1 and g_2 . Thus it belongs to one of the surfaces A, B, C, or D. We first separate surface A from B+C+D. We then imagine a dipole between gluon g_2 and an effective quark, with momentum $\bar{p}_q + \bar{p}_{g_1} \equiv \bar{P}$. Make a Lorentz boost along \bar{P} such that the momentum \bar{p}'_{g_2} of g_2 in the new frame becomes orthogonal to \bar{P} . If the momentum \bar{k}' of the new gluon in this frame is closer to \bar{p}'_{g_2} than to \bar{P} the new gluon should be associated to surface A, otherwise with surface B+C+D. (With closer we mean that the relative angle is smaller.) In the same way we can decide whether the new gluon belongs to surface D or to A+B+C. If it belongs to neither A nor D, it obviously belongs to B+C, and thus is emitted by an effective colour triplet charge. This recipe can obviously be used also for a system with an arbitrary number of gluons.

5 MC Implementation

The models presented in Sections 3.1 and 3.2 are implemented in a modified version of the Ariadne MC. In the “cascade reconnection model” we check after each emission if a reconnection involving the new gluon can give a smaller λ measure. If that is the case this configuration will be used with probability 1/8 in the continuation of the cascade. An exception is when two or more gluons originate from a single parent gluon. Such a system must be a colour octet and is therefore not allowed to be separated from the rest of the state. For this reason we keep track of the history of all emissions, as described in Section 4.2³.

In the model where reconnection is only allowed after the perturbative phase (the soft reconnection model) there are generally many gluons and many reconnection possibilities. The probability that a certain reconnection should isolate a gluon system originating from a single gluon parent is therefore very small, and has here been neglected in the MC implementation.

With an implementation of the mother-daughter relation into the MC it is possible to also include the colour suppressed contributions to the emission probabilities. Thus in the MC the emission from an “effective” (anti-)quark charge is suppressed by the factor $2C_F/C_A = 1 - 1/N_c^2$. We have, however, not found any observable which is sensitive to this correction. The effect is small, and can generally be compensated by a retuning of the parameters in the fragmentation model.

6 Results

The modifications caused by the colour reconnections are generally small and not observable in average event properties. As in [4] we also here try to find a small corner of phase space, where effects could be visible. The events we want to study are those where an isolated gluon system is moving away from the remaining system, as illustrated in Fig 9. Such states

³A similar reconnection model is developed by Lönnblad and implemented in Ariadne version 4.07. In this model, however, all emissions from a gg dipole are treated as having a gluon parent. Therefore the reconnection effects become smaller than in our calculations.

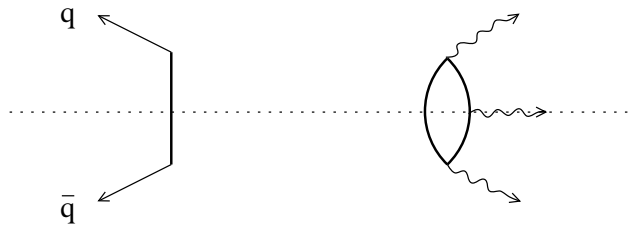


Figure 9: *We are particularly interested in situations where an isolated gluon system moves away from the remaining system, which may result in a central gap in the hadron distribution.*

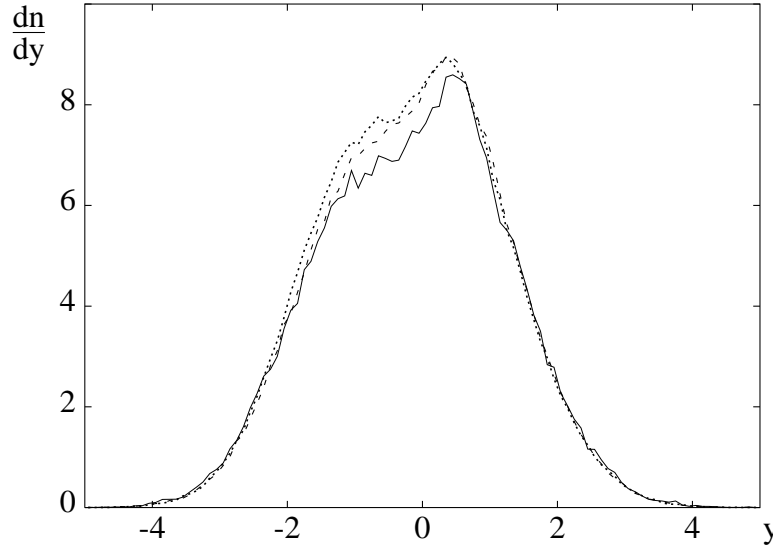


Figure 10: *Rapidity distribution of charged particles, default Ariadne (dotted line), the soft reconnection model (dashed line), and the cascade reconnection model (solid line). Both models are retuned i.e. for average events they reproduce the expected distributions. One million Z^0 decay events are analyzed. The rapidity is measured along the direction of the added $q\bar{q}$ momenta.*

could reveal themselves by a central gap in the rapidity distribution (cf also ref [18]).

To know that we have a quark and an anti-quark moving to one side we consider double tagged events with either a $b\bar{b}$ or a $c\bar{c}$ pair. To obtain a sufficient separation between the two parts in Fig 9 we have studied events where the angle between the quark and the anti-quark is less than 110° , and the rapidity axis is chosen along the sum of their momenta. In Fig 10 we show the rapidity distribution obtained in the different models; normal Ariadne, the soft connection model, and the cascade reconnection model. Here positive y -values are in the direction of the $q\bar{q}$ pair. The different Monte Carlo's are tuned to reproduce experimental data. We see a dip in the distributions from the reconnection models as compared to normal Ariadne. This difference could be a signal of non trivial effects early in the event.

The difference between the models is enhanced if we study, as in ref [4], the probability to find an event with no charged particles in a central rapidity interval. Choosing the central

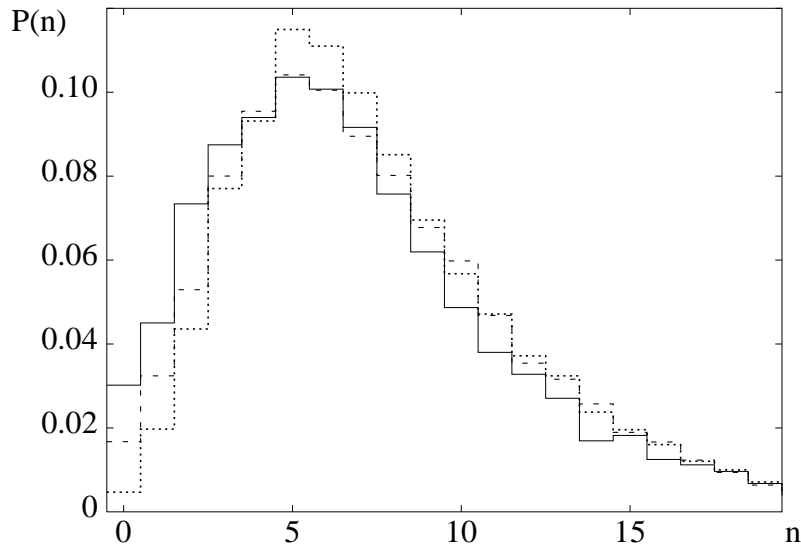


Figure 11: *Charged multiplicity in the rapidity interval $[-1, 0]$, default Ariadne (dotted line), the soft reconnection model (dashed line), and the cascade reconnection model (solid line). Both our models are retuned. The distribution is normalized w.r.t. accepted events.*

rapidity region between -1 and 0 we obtain the distributions in Fig 11, and we see significant difference between the distributions. It is 7 times more probable to find an event with no particles in the central rapidity bin in the cascade reconnection model as compared to normal Ariadne (in the soft reconnection model this factor becomes 3.5). In Fig 11 we see that there is also quite a large difference in the probability to find events with only 1 or 2 charged particles in the central rapidity bin.

With the probabilities from Fig 11 we can calculate the number of events to be expected to have no charged particles in the central rapidity bin. The results for 3 million Z events at LEP1, assuming 10% double tagging efficiency of the initial heavy quarks, are shown in the table below

Model	Number of events with n_{ch}			Total number of accepted events
	0	1	2	
Cascade reconnection	103	154	229	32700
Soft reconnection	62	130	220	37700
Background (normal Ariadne)	17	73	162	37100

Table 1: *Expected number of events with 0, 1, or 2 charged particles in a rapidity interval $-1 < y < 0$. Total events is the number of events which are left after the condition that the angle between the $c\bar{c}$ or $b\bar{b}$ momenta should be less than 110° .*

7 Conclusions

We have a very limited knowledge about how the confinement mechanism works in processes like $e^+e^- \rightarrow q\bar{q}g \dots g$, when there are several identical colour charges. The transition from a Feynman diagram to a string configuration or a cluster chain is not straight forward, as the partons can be connected in several different ways. We do not know if in such a situation Nature chooses a particular configuration at random, or if some configuration is dynamically favoured. The choice of a configuration which differs from the one initially obtained in the generation procedure is often called colour reconnection or recoupling, although the partons have not been connected before, and thus should not be called reconnected.

Also in the perturbative parton cascade we have no well founded recipe for describing the interference effects, which correspond to non-planar diagrams and are caused by identical colour charges. Although these effects are in principle calculable within perturbative QCD, this is at present not possible in practice.

To learn more about how the confinement mechanism and the interference effects work, we have studied two different models. In these models it is assumed that configurations, where the confining string connects partons which are close in phase space, are dynamically favoured.

We are in particular interested in the possibility that a colour singlet gluon system hadronizes isolated from the remainder of the state. A possible signal for such events is a central rapidity gap in events where the angle between the quark and the anti-quark is relatively small. Using double tagged events with heavy $c\bar{c}$ or $b\bar{b}$ quarks, with a relative angle less than 110° , it is possible to find a significant signal, if such events appear in Nature.

If this type of (re)connected states appear in Z decays it may also be an indication that reconnection might appear between the decay products of two W 's in the reaction $e^+e^- \rightarrow W^+W^- \rightarrow q_1\bar{q}_2Q_1\bar{Q}_2$ at LEP2. This would be important e.g. for a precision measurement of the W mass.

Acknowledgments

We would like to thank dr L. Lönnblad and dr T. Sjöstrand for valuable discussions.

References

- [1] B. Andersson, G. Gustafson, G. Ingelman, and T. Sjöstrand, *Phys. Rep.* **97** 31 (1983)
- [2] G. Marchesini, B.R. Webber, *Nucl. Phys.* **B238** 1 (1984)
B.R. Webber, *Nucl. Phys.* **B238** 492 (1984)
- [3] G. 't Hooft, *Nucl. Phys.* **B190** 455 (1981)
- [4] G. Gustafson, and J. Häkkinen, *Z. Phys.* **C64** 659 (1994)
- [5] G. Gustafson, U. Petterson, and P.M. Zerwas, *Phys. Lett.* **B290** 90 (1988)
- [6] T. Sjöstrand, and V. Khoze, *Z. Phys.* **C62** 291 (1994)
T. Sjöstrand, and V. Khoze, *Phys. Rev. Lett.* **72** 28 (1994)
- [7] L. Lönnblad, CERN TH/95-218
- [8] G. Gustafson, *Phys. Lett.* **B175** 453 (1986)
G. Gustafson, and U. Petterson, *Nucl. Phys.* **B306** 746 (1988)
B. Andersson, G. Gustafson, L. Lönnblad, *Nucl. Phys.* **B339** 393 (1990)
- [9] A.H. Mueller, *Phys. Lett.* **B104** 161 (1981)
B.I. Ermolaev, and V.S. Fadin, *JETP Lett.* **33** 269 (1981)
A. Bassetto, M. Ciafaloni, G. Marchesini, and A.H. Mueller, *Nucl. Phys.* **B207** 189 (1982)
- [10] L. Lönnblad, *Comp. Phys. Comm.* **71** 15 (1992)
- [11] G. Marchesini, B.R. Webber, G. Abbiendi, I.G. Knowles, M.H. Seymour, and L. Stanco, *Comp. Phys. Comm.* **67** 465 (1992)
- [12] T. Sjöstrand, *Comp. Phys. Comm.* **82** 74 (1994)
- [13] G. Gustafson, *Z. Phys.* **C15** 155 (1982)
- [14] See e.g. M. Schmelling, CERN-PPE/95-129
- [15] B. Andersson, P. Dahlqvist, and G. Gustafson, *Phys. Lett.* **B214** 604 (1988)
B. Andersson, P. Dahlqvist, and G. Gustafson, *Z. Phys.* **C44** 455 (1989)
- [16] G. Gustafson, *Nucl. Phys.* **B392** 251 (1993)
- [17] Ya.I. Azimov, Yu.L. Dokshitzer, V.A. Khoze, and S.I. Troyan, *Phys. Lett.* **B165** 147 (1985)
- [18] J.D. Bjorken, S.J. Brodsky, and H.J. Lu, *Phys. Lett.* **B286** 153 (1992)
H.J. Lu, S.J. Brodsky, and V.A. Khoze, *Phys. Lett.* **B312** 215 (1993)

Paper V

$b\bar{b}$ -fragmentation and $B\pi$ correlations

Jari Häkkinen¹

Department of Theoretical Physics, Lund University,
Sölvegatan 14A, SE-223 62 Lund, Sweden

Submitted to
Z. Phys.

Abstract:

We show that experimental data are in very good agreement with predictions from the string fragmentation model by Bowler and Morris. We present a physical interpretation and discuss the relation to results obtained from Perturbative QCD and Local Hadron Parton Duality (LPHD). We also present implications for $B\pi$ correlations and the possibility to use these as a tag to study CP violation in B decays.

¹jari@thep.lu.se

1 Introduction

An understanding of hadronization in b-quark jets is important for several reasons.

- It can help to understand the confinement mechanism.
- A good description of jet fragmentation is essential to reconstruct an underlying hard parton interaction. Thus e.g. a measurement of the reaction $e^+e^- \rightarrow W^+W^- \rightarrow q_1\bar{q}_2q_3\bar{q}_4$ at LEP2 is important for determination of the W mass, which can give information about virtual corrections involving the Higgs particle.
- As proposed in [1] particle correlations in b and \bar{b} jets can be used as a tag which e.g. can improve a determination of CP violation in B decay.

The Lund string fragmentation model [2] (implemented in the Jetset MC [3]) and the cluster fragmentation model [4] (implemented in the Herwig MC [5]) have been frequently used by experimental groups to describe the hadronization process in the analysis of their data. Previous official versions (up to v7.3) of the Jetset MC have in the default version given a too hard B meson spectrum, and in consequence too low total multiplicity in $b\bar{b}$ events. To describe the data, experimentalists have instead often used the Peterson et al. model [6] for the B meson momentum, combined with string fragmentation for the remainder of the jet. That model contains one free parameter which can be adjusted to the experimental data. The two most essential experimental observables are the average B-meson energy (or \bar{x}_B) and the average total charged multiplicity \bar{n} . In the Jetset MC it is assumed that after separation of the B hadron, the rest of the jet corresponds to a light quark jet with the remaining energy, and therefore there is a correlation between \bar{x}_B and \bar{n} . It is noteworthy that this correlation agrees well with data. Bowler and Morris [7] have proposed a modification of the initial Lund Model for the fragmentation of heavy b or c quarks. This model has no free parameter, and therefore gives a definite prediction. In the present paper we will demonstrate that the model

- agrees well with expectations from a string dynamics scenario.
- agrees qualitatively with expectations from perturbative QCD and local parton hadron duality or cluster fragmentation.
- agrees very well with experimental data.

Equipped with a description of b fragmentation, we will in this paper also study the $B\pi$ correlations and estimate the efficiency of the tagging method proposed in ref [1] for a study of CP violation in B decays.

2 b jet fragmentation

The Lund string fragmentation model is implemented in Jetset to take care of the fragmentation of $q\bar{q}$ strings. The main idea in the fragmentation of the original $q\bar{q}$ pair, i.e. $e^+e^- \rightarrow Z^0, \gamma \rightarrow q\bar{q}$, is that new quark–anti-quark (diquark–anti-diquark) pairs are produced in the colour field stretched between the original quark pair. The constituents of a new pair obtain their transverse mass through the tunneling process needed to create them [2]. There is a flavour ordering present throughout the string so that the flavour quantum number is preserved. Details of how these properties are given to hadrons produced in

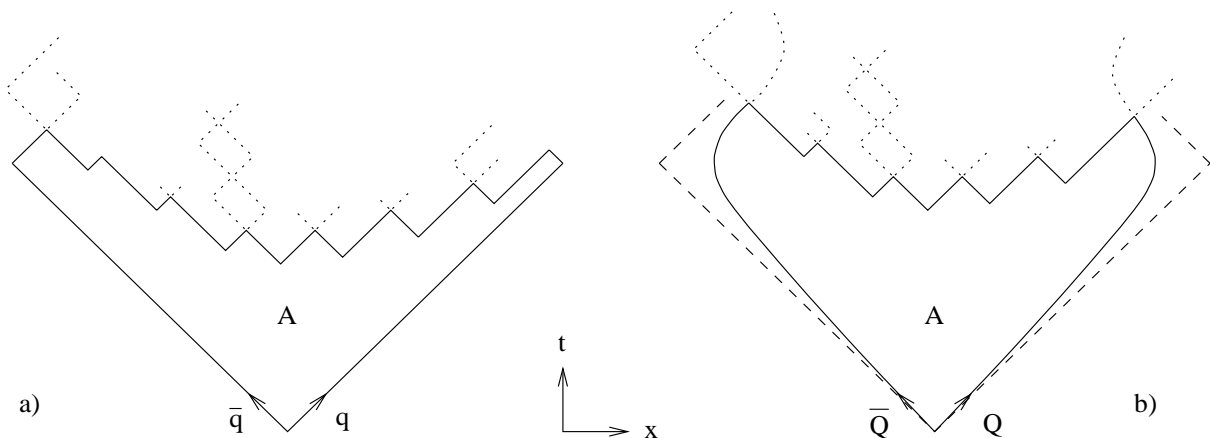


Figure 1: *Quark trajectories in the Lund model. Light quarks move along light cones a), while heavy quarks move along hyperbolae b). The finite mass of heavy quarks decreases the area bounded by the solid lines resulting in softer B spectrum.*

Jetset will not concern us here. Instead we are going to study the energy and longitudinal momentum distribution of the produced hadrons.

A basic assumption in the Lund model is “left-right symmetry”, which means that the fragmentation process should look the same irrespective to which end of the string we start from in an iterative process. From this assumption follows that the probability dP to obtain a definite final state with hadron momenta p_i (being 1+1 dimensional vectors if we neglect the transverse dimensions) with masses m_i is given by [8]

$$dP \propto \prod_i N_i d^2 p_i \delta(p_i^2 - m_i^2) \delta(\sum_k p_k - p_{total}) \exp(-bA) \quad (1)$$

where A is the area indicated in Fig 1. It is suggestive that this expression is the product of a phase space factor and the exponent of an area, which can be interpreted as (the imaginary part of) an action and is similar to a Wilson loop integral.

The distribution in Eq (1) can be generated iteratively starting from one end of the quark–anti-quark system. With the other properties fixed, the probability to give a hadron a fraction z of the available energy is given from a splitting function,

$$f(z) \propto \frac{1}{z} z^{a_i} \left(\frac{1-z}{z}\right)^{a_k} \exp\left(-\frac{bm_{\perp}^2}{z}\right). \quad (2)$$

The parameters a_i could in principle depend on the flavour of the associated quark–anti-quark pair. In Eq (2) the index i corresponds to the flavour of the previously produced $q\bar{q}$ pair and k to the latest produced flavour pair. Since experimental data seems to need the use of only two different a -values in connection with quark–anti-quark and diquark–anti-diquark production respectively (the latter leading to baryon–anti-baryon production), two different a -values have been used in most applications.

We also note that in the string model it is assumed that heavy quarks like c or b can only be produced perturbatively, either directly from the initial γ or Z , or in the process $g \rightarrow q\bar{q}$,

and not in the soft string breaking process. Thus a b-quark is always at the end of a string, and the argument based on left-right symmetry is really not applicable for the B hadrons. The fragmentation will always be left-right symmetric whatever energy is given to the B and the \bar{B} at the ends of the string. A modification of the splitting function in Eq (2), based on the physical ideas behind the string model, was proposed by Bowler and Morris in [7]. If the initial $q\bar{q}$ pair is a heavy $c\bar{c}$ or $b\bar{b}$ pair, these quarks do not move along the light cones but instead along hyperbolae in the $x-t$ diagram as shown in Fig 1b. It is then natural to insert in Eq (1) the area bounded by the quark trajectory as indicated in Fig 1b [7]. The result is a softer spectrum for the leading B meson, which is well approximated by the expression

$$f(z) \propto \frac{1}{z^{1+r_Q} b M_Q^2} z^{a_i} \left(\frac{1-z}{z}\right)^{a_k} \exp\left(-\frac{b m_{\perp}^2}{z}\right). \quad (3)$$

Here r_Q is predicted to be equal to 1, but is introduced as a parameter in Jetset. This is done to make it possible to control the effect of the modification.

A relativistic string or a homogeneous (colour-)electric field is invariant under longitudinal boosts, which in the string model is reflected in a smooth distribution in rapidity for the produced hadrons. Although it is not at all a definite consequence, we feel that from the physical picture of hadrons formed from the energy stored in a string-like field, it is most natural that the distribution of light hadrons stretch up to the rapidity of the leading heavy B meson (or D meson in case of a c quark jet). Thus there should neither be a large rapidity gap nor should the rapidity distribution of the light hadrons continue beyond the rapidity of the heavy meson. This is actually the case for the splitting function in Eq (3), while for the function in Eq (2) a large gap is obtained between the leading B-meson and the remainder of the jet. The average rapidity difference, $\overline{\Delta y}$, between the B meson and the first rank meson in the remainder is 0.88 which should be compared with the rapidity difference 0.91 between neighbouring light mesons in the middle of the string. The corresponding numbers for the harder distribution is 1.96 and 0.92, respectively. (As representative for a light meson we have used ρ mesons to avoid kinematical effects from the exceptionally low pion mass, cf the discussion in [9].) The difference between the two distributions is further illustrated in Fig 2. This figure shows the rapidity difference distributions between differently flavoured neighbouring mesons. The large (compared to the light mesons within the string) rapidity difference between the leading heavy B and the light ρ is present for the hard distribution while the softer gives similar distributions irrespective to flavour and rank.

Such a smooth rapidity distribution is also expected in PQCD assuming LPHD or cluster fragmentation. This is a consequence of the fact that the initial b-quark radiates gluons with (pseudo-)rapidities up to the rapidity of the b-quark, but not beyond this value. The region of larger rapidities has been called the dead cone [10].

To be able to describe LEP $e^+e^- \rightarrow q\bar{q}$ data correctly gluons must be included. In all simulations below gluons are radiated before string breakup. When we use the original symmetric Lund fragmentation formula (Eq (2)) in the simulations we find that the average $\overline{x_E}$ for B-mesons decreases to 0.77. This is well outside the experimental value, $0.702 \pm 0.002 \pm 0.008$ (average of the results reported from L3, ALEPH, OPAL and DELPHI experiments at LEP in 1994) [11]. Using the modified formula, Eq (3), we find that $r_Q = 1.05 \pm 0.07$, gives an $\overline{x_E}$ within the experimental errors. We note that this is in very good agreement with the

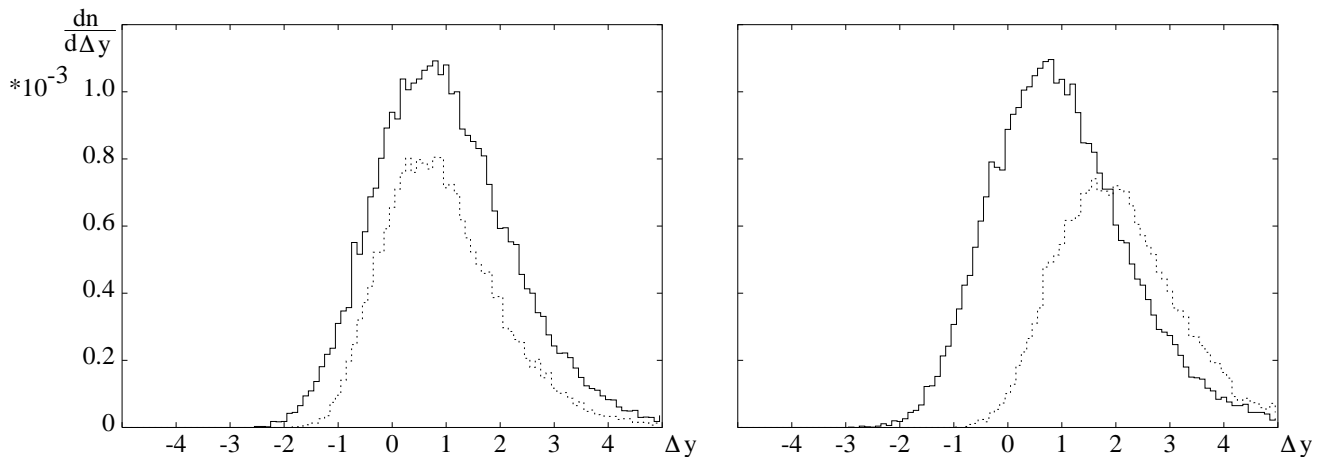


Figure 2: a) *The full line shows the rapidity difference between rank 2 and rank 3 ρ 's, and the dotted line shows the rapidity difference between B and rank 2 ρ 's, obtained by the modified splitting function, Eq (3). b) Shows the same distributions when the original splitting function, Eq (2), is used.*

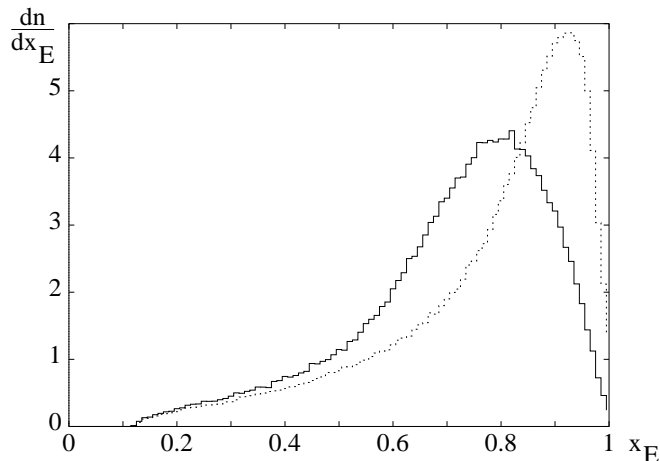


Figure 3: *Combined $B^0 B^+$ energy spectrum obtained at the Z pole, using the original (dotted line), and the modified (solid line) splitting functions, Eqs (2) and (3), respectively. (Gluon radiation is included before fragmentation.)*

theoretically expected value 1. In Fig 3 we show the combined B^0 and B^+ energy spectrum using Eq (2) and Eq (3), respectively. We see that the spectrum is considerably softened by the modified function.

The acceptable values of r_Q shift down to 0.98 ± 0.08 when 30% of the produced mesons have orbital angular momentum (tensor mesons) in the simulations. The B meson energy spectrum is softened by the $(B\pi)$ resonance states, and in consequence the splitting function can be harder as compared with simulations without tensor mesons.

Using the softer b hadron energy distribution (Eq (3) with $r_Q = 1$) will increase the average number of charged particles produced in Jetset. The average difference between

Splitting function	Tensors	Corr.	a	b	ϵ_b	$\bar{n}_b - \bar{n}_{uds}$	x_E	$\langle \text{Thrust} \rangle$
Original Lund Eq (2)	0	no	0.30	0.49	-	1.2	0.77	0.93
	0.30	no	0.30	0.75	-	0.8	0.77	0.93
	0	yes	0.50	0.22	-	2.0	0.70	0.92
	0.30	yes	0.50	0.52	-	1.2	0.74	0.93
Modified Lund Eq (3)	0	no	0.30	0.58	-	3.1	0.71	0.93
	0.30	no	0.30	0.90	-	3.0	0.72	0.93
	0	yes	0.90	0.44	-	3.3	0.66	0.93
	0.30	yes	0.90	0.90	-	3.0	0.69	0.93
Peterson <i>et al.</i>	0	no	0.30	0.53	0.0013	1.9	0.74	0.93
	0.30	no	0.30	0.85	0.0003	1.43	0.76	0.93
	0	yes	0.50	0.22	0.0082	2.4	0.68	0.92
	0.30	yes	0.50	0.57	0.0017	2.1	0.71	0.93
Experimental data						3.14 [11] ± 0.44	0.702 [11] ± 0.002 ± 0.008	0.9349 [13] ± 0.0006 ± 0.0024

Table 2: *Some typical results obtained when the fragmentation models are tuned to retain the charged multiplicity at LEP1. The 'Tensor' column shows the fraction of tensor meson production in the simulations, and the 'Corr.' column shows if flavour correlations are included.*

the number of charged particles produced in b events compared to uds events, $\bar{n}_b - \bar{n}_{uds}$, becomes $3.06_{-0.09}^{+0.29}$ ($2.63_{-0.26}^{+0.12}$ for 30% tensor mesons). This is in agreement with the experimental value, 3.14 ± 0.44 [11]. Compared with an analytic MLLA calculation which gives 5.5 ± 0.8 [12], there is a large discrepancy. Despite this discrepancy we see that a detailed MC, with the same fundamental properties as MLLA, agrees with experimental data. The original splitting function in Eq (2), however, gives an average difference between the number of charged particles in b and uds events of 1.21, which is well below the experimental value.

Similar calculations have also been performed using other fragmentation models implemented in the Jetset MC: the Peterson *et al.* model for heavy quark fragmentation, inclusion of tensor meson production, and introduction of transverse momentum correlations and flavour correlations between neighbouring string breakups presented in [9]. In all simulations an optimization of the fragmentation parameters, a , b , and ϵ_b , have been performed in order to try to retain several experimental observables (\bar{n}_{ch} , $\bar{n}_b - \bar{n}_{uds}$, \bar{x}_E for B mesons, and average thrust) at LEP1 energies. In Table 2 we list results obtained when the different fragmentation models are used. The a and b parameters are chosen to give the best compromise for a given model, with the condition that the observed charged particle multiplicity at LEP1 is retained.

We see that the Peterson *et al.* model, and the original splitting function, do not reproduce the experimental data. When no flavour correlations are included the modified splitting function performs well. However, in the presence of flavour correlations there seems to be a need of some amount of tensor meson production. We believe the fraction of tensor

meson production used in the MC's are extreme values of the real fraction at LEP1, and note that the OPAL Collaboration expects the fraction to be at least 20% [14]. Inclusion of flavour correlations in the simulations improve the performance of MC's when the Peterson *et al.* model or the original splitting function is used, but the discrepancy with experimental data is still quite large.

We conclude that the splitting function in Eq (3) is both physically motivated and in better agreement with experimental data than the other fragmentation models implemented in Jetset, although these cannot be fully ruled out on the basis of above considerations.

3 $B\pi$ correlations as a flavour tag and CP violation

In [1] it was suggested to use $B\pi$ correlations as a flavour tag in a study of CP violation in B decays. In this section we will study these correlations and estimate the efficiency in CP violation studies. We will also study how the relation between efficiency and purity varies with the mass of the $B\pi$ pair.

$B\pi$ correlations depend on the properties of b-jet fragmentation, and also on the production rate for B resonances decaying into a $B\pi$ pair. In the default version of the Jetset MC there are no correlations in flavour or transverse momentum between neighbouring $q\bar{q}$ string breakups. In [9] it is argued that due to the exceptionally small pion mass (the pions have also properties corresponding to a Goldstone boson) such correlations are expected to some degree. These flavour correlations could influence the $B\pi$ correlations, even if their effect on \bar{x}_B and the inclusive spectra is negligible. In the following we will also study this possibility.

If a B^0 ($\bar{b}d$) meson is produced in a $\bar{b}b$ event the associated \bar{d} is likely to end up in a π^+ near in momentum space. This π^+ could be part of the remaining jet, either as a directly produced pion or the decay product from e.g. a ρ meson. The $B^0\pi^+$ pair can also be decay products from a parent B resonance. From iso-spin invariance the $B^0\pi^+$ correlations are related to $B^\pm\pi$ correlations, which are experimentally studied by the OPAL collaboration [14].

Let us first study the case where the \bar{d} partner of a B^0 is a leading parton in the remaining jet. The tagging possibility relies on the fact that the excess positive charge from the \bar{d} is found in the leading end of the jet, usually in the first rank hadron (of the remaining jet). If it is found in the first rank hadron the characteristic invariant $B\pi$ mass is determined by the relation

$$M_{B\pi}^{char} \approx M_B + m_\perp \cosh \Delta' \quad (4)$$

where m_\perp is the transverse mass of the pion and Δ' is the rapidity difference between the B and the pion or the parent resonance if the pion comes from e.g. a ρ meson. Since the energy spectrum for the B mesons is strongly peaked at high energies, with an average around $\bar{x}_E \approx 0.7$, the $B\pi$ mass increase rapidly for higher rank pions with lower energy in the cms. Thus to enhance the signal it is favourable to study only pairs with mass below 5.8GeV. We also note that low energy B mesons can be produced in perturbative gluon splittings, $g \rightarrow b\bar{b}$, but this is estimated to be a very small contribution at LEP1 energies [15].

In ref [14] it is assumed that the next $q\bar{q}$ pair in the string breakup has the same probability to be a $u\bar{u}$ as a $d\bar{d}$ pair. This is not necessarily the case, even if the fragmentation is iso-spin invariant. Consider a toy model in which only pions are produced. Then iso-spin invariance implies equal numbers of π^+ , π^0 , and π^- , which means that a $d\bar{d}$ pair must be followed by a $u\bar{u}$ with probability 2/3 and a $d\bar{d}$ only with probability 1/3. (Equal probabilities would give twice as many π^0 as π^+ or π^- .) This is the type of flavour correlations discussed in ref [9].

From our estimates the effect of a realistic degree of flavour correlations is small. It could conceivably affect an estimate of $B\pi$ resonance by distorting the background. The flavour correlations imply that the excess positive charge is over compensated in the first rank meson, followed by a negative contribution in the second rank, a still smaller positive contribution in the third rank meson, etc. We want in the future to estimate the magnitude of such a possible distortion, to see if it could have a noticeable affect on the experimental results. We note that the OPAL Collaboration estimates that $(B\pi)$ resonances contributes with at least 20% of the total production of B mesons in $Z^0 \rightarrow b\bar{b}$ fragmentation [14].

In [1] a mass estimate for the $(B\pi)$ resonance is obtained from extrapolation of charmed meson data to B mesons. The estimate puts an upper limit on the resonance mass at 5.8GeV. This estimate is supported by OPAL data where an excess, as compared with simulations where no resonance meson production was included, of $B^+\pi$ pairs is found at 5.7GeV. The $(B\pi)$ resonance will eventually decay to a $B\pi$ pair close in phase space, and contribute to this excess.

Pions produced in the center of the string have a fairly large momentum relative to the B^0 meson. If we want to retain $B^0\pi$ pairs close in phase space, the relative momentum between central pions and the B puts kinematical constraints on the B energy, forcing the B energy to be small. We have seen above that the average x_E for B mesons is 0.70, so central pions will have small chances of making a small mass pair with the B.

The method to trace CP violating B mesons proposed in ref [1] depends on the correlation of B^0 (\bar{B}^0) mesons with pions nearby in the phase space, *and* the detection of a CP eigenstate f as a B^0 or \bar{B}^0 decay product in conjunction with a similar pion.

The suggested method leads to a dilution of *any* real CP violating asymmetry. Starting with the time integrated asymmetry [16]

$$A(f) \equiv \frac{\Gamma(B_{t=0}^0 \rightarrow f) - \Gamma(\bar{B}_{t=0}^0 \rightarrow f)}{\Gamma(B_{t=0}^0 \rightarrow f) + \Gamma(\bar{B}_{t=0}^0 \rightarrow f)}, \quad (5)$$

where f denotes a CP eigenstate and $\Gamma(B_{t=0}^0 \rightarrow f)$ is the decay width when the state f is produced as a decay product of a state starting out as a B^0 at $t=0$.

Expressing the asymmetry in final states we get

$$A(f) = \frac{1}{1+x^2} \frac{[N(\bar{T}\pi^-) + N(T\pi^-)]N_{f+} - [N(T\pi^+) + N(\bar{T}\pi^+)]N_{f-}}{[N(\bar{T}\pi^-) - N(T\pi^-)]N_{f+} + [N(T\pi^+) - N(\bar{T}\pi^+)]N_{f-}}. \quad (6)$$

T is a flavoured state we know to come from a B^0 , and is used to determine the flavour of the B meson. $N(T\pi)$ is the relative number (probability) of states T in conjunction with a pion.

$N_{f\pm}$ denotes the number of final states $f\pi^\pm$. x is the mass mixing parameter $x \equiv (\Delta m/\Gamma)$. (Notation taken from [1].)

Considering a charge symmetric production process ($p\bar{p}$ or e^+e^-) where B^0 and \bar{B}^0 production should be equal, i.e. $N(T\pi^-) = N(\bar{T}\pi^+)$ and $N(T\pi^+) = N(\bar{T}\pi^-)$, gives

$$A_{obs} \equiv \frac{N_{f^+} - N_{f^-}}{N_{f^+} + N_{f^-}} = \frac{N(T\pi^+) - N(T\pi^-)}{N(T\pi^+) + N(T\pi^-)}(1 + x^2)A(f), \quad (7)$$

and we see that the tagging process suppresses the experimentally observed asymmetry. We are going to estimate the efficiency of the suggested tagging method by calculating the dilution factor,

$$\xi \equiv \frac{N(T\pi^+) - N(T\pi^-)}{N(T\pi^+) + N(T\pi^-)}, \quad (8)$$

of Eq (7) for the reaction $e^+e^- \rightarrow b\bar{b} \rightarrow X$ as a function of the $B\pi$ pair mass. From the B production considerations above we expect an excess of low mass $B^0\pi^+$ pairs giving a non vanishing dilution factor.

In the calculations we use Jetset with the softer fragmentation distribution, Eq (3), since this is in best agreement with experimental data. As the tagged state we use the B^0 meson and accept all possible $B^0\pi$ pairs. In Fig 4a we show the invariant mass multiplicity distribution for $B^0\pi$ pairs from 10^6 mixed flavour events at LEP1 energies. Of these approximately 218000 events will be $b\bar{b}$ events giving b hadrons. In the figure we clearly see a difference between the $B^0\pi^+$ and $B^0\pi^-$ distributions. Continuing to large $m(B\pi)$ the difference decreases since the $B\pi$ -charge correlations vanishes.

In the calculation of the average dilution factor we only include $B\pi$ pairs with masses below 5.8GeV. This restriction eliminates the chance of using central pions in the pair and emphasize the contributions from $(B\pi)$ resonances which are more probable to give a right charged pion. Accepting all possible pairs with $m(B^0\pi) \leq 5.8\text{GeV}$ the average dilution factor is $\xi = 0.13-0.17$. The variation in ξ is mainly due to different production fractions of tensor mesons allowed in the simulations, and we note that a larger fraction of resonance meson production will enhance the efficiency of the tagging method.

The efficiency of the proposed tagging method will increase if only the most correlated pion in an event is taken into account. This pion should be the fastest one in the event. In Fig 2 we have plotted the rapidity difference between rank 2 and rank 3 mesons in the Lund string. Indeed we see that in general the fastest meson is the rank 2 particle, i.e. the neighbour to the b hadron. (In Fig 2 we show distributions for ρ mesons, but similar results are obtained for any directly produced particles.) Considering only this pion in every event gives a more peaked invariant mass distribution as can be seen in Fig 4b. The average dilution factor, for pairs with $m(B\pi) \leq 5.8\text{GeV}$, increases to 0.17-0.20. Again the dilution factor depends on the fraction of tensor mesons produced in the simulations.

The distributions in Fig 4 can be used to calculate the dependence of the dilution factor on the $B\pi$ invariant mass. The result is plotted in Fig 5. We see that at $m(B\pi) = 5.5\text{GeV}$ the dilution factor is about 0.10 and grows to a maximum at $m(B\pi) = 5.8\text{GeV}$. The growth is much larger if only the fastest pion is used as can be seen in Fig 5b. The large difference

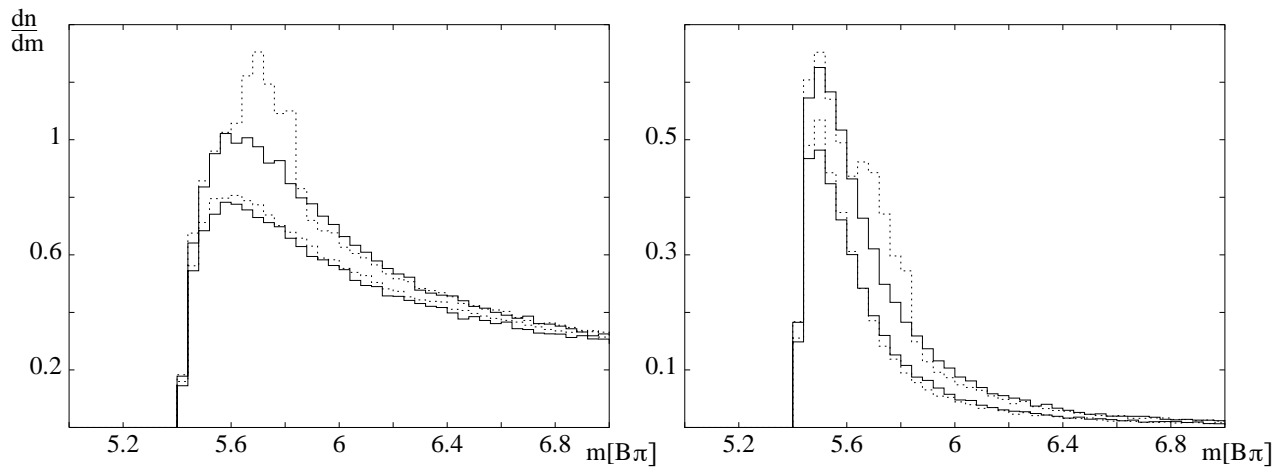


Figure 4: *Invariant mass multiplicity distributions.*

a) *Events where all possible $B^0\pi$ pairs are considered. The full lines are data from events without any tensor mesons. The upper full line is for $B^0\pi^+$ pairs, and the lower full line is for $B^0\pi^-$ pairs. The dashed lines are for events with a tensor meson fraction of 30%. Again the upper (dashed) line is for $B^0\pi^+$ and the lower for $B^0\pi^-$.*

b) *Events where only the fastest pion is paired with the B meson. The different lines describe the same sort of data as in a).*

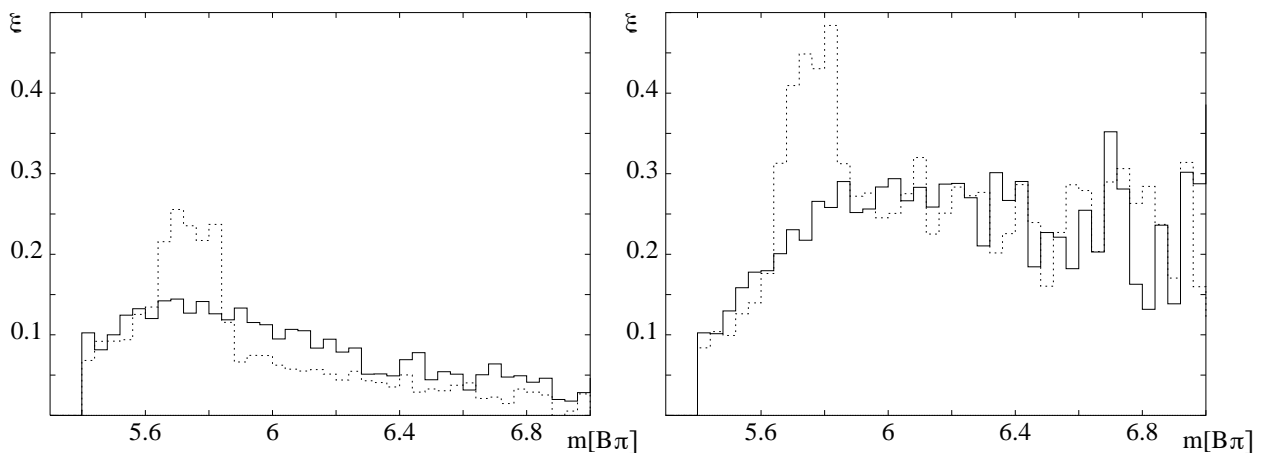


Figure 5: *Dilution factor as a function of invariant mass.*

a) *Events where all possible $B^0\pi$ pairs are considered. The full line is for events without any tensor mesons, and the dashed line is for events with a tensor meson fraction of 30%.*

b) *Events where only the fastest pion is paired with the B meson. The two lines describe the same sort of data as in a).*

in the maximum of $\xi =$ around 5.8GeV depend on whether tensor mesons are produced or not, since the decay of B^{**} mesons contributes to the $B^0\pi^+$ and therefore enhance the dilution factor. In Fig 5b ξ remains around 0.25 above $m(B\pi) = 6$ GeV, but very low rates are expected above this mass, cf. Fig 4b.

When the tensor meson production rate is assumed to be within 20–30%, we calculate the dilution factor in the invariant mass range $5.6 < m(B^0\pi) < 5.9\text{GeV}$ to be 0.31–0.35. The OPAL Collaboration finds a similar value, 0.364 ± 0.024 , in their $B^+\pi$ studies [14], where it is expected that at least 20% of the B mesons are produced as decay products of heavier resonances at LEP1

We have also performed the same calculations with an MC where we included flavour correlations between neighbouring $q\bar{q}$ pairs. The results from these runs are very similar to those found above without such flavour correlations.

4 Conclusions

A modification of the original Lund string fragmentation function (Eq (2)), where the reduction in the “colour coherence area” due to the large mass of heavy quarks is taken into account, will give a softer energy distribution for heavy mesons. Experimental data are reproduced by tuning the parameter r_Q to 1.05 ± 0.07 (cf. Eq (3)), which is consistent with the theoretically derived $r_Q \equiv 1$. The Lund string model, together with the modified splitting function, also gives rapidity distributions in agreement with PQCD assuming LPHD or cluster fragmentation. The Jetset MC is found to perform better when the modified splitting function is used, as compared to the the original splitting function or the Peterson *et al.* fragmentation model.

The possibility to experimentally observe CP violating B mesons using pion charge to tag the flavour of the leading B^0 is always diluted. This dilution depends on the fraction of resonance B meson production. In the OPAL measurement [14] it is found that at least 20% of the B mesons are produced as decay products of heavier resonances at LEP1. We estimate the dilution factor, defined in Eq (8), in the invariant mass range, $5.6 < m(B^0\pi) < 5.9\text{GeV}$ to be 0.31–0.35. The uncertainty is due to the fraction of resonance production, here we have used 20–30%. The OPAL Collaboration finds a similar value, 0.364 ± 0.024 , in their $B^+\pi$ studies [14].

Acknowledgments

I would like to thank prof Gösta Gustafson and dr Torbjörn Sjöstrand for valuable discussions.

References

- [1] M. Gronau, A. Nippe, J.L. Rosner, *Phys. Rev.* **D47** 1988 (1993)
- [2] B. Andersson, G. Gustafson, G. Ingelman, T. Sjöstrand, *Phys. Rep.* **97** 31 (1983)
- [3] T. Sjöstrand, *Comp. Phys. Comm.* **82** 74 (1994)
- [4] B.R. Webber, *Nucl. Phys.* **B238** 492 (1984)
G. Marchesini, B.R. Webber, *Nucl. Phys.* **B238** 1 (1984)

- [5] G. Marchesini *et al.*, *Comp. Phys. Comm.* **67** 465 (1992)
- [6] C. Peterson, D.Schlatter, I. Schmitt, P. Zerwas, *Phys. Rev.* **D27** 105 (1983)
- [7] M.B. Bowler, *Z. Phys.* **C11** 169 (1981)
D.A. Morris, *Nucl. Phys.* **B313** 634 (1989)
- [8] B. Andersson, G. Gustafson, and B. Söderberg, *Z. Phys.* **C20** 317 (1983)
- [9] B. Andersson, G. Gustafson, J. Samuelsson, *Z. Phys.* **C64** 653 (1994)
- [10] Yu.L. Dokshitzer, V.A. Khoze, S.I. Troyan, *J. Phys.* **G17** 1602 (1991)
- [11] A. De Angelis, in Proceedings of the XXIV International Symposium on Multiparticle Dynamics, (Vietri sul Mare, Italy, 1994), eds. A. Giovannini, S. Lupia and R. Ugoccioni, World Scientific (Singapore, 1995), p. 359
- [12] B.A. Schumm, Yu.L. Dokshitzer, V.A. Khoze, D.S Koetke, *Phys. Rev. Lett.* **69** 3025 (1992)
- [13] The L3 Collab, *Z. Phys* **C55** 39 (1992) The ALEPH Collab, *Z. Phys* **C55** 209 (1992)
The DELPHI Collab, *Z. Phys* **C59** 21 (1993) The OPAL Collab, *Z. Phys* **C59** 1 (1993)
- [14] The OPAL Collab., *Z. Phys.* **C66** 19 (1995)
- [15] Helenka Przysiezniak-Frey, Talk given at Moriond: QCD and High Energy Hadronic Interactions 1996
- [16] I. Dunetz, J.L. Rosner, *Phys. Rev.* **D34** 1404 (1986)
I. Dunetz, *Ann. Phys. (N.Y.)* **184** 350 (1988)

Paper VI

Colour: A Computer Program for QCD Colour Factor Calculations

Jari Häkkinen, Hamid Kharraziha¹
Department of Theoretical Physics, Lund University,
Sölvegatan 14A, SE-223 62 Lund, Sweden

Submitted to
Computer Physics Communications

Abstract:

A computer program for evaluating colour factors of QCD Feynman diagrams is presented, and illustrative examples on how to use the program to calculate non trivial colour factors are given. The program and the discussion in this paper is based on a diagrammatic approach to colour factors.

¹jari@thep.lu.se, hamid@thep.lu.se

Program Summary

Title of program: colour

Program obtainable from: <http://www.thep.lu.se/tf2/hep>
or <ftp://thep.lu.se/pub/LundPrograms/Misc/colour.tar.Z>

Computer for which program is designed: Computers with an ANSI C compiler.

Program language used: C

Peripherals used: terminal and mass storage for input, terminal for output

Number of lines in combined program: ≈ 1000

Keywords: Feynman diagrams, QCD colour factors

Nature of the physical problem: In many QCD Feynman diagrams there is a need to calculate the colour factor. This program calculates colour factors fast and accurately.

Method of solution: QCD Feynman diagrams, with no four-gluon vertices, factorize into a colour (group) factor and a kinematical factor. The colour part of any closed QCD Feynman diagram can be transformed into a sum of diagrams including only closed quark (colour) lines. In each such term, the number of quark (colour) loops is counted, giving factors of 3 (or N_c). The sum of these terms is then the desired colour factor.

To perform the translation, we need to have rules to interpret gluons and vertices into quark lines. There is in principle only need for three equalities to be able to calculate any closed QCD diagram (not containing four gluon vertices). To achieve good computing performance further equalities have been introduced. The most essential ones are listed in Appendix A.

Restriction of complexity of the problem: Four gluon vertices cannot be included directly in diagrams to be calculated. The number of gluons in diagrams to be calculated are limited to 200, but can easily be changed prior to compiling.

Typical running time: For typical diagrams, fractions of a second. Complicated diagrams - a few seconds to hours.

1 Introduction

There are several programs available to perform momentum Feynman diagram calculations, either symbolically or numerically [1]. Some of these perform QCD calculations, but usually the QCD calculating programs do not calculate the colour factors for a given diagram. The users have to calculate these factors themselves. This can be done in different ways, the most appealing method is presented in [2, 3] where only diagrammatic manipulations are needed to calculate colour factors of diagrams.

In this paper we present a computer program for calculating colour factors of QCD diagrams using the rules and equalities derived in [2]. An introduction is given on how to use the program and which results can be obtained. Using a set of projection operators non trivial results can be achieved, such as how the interaction probability between two gluons depend on their common colour state. Only closed Feynman diagrams (vacuum QCD diagrams, i.e. diagrams with no external legs) can be calculated, but this is not a real problem since the restriction can be circumvented as will be shown. We also present a short introduction to the group theory part of the calculations.

2 Theory in brief

The program presented here is based on the results in [2] and [3]. These results has been further developed and explained to us by Yuri Dokshitzer and Bo Söderberg [4]. In this section and the appendices we give a brief presentation of the main results.

The existence of colour factors in QCD originates from the invariance of the Lagrangian under colour transformations. For a certain interaction, with incoming and outgoing particles, intermediate propagators and different kinds of vertices, one has to sum over all possible colours, if they are not explicitly specified. Since the kinematical factor in the interaction probability is equal for all these diagrams (excluding diagrams containing four-gluon vertices), we therefore have a multiplicative factor to the probability, which we get by counting the colours.

Two preliminary remarks. When we discuss colours and anti-colours we often use quarks and anti-quarks, respectively, to describe the colour flow. In most expressions we keep N_c as a free variable in order to be general. Whenever the number of colours is specified, $N_c = 3$ has been used.

Every $3^m \otimes \bar{3}^n$ space can be divided into a set of irreducible subspaces. In the simplest example of a quark and an anti-quark system, the irreducible representation is the singlet and the octet state, i.e. $3 \otimes \bar{3} = 1 \oplus 8$, where the octet state corresponds to the gluons. The equation

$$\begin{array}{c} \longrightarrow \\ \longleftarrow \end{array} = \frac{1}{N_c} \begin{array}{c} \longrightarrow \\ \longrightarrow \end{array} \begin{array}{c} \longleftarrow \\ \longleftarrow \end{array} + 2 \begin{array}{c} \longrightarrow \\ \longrightarrow \end{array} \begin{array}{c} \longleftarrow \\ \longleftarrow \end{array} \quad (1)$$

states this fact in equation form. (The factor of 2 in the second term is due to the Gell-Mann normalization of gluons, see discussion in Appendix B. We have adopted Gell-Mann

normalization in all calculations in this paper.) In the LHS of Eq (1) a colour and an anti-colour state, $3 \otimes \bar{3}$, are divided into irreducible singlet and octet states on the RHS. The degeneracy (multiplicity) of a state is given by taking the trace of the representation of the state. Calculating the trace in this diagrammatic representation corresponds to connecting the incoming legs and the outgoing colour flow. For the LHS we find

$$\text{Tr} [\text{LHS}] = \text{Tr} \left[\begin{array}{c} \longrightarrow \\ \longleftarrow \end{array} \right] = \begin{array}{c} \text{---} \\ \text{---} \\ \text{---} \end{array} = N_c^2$$

as expected, and for the RHS

$$\text{Tr} [\text{RHS}] = \frac{1}{N_c} \begin{array}{c} \text{---} \\ \text{---} \\ \text{---} \end{array} + 2 \begin{array}{c} \text{---} \\ \text{---} \\ \text{---} \end{array} = 1 + (N_c^2 - 1)$$

Another observation is that the two diagrams, P_1 and P_2 , in the RHS of Eq (1) are disjoint projection operators since the terms satisfy $P_i^2 = P_i$ and $P_i P_j = 0, P_j P_i = 0$. These can be used to split any quark–anti-quark diagram into an irreducible representation

$$\begin{array}{c} \longrightarrow \\ \longleftarrow \end{array} \boxed{} = \lambda_1 P_1 + \lambda_8 P_8$$

The projection operators can be used to ask specific questions about the colour states particles are in, e.g. what is the probability to find two free gluons in an anti-symmetric octet state. This is easily solved by calculating colour states. The two gluons are in a $8 \otimes 8$ state with degeneracy 64, and the irreducible representation of the $8 \otimes 8$ space contains an anti-symmetric octet (with degeneracy 8), i.e. the answer is 8/64 since the probability is equal for all states. In the next section we will give a few other examples on these issues and describe how to perform the calculations using the program.

Given a problem concerning colour states, the problem of finding solutions boils down to finding the projection operators for reduced representations. Once this is done all interesting numbers can be calculated using the program. In Appendix B we have listed the (irreducible representation) projection operators for a few states.

The triple gluon coupling is anti-symmetric in colour. We have generalized the program to include also a symmetric coupling between three colour octets (“gluons”).

3 Using the program

A straight forward use of the program is to calculate QCD vacuum diagrams. This might not be too exciting. Using projection operators more interesting results can be obtained. A few illustrative examples will be given below.

The program interacts with the user through input files. The diagram to be calculated is defined in one input file which is read by the program, the diagram is calculated and the result is written on the screen. No interaction with the user is needed after the program has been started.

The command line syntax to start the program is:

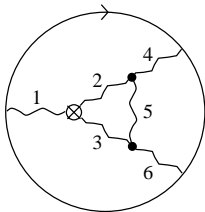
where

- df Changes the input file name. The default name is *colour.in*.
- h or -help Prints a small description of the program and a list of valid options.

There are few rules for defining a qcd diagram in the input file.

- Every gluon line is assigned a unique number.
- Triple anti-symmetric gluon vertices are represented by a letter f followed by the three incoming gluon numbers.
- Symmetric triple vertices² are represented in the same way as the anti-symmetric vertices but with the letter d .
- Quark loops are represented by a letter t , followed by all gluons connected to the quark loop.
- Four-gluon vertices cannot be directly included in the program since the colour and the kinematical parts of the cross section do not factorize. This can, however, be taken care of by separating the four-gluon vertex in factorizable terms, as discussed further in Appendix A.
- Ghosts can also be included since these couple to gluons with the same colour factor as gluons themselves. Thus ghost vertices can be represented with a letter f .
- For the quark loops and the anti-symmetric gluon vertex the order of the gluons are important since $f_{abc} = -f_{bac}$. So when translating a diagram into a file all loops and f vertices must be written down in the same order (clockwise or anti-clockwise).
- Composite objects, d , f , and t , must be separated with a newline character, while gluon numbers are separated with a space. All other separation characters are invalid and will stop the execution of the program.

For example, the diagram



would transform to a file like

```
d 1 2 3
f 2 4 5
f 3 5 6
t 1 4 6
```

The numbers assigned to every gluon are arbitrary and occur twice in the file since every gluon is connected to two vertices in the diagram. If you run this file, the answer will be: $\frac{1}{2^3}(N_c^4 - 5N_c^2 + 4)$ and is equal to 5 using $N_c = 3$.

²As mentioned above these are not physical QCD gluon vertices, but are included for generality. The vertex is also used in projection operators.

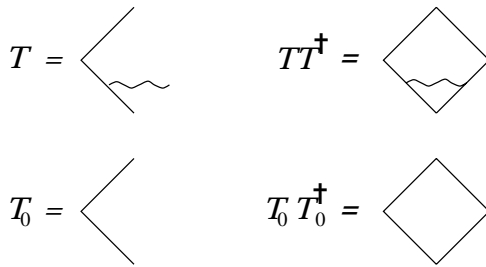


Figure 1: *Diagrams used to calculate C_F .*

3.1 Example 1: Colour factor for gluon emission from quarks

Let us start with the problem of calculating the colour factor, often denoted C_F , for emission of a gluon from a quark line. This can be easily done by hand, but it is a nice example to demonstrate how the program can be used.

We will study a transition matrix T , defined in Fig 1. A colour singlet comes in, a quark–anti-quark pair is created and a gluon is emitted from one of the quark legs. We have chosen to use a singlet state since the program can only handle closed diagrams³. By definition, C_F is a multiplicative factor to the transition probability, due to the emission of a gluon from the quark leg. For the transition probability, we have to square the matrix by multiplying it with its conjugate (reversing the colour flow and using the mirror image). The result then must be normalized by dividing by the squared amplitude of just creating the quark–anti-quark pair.

Consequently, to obtain C_F we have to run the program twice, one time with the diagram TT^\dagger and once with the diagram $T_0T_0^\dagger$.

In order to use the program we have to translate the diagrams into an input file. This can be done as

Diagram	Input file	Result
TT^\dagger	t 1 1	$\frac{1}{2} [N_c^2 - 1]$
$T_0T_0^\dagger$	t	N_c

Thus, we get that

$$C_F = \frac{N_c^2 - 1}{2N_c} = \frac{4}{3}.$$

3.2 Example 2: Partitioning into irreducible representations

Any diagram in the $8 \otimes 8$ space can be written as a sum of the projection operators described in Appendix B (and crossing operators which are built from operators of the same multiplicity). Consider e.g. the gluon-gluon scattering matrix T in Fig 2. This matrix can

³There are obviously other diagrams which would enable us to calculate C_F , but these involve obscuring technicalities.

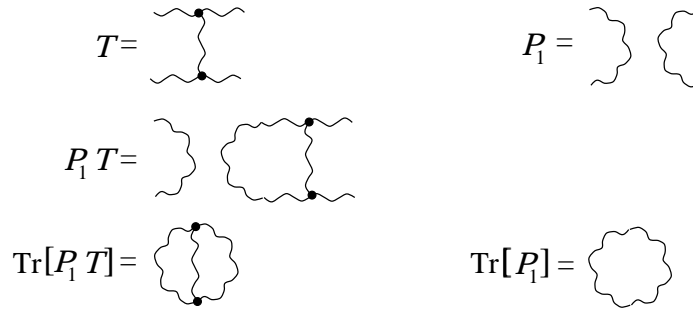


Figure 2: *Diagrams used to calculate the singlet eigenvalue, λ_1 , for the state T .*

be written as a sum of projection operators solely, that is without any crossing operators,

$$T = \sum \lambda_i P_i.$$

The eigenvalues can easily be found. To be concrete we will determine λ_1 corresponding to the singlet state, and the other eigenvalues are derived in the same way. To calculate this, we apply the operator to the matrix T , thus projecting out the singlet part of the diagram. Then we take the trace of PT and divide the result with the trace of just the operator,

$$TP_1 = \lambda_1 P_1, \quad \lambda_1 = \frac{\text{Tr}(P_1 T)}{\text{Tr}(P_1)}.$$

The translation into a file looks like

Diagram	Input file	Result
$\text{Tr}(P_1 T)$	f 1 2 3	$N_c [N_c^2 - 1]$
	f 1 3 2	
$\text{Tr}(P_1)$	See Sec 3.4	$N_c^2 - 1$

Running the program we find that $\lambda_1 = N_c$.⁴

3.3 Example 3: Probability of an octet state

The question here is: If we have a transition matrix of some kind containing two gluons, what is the probability for them to be in any of the states described in Fig 6 in Appendix B. Take for example the transition matrix T in Fig 3, what is the probability for the two incoming gluons to be in the anti-symmetric octet state P_{8a} ?

To solve this problem, the first step is to square the matrix, thus getting the symmetric matrix TT^\dagger which correspond to the probability. Then the antisymmetric octet part of the amplitude is projected out, by applying the operator. The probability is given by the multiplicity of the projected part, divided by the total multiplicity of the amplitude,

$$\text{Prob}(P_{8a}|T) = \frac{\text{Tr}(P_{8a} T T^\dagger)}{\text{Tr}(T T^\dagger)}.$$

⁴Note that the eigenvalues depend on the normalization of the gluon, see Appendix B.

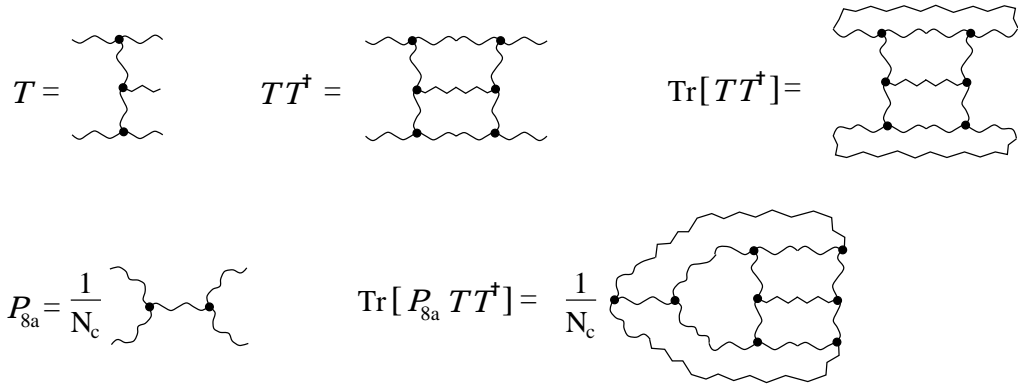


Figure 3: *Diagrams used in Example 3.3.*

For this we have to run the program twice, once with the diagram $Tr(TT^\dagger)$ and once with the diagram $Tr(P_{8a}TT^\dagger)$.

The translation into a file looks like

Diagram	Input file	Result
	f 1 4 2 f 4 7 5 f 7 9 8 f 6 8 9 f 3 5 6 f 1 2 3	$N_c^3 [N_c^2 - 1]$
$N_c Tr(P_{8a}TT^\dagger)$	f 1 4 2 f 4 7 5 f 7 9 8 f 6 8 12 f 3 5 6 f 11 2 3 f 1 10 9 f 10 11 12	$\frac{1}{8} [N_c^6 + 11N_c^4 - 12N_c^2]$

Putting it all together gives a probability of 7/24 (with $N_c = 3$) to find the two incoming gluons in an octet state.

3.4 Limitations

There are some limits in the program. First, the physics limitations. Four-gluon vertices are not included and therefore diagrams containing these vertices cannot be calculated directly. The four-gluon vertex must be replaced with three other diagrams, which have to be calculated separately (see Appendix A). There is also one specific diagram that the program cannot evaluate, a gluon ring, but the colour factor for this diagram is simply the number of different gluons, $N_c^2 - 1$. This is purely technical and the diagram could in principle be

implemented into the program as a special case, but the gain is not worth the effort. Secondly, local implementation limits. There is a limit on the number of gluons which can be included in the program. This is set to 200 but can easily be changed by the user before compiling. There is also a limit to which power in N_c calculations can be done, the default range is $N_c^{-100} - N_c^{99}$, this can also easily be changed prior to compiling the program. A warning message will appear if over- or underflow occurs.

4 Acknowledgments

We would like to thank Yuri Dokshitzer and Bo Söderberg for introducing us into the world of colour factors.

References

- [1] H. Strubbe, *Comp. Phys. Comm.* **8** 1 (1974)
J. Kühlbeck, M. Böhm, A. Denner, *Comp. Phys. Comm.* **60** 165 (1990)
R. Mertig, M. Böhm, A. Denner, *Comp. Phys. Comm.* **64** 345 (1991)
- [2] Yu.L. Dokshitzer, S.I. Manaenkov, Quantum Chromodynamics for Beginners. Color Algebra, Leningrad Nuclear Physics Inst. Preprint 1103, Leningrad, September 1985
- [3] P. Cvitanović, Group Theory, Nordita Classics Illustrated, 1984
- [4] Yu.L. Dokshitzer, Introduction to Colour Dynamics, Seminars based on [2], given at Department of Theoretical Physics, Lund University, Spring 1992.
B. Söderberg, Private communications

A Colour Rules

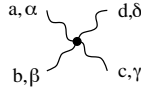
The set of rules in Fig 4, taken from [2], are implemented in the program with the exception of the gluon loop C1b. The equation numbers are the ones to be found in [2], and as indicated we do not list all of them. We note that in principle it is enough to use equations C11 and C19 to translate any diagram without four-gluon vertices to diagrams containing only quark loops. The other equalities are implemented in order to increase the computing performance.

$$\begin{array}{lcl}
 \begin{array}{c} \circlearrowright \end{array} = N_c & & \text{C1a} \\
 \begin{array}{c} \text{gluon loop} \end{array} = N_c^2 - 1 & & \text{C1b} \\
 \begin{array}{c} \text{gluon line} \circlearrowright \end{array} = 0 & & \text{C2} \\
 \begin{array}{c} \text{gluon line} \text{gluon loop} \end{array} = 0 & & \text{C7} \\
 \begin{array}{c} \text{quark line} \text{quark loop} \end{array} = \frac{1}{N_c} \begin{array}{c} \text{quark line} \text{quark loop} \end{array} + 2 \begin{array}{c} \text{quark line} \text{quark loop} \text{gluon line} \end{array} & & \text{C11} \\
 \begin{array}{c} \text{gluon loop} \text{quark line} \end{array} = C_F \text{quark line} & & \text{C14} \\
 \begin{array}{c} \text{gluon line} \text{gluon loop} \end{array} = -\frac{1}{2N_c} \begin{array}{c} \text{gluon line} \end{array} & & \text{C15} \\
 \begin{array}{c} \text{gluon line} \circlearrowright \text{gluon line} \end{array} = \frac{1}{2} \begin{array}{c} \text{gluon line} \end{array} & & \text{C18} \\
 \begin{array}{c} \text{quark line} \text{quark loop} \text{quark line} \end{array} - \begin{array}{c} \text{quark line} \text{quark loop} \text{quark line} \end{array} = \frac{1}{2} \begin{array}{c} \text{quark line} \text{quark loop} \text{quark line} \end{array} & & \text{C19a} \\
 \begin{array}{c} \text{quark line} \text{quark loop} \text{quark line} \end{array} + \begin{array}{c} \text{quark line} \text{quark loop} \text{quark line} \end{array} = \frac{1}{2} \begin{array}{c} \text{quark line} \text{quark loop} \text{quark line} \end{array} & & \text{C19b}
 \end{array}$$

Figure 4: *Rules for diagram manipulations.*

The four-gluon vertex has not been included in the program since QCD diagrams containing four-gluon vertices do not factorize into a colour (group theoretical) part and a

kinematical part. The four-gluon vertex,



has the form

$$f_{abn}f_{ncd}[g^{\alpha\gamma}g^{\beta\delta} - g^{\alpha\delta}g^{\beta\gamma}] + f_{and}f_{bcn}[g^{\alpha\gamma}g^{\beta\delta} - g^{\alpha\beta}g^{\gamma\delta}] + f_{anc}f_{bdn}[g^{\alpha\delta}g^{\beta\gamma} - g^{\alpha\beta}g^{\gamma\delta}].$$

Thus a diagram with such a vertex can be split into three pieces, each of which has a factorized form (this separation is not unique). Each piece has a colour factor corresponding to a diagram where the four-gluon vertex is replaced by two three-gluon vertices, as symbolically shown in Fig 5.

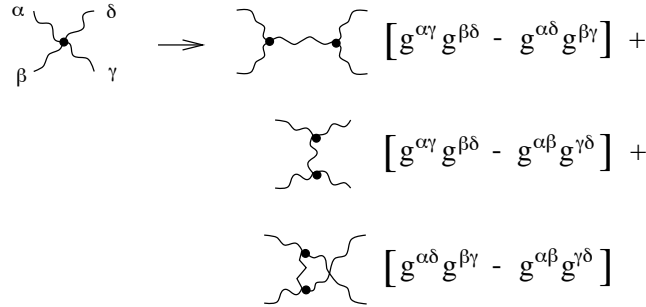


Figure 5: *Symbolic representation of the colour factors in a four-gluon vertex.*

B Projection Operators

In Figs 6–9 we present the set of projection operators needed to obtain irreducible representations of the $8 \otimes 8$, $3 \otimes \bar{3}$, $3 \otimes 3$, and $3 \otimes 3 \otimes 3$ spaces, respectively. For the derivation of these operators we refer to Cvitanović [3].

There are different normalizations adopted for gluons and the coupling constant α_s . A difference in the overall normalization of the projection operators is not a problem as long as it is used consistently. The overall normalization is factorized out in most cases, as in the Examples 3.2 and 3.3. In Example 3.1 we have adopted the Gell-Mann (conventional) normalization of the gluons.

The difference in normalization, lies in how we interpret the curly lines, representing the gluons, and also in the interpretation of the triple vertices. With the Gell-Mann normalization, the gluon is interpreted as the octet projection in the $3 \otimes \bar{3}$ space together with a factor $1/2$ (compare Eq C11 of Appendix A). This factor originates from the conventional QCD normalization of the generators of the SU(3) group, i.e.

$$t^a = \frac{1}{2}\lambda^a. \quad (2)$$

$$\begin{aligned}
P_{10} &= \frac{1}{4} \left[\begin{array}{c} \text{Diagram 1} \\ \text{Diagram 2} \end{array} - \text{Diagram 3} + (4) \begin{array}{c} \text{Diagram 4} \\ \text{Diagram 5} \end{array} - (4) \begin{array}{c} \text{Diagram 6} \\ \text{Diagram 7} \end{array} - (2) \frac{1}{N_c} \left. \text{Diagram 8} \right\} \left. \text{Diagram 9} \right\} \left. \right] \\
P_{10} &= \frac{1}{4} \left[\begin{array}{c} \text{Diagram 1} \\ \text{Diagram 2} \end{array} - \text{Diagram 3} - (4) \begin{array}{c} \text{Diagram 4} \\ \text{Diagram 5} \end{array} + (4) \begin{array}{c} \text{Diagram 6} \\ \text{Diagram 7} \end{array} - (2) \frac{1}{N_c} \left. \text{Diagram 8} \right\} \left. \text{Diagram 9} \right\} \left. \right] \\
P_{27} &= \frac{1}{4} \left[\begin{array}{c} \text{Diagram 1} \\ \text{Diagram 2} \end{array} + \text{Diagram 3} + (4) \begin{array}{c} \text{Diagram 4} \\ \text{Diagram 5} \end{array} + (4) \begin{array}{c} \text{Diagram 6} \\ \text{Diagram 7} \end{array} - (2) \frac{1}{N_c + 2} \left. \text{Diagram 8} \right\} \left. \text{Diagram 9} \right\} \left. \text{Diagram 10} \right\} \left. \text{Diagram 11} \right\} \left. \right] \\
P_0 &= \frac{1}{4} \left[\begin{array}{c} \text{Diagram 1} \\ \text{Diagram 2} \end{array} + \text{Diagram 3} - (4) \begin{array}{c} \text{Diagram 4} \\ \text{Diagram 5} \end{array} - (4) \begin{array}{c} \text{Diagram 6} \\ \text{Diagram 7} \end{array} - (2) \frac{1}{N_c - 2} \left. \text{Diagram 8} \right\} \left. \text{Diagram 9} \right\} \left. \text{Diagram 10} \right\} \left. \text{Diagram 11} \right\} \left. \right] \\
P_1 &= \frac{1}{N_c^2 - 1} \left. \text{Diagram 12} \right\} \left. \text{Diagram 13} \right\} \\
P_{8_s} &= (2) \frac{N_c}{2(N_c^2 - 4)} \left. \text{Diagram 14} \right\} \left. \text{Diagram 15} \right\} \\
P_{8_a} &= (2) \frac{1}{2N_c} \left. \text{Diagram 16} \right\} \left. \text{Diagram 17} \right\}
\end{aligned}$$

Figure 6: *Projection operators needed to obtain the irreducible representations of the $8 \otimes 8 = 0 \oplus 1 \oplus 8_a \oplus 8_s \oplus 10 \oplus \overline{10} \oplus 27$ space.*

A more convenient way to normalize the gluon is to let the factor of $\frac{1}{2}$ in Eq 2 go into α_s , i.e. to let the gluon represent just the octet projection, without any factors. In the same spirit, the triple gluon vertices (symmetric and anti-symmetric) can be defined without any factors.

The program output comes with both normalizations. The answer which is expressed as a polynomial in N_c , is normalized with the second convention. If you use the polynomial ignoring the overall factor (and the numerical answer), you should replace the factors within parenthesis, in the operators in Figures 6 and 7, by a factor 1. If you prefer to use the Gell-Mann normalization, you must make use of the factors within parenthesis.

The projection operator, P_0 , has the multiplicity 0 when the number of colours is 3. This subspace exists e.g. in SU(2) where it has multiplicity 3 and corresponds to a real state.

$$\begin{aligned}
P_1 &= \frac{1}{N_c} \left[\begin{array}{c} \text{---}\overrightarrow{\hspace{1cm}}\text{---} \\ \text{---}\overleftarrow{\hspace{1cm}}\text{---} \end{array} \right] \left[\begin{array}{c} \text{---}\overrightarrow{\hspace{1cm}}\text{---} \\ \text{---}\overleftarrow{\hspace{1cm}}\text{---} \end{array} \right] \\
P_8 &= \begin{array}{c} \text{---}\overrightarrow{\hspace{1cm}}\text{---} \\ \text{---}\overleftarrow{\hspace{1cm}}\text{---} \end{array} - \frac{1}{N_c} \left[\begin{array}{c} \text{---}\overrightarrow{\hspace{1cm}}\text{---} \\ \text{---}\overleftarrow{\hspace{1cm}}\text{---} \end{array} \right] \left[\begin{array}{c} \text{---}\overrightarrow{\hspace{1cm}}\text{---} \\ \text{---}\overleftarrow{\hspace{1cm}}\text{---} \end{array} \right] \equiv (2) \left[\begin{array}{c} \text{---}\overrightarrow{\hspace{1cm}}\text{---} \\ \text{---}\overleftarrow{\hspace{1cm}}\text{---} \end{array} \right] \text{---} \text{---} \left[\begin{array}{c} \text{---}\overrightarrow{\hspace{1cm}}\text{---} \\ \text{---}\overleftarrow{\hspace{1cm}}\text{---} \end{array} \right]
\end{aligned}$$

Figure 7: Projection operators needed to obtain the irreducible representations of the $3 \otimes \bar{3} = 1 \oplus 8$ space.

$$\begin{aligned}
P_{\bar{3}} &= \frac{1}{2} \left[\begin{array}{c} \text{---} \\ \text{---} \end{array} - \begin{array}{c} \diagup \\ \diagdown \end{array} \right] \\
P_6 &= \frac{1}{2} \left[\begin{array}{c} \text{---} \\ \text{---} \end{array} + \begin{array}{c} \diagup \\ \diagdown \end{array} \right]
\end{aligned}$$

Figure 8: Projection operators needed to obtain the irreducible representations of the $3 \otimes 3 = \bar{3} \oplus 6$ space.

$$\begin{aligned}
P_1 &= \frac{1}{6} \left[\begin{array}{c} \text{---} \\ \text{---} \\ \text{---} \end{array} + \begin{array}{c} \diagup \\ \diagdown \\ \diagup \\ \diagdown \end{array} + \begin{array}{c} \diagdown \\ \diagup \\ \diagdown \\ \diagup \end{array} - \begin{array}{c} \diagup \\ \diagdown \end{array} - \begin{array}{c} \diagdown \\ \diagup \end{array} - \begin{array}{c} \text{---} \\ \text{---} \end{array} \right] \\
{}^1P_8 &= \frac{1}{6} \left[2 \begin{array}{c} \text{---} \\ \text{---} \\ \text{---} \end{array} - \begin{array}{c} \diagup \\ \diagdown \\ \diagup \\ \diagdown \end{array} - \begin{array}{c} \diagdown \\ \diagup \\ \diagdown \\ \diagup \end{array} + 2 \begin{array}{c} \diagup \\ \diagdown \end{array} - \begin{array}{c} \diagdown \\ \diagup \end{array} - \begin{array}{c} \text{---} \\ \text{---} \end{array} \right] \\
{}^2P_8 &= \frac{1}{6} \left[2 \begin{array}{c} \text{---} \\ \text{---} \\ \text{---} \end{array} - \begin{array}{c} \diagup \\ \diagdown \\ \diagup \\ \diagdown \end{array} - \begin{array}{c} \diagdown \\ \diagup \\ \diagdown \\ \diagup \end{array} - 2 \begin{array}{c} \diagup \\ \diagdown \end{array} + \begin{array}{c} \diagdown \\ \diagup \end{array} + \begin{array}{c} \text{---} \\ \text{---} \end{array} \right] \\
P_{10} &= \frac{1}{6} \left[\begin{array}{c} \text{---} \\ \text{---} \\ \text{---} \end{array} + \begin{array}{c} \diagup \\ \diagdown \\ \diagup \\ \diagdown \end{array} + \begin{array}{c} \diagdown \\ \diagup \\ \diagdown \\ \diagup \end{array} + \begin{array}{c} \diagup \\ \diagdown \end{array} + \begin{array}{c} \diagdown \\ \diagup \end{array} + \begin{array}{c} \text{---} \\ \text{---} \end{array} \right]
\end{aligned}$$

Figure 9: Projection operators needed to obtain the irreducible representations of the $3 \otimes 3 \otimes 3 = 1 \oplus 8 \oplus 8 \oplus 10$ space.